

THE CURE REACTION OF AN AROMATIC THERMOSETTING
POLYIMIDE

A Thesis

Presented to

The Faculty of the Department of Chemistry
The College of William and Mary in Virginia

In Partial Fulfillment
of the Requirements for the Degree of
Master of Arts

by

Michael E. Whitham

1986

APPROVAL SHEET

This thesis is submitted in partial fulfillment of the
requirements for the degree of

MASTER OF ARTS

Michael Edward Whitham
Michael Edward Whitham

Approved, May, 1986

David E. Kranbuehl
David Kranbuehl

Robert L. Orwoll
Robert Orwoll

Gary C. DeFotis
Gary DeFotis

DEDICATION

To my wife, family, and friends, who had the determination that I would finish in spite of myself.

TABLE OF CONTENTS

	Page
ACKNOWLEDGEMENTS.....	v
LIST OF TABLES.....	vi
LIST OF FIGURES.....	vii
ABSTRACT.....	x
CHAPTER I. INTRODUCTION TO THE CHEMISTRY.....	2
CHAPTER II. INTRODUCTION TO DYNAMIC DIELECTRIC ANALYSIS.....	11
CHAPTER III. ANALYSIS OF A POLYIMIDE CURE.....	34
CHAPTER IV. AGEING STUDY AT 0% AND 90% HUMIDITY....	49
CHAPTER V. WHAT IS A DIFFERENTIAL SCANNING CALORIMETER?.....	60
CHAPTER VI. MEASUREMENT OF HEAT CAPACITY BY DIFFERENTIAL SCANNING CALORIMETRY.	68
CHAPTER VII. ANALYSIS OF DSC SCANS.....	87
CHAPTER VIII. ACTIVATION ENERGY BY DSC.....	100
CHAPTER IX. PRESSURE RUNS ON THE DSC.....	115
CHAPTER X. THE CROSSLINKING REACTION.....	122
BIBLIOGRAPHY.....	128

ACKNOWLEDGEMENTS

I wish to express my appreciation for the assistance and encouragement given me by the faculty of the chemistry department. I want to thank my wife for helping me prepare some of the curves used in this text, and my father for typing most of the mathematical expressions in the text. Professor David E. Kranbuehl deserves credit for keeping my research on track and for helping me develop a sense of scientific understanding. Melanie Hoff and Sue Delos helped guide my day to day activities in the laboratory and have helped me overcome innumerable difficulties. Special thanks goes to Dr. John Benzel in the physics shop for his aid in the adaptation of a pressure head to the differential scanning calorimeter.

LIST OF TABLES

TABLE		Page
1.	Enthalpy at Different Scanning Speeds.....	70
2.	Enthalpy for Different Masses.....	70
3.	Heat Capacity of Indium.....	73
4.	Heat Capacity of Zinc.....	73
5.	Heat Capacity of Zinc, Different Method.....	74
6.	Heat Capacity of the Polyimide.....	76
7.	Delta H for Crosslinking Reaction.....	103
8.	Reaction Order for Crosslinking.....	104
9.	Reaction Rate for Crosslinking.....	104

LIST OF FIGURES

Figure		Page
1.	Polyimide Reaction Sequence.....	7
2.	Incorrect Polyimide Reaction Sequence.....	8
3.	Formation of Tetra-acid.....	8
4.	Reverse Diels-Alder Reaction.....	8
5.	Imidization Mechanism.....	9
6.	Polarization in a Capacitor.....	13
7.	In Phase Relationship.....	18
8.	Resistive Circuit.....	18
9.	Out of Phase Relationship.....	19
10.	Capacitave Circuit.....	19
11,12.	Phasor Diagrams of Circuits.....	19
13.	Model and Circuit Equivalency.....	22
14.	Circuit Measurement Equivalency.....	24
15.	Real and Complex Curves.....	30
16.	Apparatus for Dielectrometry.....	31
17.	Polymer Experiment Layup.....	32
18,19.	Real and Imaginary Components of the Polyimide.....	40,41
20,21.	Frequency Plots for Low Temperatures.....	42,43
22,23.	Frequency Plots for High Temperatures.....	44,45

Figure	Page
24,25.	Master Plots for Real and Complex Components.....46,47
26,27.	Comparison Plots of Real Component in Humidity Study.....53,54
28,29.	Comparison Plots of Complex Component in Humidity Study.....55,56
30,31.	Comparison Plots Considering Hurricane Gloria.....57,58
32.	Schematic of Scanning Calorimeter.....66
33.	Scan of Pure Indium.....78
34,35.	Heat Capacity Scans for Pure Indium.....79,80
36,37.	Heat Capacity Scans for Pure Zinc.....81,82
38,39.	Heat Capacity Scans for the Polyimide.....83,84
40.	Complete Cure of the Polyimide.....91
41.	Scan of the Imidization Region.....92
42.	Scan of BTDE-MDA mix.....93
43.	Scan of NE-MDA mix.....94
44.	Scan of NE.....95
45.	Scan of NA.....96
46.	Scan of BTDE.....97
47.	Scan of BTDA.....98
48.	Scan of MDA.....99
49.	Scan of Crosslink Region.....106
50,51, 52,53.	Isothermal Scans in the Crosslinking Region.....107,108 109,110
54.	Plot to Determine Reaction Order.....111

Figure		Page
55.	Plot to Determine Reaction Rate.....	112
56.	Plot to Determine Activation Energy.....	113
57.	Latent Heat of Vaporization for Water.....	119
58.	Scan of Boiling for Water.....	120
59.	Proposed Free Radical Crosslink Mechanism...	125
60.	Reaction Sequence for Model Compound Crosslink.....	126

ABSTRACT

The purpose of this investigation was to gain information on the cure reaction of an aromatic thermosetting polyimide. Dynamic dielectric analysis and differential scanning calorimetry were used to accomplish this goal.

The first part of this study reviews the chemistry of the polyimide which was determined by traditional chemical methods. The monomers and reaction sequence are presented.

The second part of this study is concerned with dielectric data. The theory of dielectrics is reviewed first and then a dielectric spectra of a fresh resin system is analyzed. A study related to age and storage conditions is also presented.

The last part of this study deals with differential scanning calorimetry. The theory of differential scanning calorimetry is reviewed. Methods for obtaining specific heats and activation energies are presented. Scans of the polyimide and its monomers are interpreted. A method for operating the differential scanning calorimeter under pressure is also presented.

The objective of this thesis is to provide the reader with a modest understanding of dielectric analysis and scanning calorimetry and to show how these powerful tools can be applied to the study of polymerization of an aromatic thermosetting polyimide.

THE CURE REACTION OF AN AROMATIC THERMOSETTING
POLYIMIDE

CHAPTER I

Introduction to the Chemistry

A mixture of a monomethyl ester of 5-norbornene-2,3-dicarboxylate (NE), a dimethyl ester of 3,3',4,4'-benzophenone tetracarboxylate (BTDE), and 4,4'-methylenedianiline (MDA) reacts at elevated temperatures to form an aromatic thermosetting polyimide. The curing reaction of these monomers to form a polymer is investigated in this report.

The molar ratio of the components is,

$$(n) \text{ (BTDE)} : (n+1) \text{ (MDA)} : (2) \text{ (NE)}$$

Dr. Serafini developed the idea of dissolving these monomers in a low boiling solvent and then impregnating reinforcing fibers with the mixture. The monomer reactants would polymerize in situ upon heating the impregnated fibers.¹ Dr. Serafini's laboratory found that the value for n in the molar ratio which provided the best balance of thermo-oxidative stability and processing characteristics was $n=2.087$. The aromatic thermosetting polyimide has been referred to as "PMR 15" by Dr. Serafini to signify the material's formulated molecular weight of 1500.

The samples studied in this report were prepared either at William and Mary by Sue Delos or at General Electric by Dick Griffen. They are prepared in a 50% weight methanol solution. The samples are stored in a freezer at -10 C. Samples kept under these storage conditions remain stable for six months.² Samples are removed from storage bottles by first allowing the bottle and the mixture to come to room temperature, then removing the sample, and then returning the storage bottles to the freezer. Care is exercised during the sampling procedure because dielectric data have shown the handling history of the mixture affects the cure reactions.

The polymerization occurs by making long chain polyimides at lower temperatures, $T < 200$ C, and then crosslinking the polyimides into a resin matrix at higher temperatures, $T > 200$ C. IR and ^{13}C -NMR studies conducted in Dr. Kranbuehl's laboratory have demonstrated that NE imidizes with MDA faster and at lower temperatures than BTDE.^{3,4} Figure Chem 1 illustrates the reaction sequence of the polyimide. Notice that at room temperature short chains of nadic imide (NE-MDA) and bisnadimide (NE-MDA-NE) are formed. The bisnadimide chains will obviously not undergo further imidization but will be able to crosslink later in the cure. The nadic imide chains are extended by imidization reactions with BTDE and MDA as the temperature is increased. Chains are terminated by reacting with any

NE left in solution or by reacting with a nadic imide unit. The result of this type of reaction sequence is that some very short chains will be crosslinked with some long chains.

Dr. Lauver reported kinetic data showing that two distinct stages of imidization exist.⁵ In his experiment he determined the fraction of polymer imidized by assuming that the concentration of imide groups formed is directly proportional to the absorbance observed at 1370cm^{-1} in an IR spectra. Dr. Lauver did not have an explanation for his results but his data does corroborate the work performed in Dr. Kranbuehl's laboratory.

^{13}C -NMR studies conducted in Dr. Kranbuehl's laboratory clearly indicate that complete imidization is favored over a stepwise order of forming an amide then an imide.³ Data showed that the amide may be formed as an intermediate but that no appreciable build up in the concentration of the amide is observed. The quick formation of the imide is expected because 5 membered rings are favored by entropy. Figure Chem 2 is the incorrect reaction sequence published in the earlier literature. Figure Chem 3 reports the corrected mechanism used to form an imide with NE and MDA. Imides formed with BTDE and MDA react by the same mechanism.

^{13}C -NMR studies have also shown that BTDE and NE hydrolyze in the presence of moisture.⁴ Dielectric

studies show that the diacid of NE and the tetraacid of BTDE react faster than the esters.⁴ Figure Chem 4 illustrates the reaction.

It is presumed that a retro-Diels Alder reaction is the rate limiting step for the crosslinking reaction.⁵ Figure Chem 5 provides an illustration.

From the above information it can be said that the storage and handling history of the monomer reactant mixture can affect the polyimide which is formed. If the monomer mixture is allowed to sit at room temperature for more than a few hours, most of the endcapping monomer (NE) will react, forming bisnadimide. The end result of having several short chains of bisnadimide is that extremely long chains of the polyimide will be formed on the free nadic imide. A crosslinked matrix of this composition would be different from one prepared by curing the monomer mixture straight from the freezer. If the monomer mixture is stored in a humid environment a similar result as the above can be expected. To obtain reproducible results in the processing and thermo-oxidative properties of the polyimide resin the monomer reactants must be stored in a cold, dry environment.

Visual Temperature Experiment

A sample of the monomer mixture prepared at General Electric was poured into an aluminum foil weighing pan and was heated. The objective of the experiment was to see the physical changes the monomer mixture experiences as it is cured to its final state of a polyimide thermoset.

<u>Temperature</u>	<u>Appearance</u>
25 C	Viscous, brown solution.
63 C	Bubbles formed.
74 C	Rapid boiling due to methanol evaporating.
98 C	Large bubbles formed. Solution is thicker and can hold air bubbles.
120 C	Solution is much thicker. Rod sticks to solution when pricked.
155 C	No bubbling is visible.
192 C	Solution is hard and powdery.
225 C	Resin has softened.
253 C	Resin is spongy.
288 C	Resin begins to set up.
301 C	Resin is hard.
>301 C	Resin is hard.

Figure Chem 1

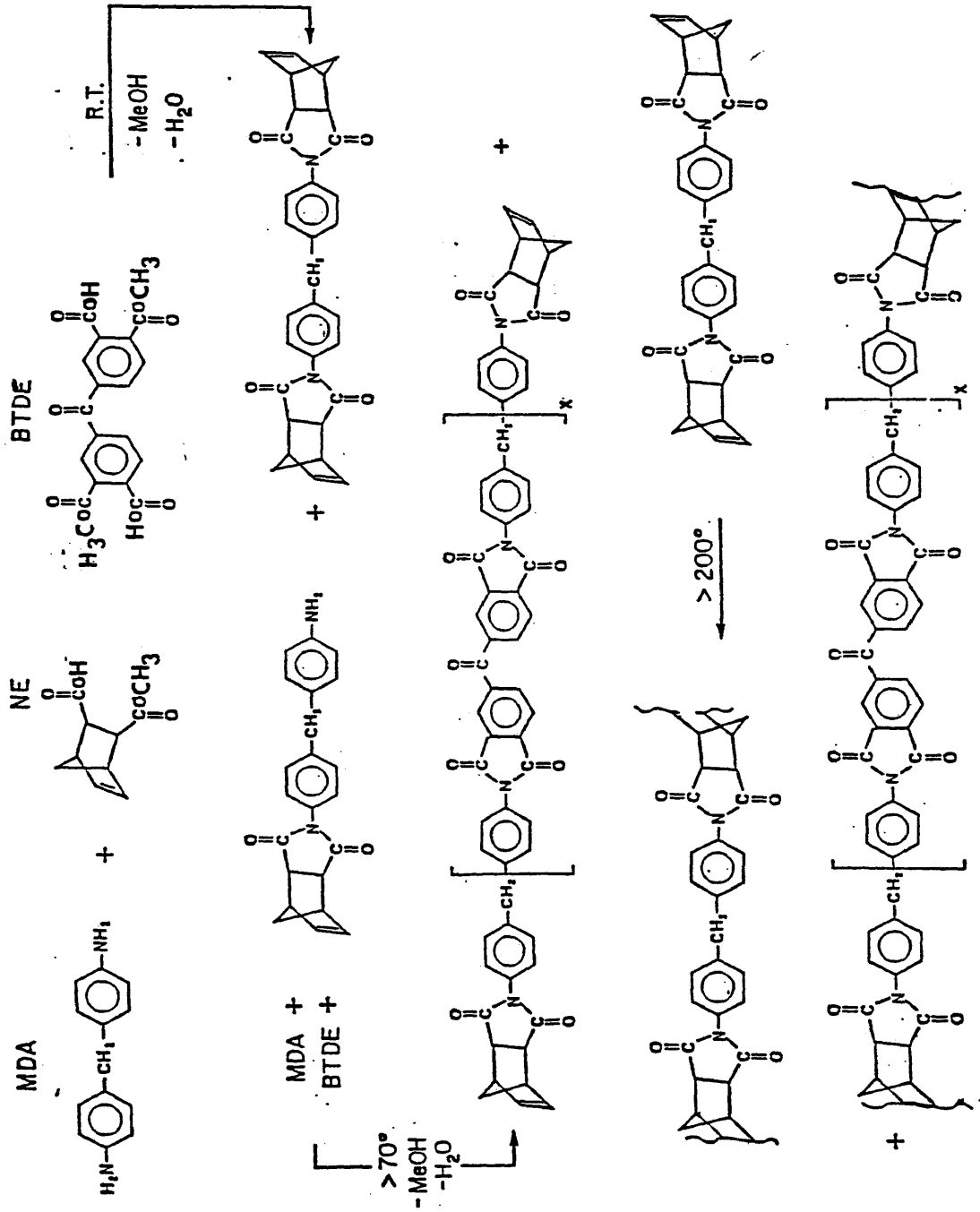


Figure Chem 2

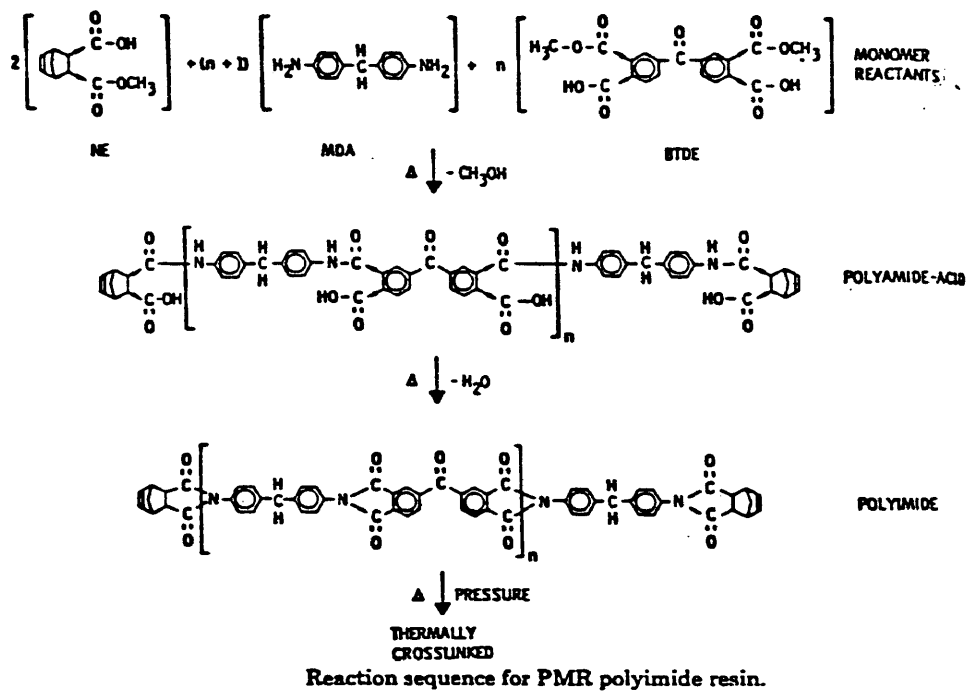


Figure Chem 4

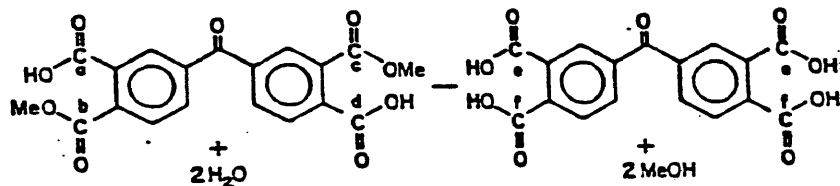


Figure Chem 5

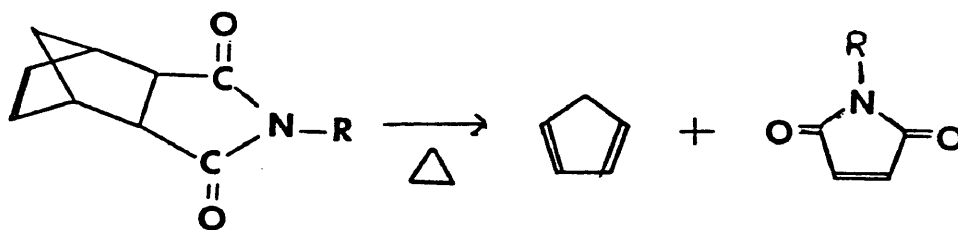
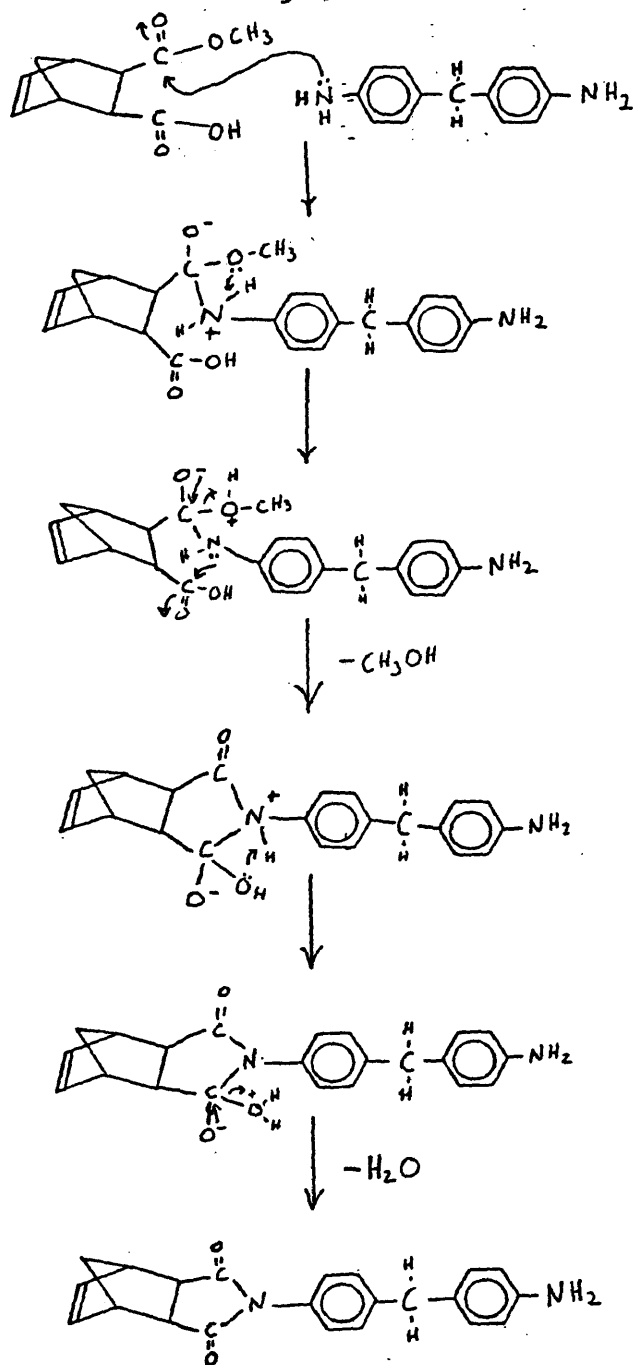


Figure Chem 3



NOTES FOR CHAPTER I

1. Tito T. Serafini, "Resins for Aerospace," The American Chemical Society, New York, N.Y., 1980.
2. R. W. Lauver, W. B. Alson, and R. D. Vanucci, NASA-TM-79063, (N79-16921) (1979).
3. S. E. Delos, R. K. Schellenberg, J. E. Smedley, and D. E. Kranbuehl, J. Ap. Poly. Sci., 27, 4295 (1982).
4. D. E. Kranbuehl, S. E. Delos, E. C. Yi, and J .T. Mayer, Proc. of the 2nd Intl. Conf. on Polyimides, 469 (1985).
5. Richard W. Lauver, J. Poly. Sci., 17, 2529 (1979).

CHAPTER II

Introduction to Dynamic Dielectric Analysis

Dynamic Dielectric Analysis (DDA) is a method of electronically monitoring the cure reaction of polymer systems. DDA provides the benefits of being nondestructive to the sample, and of continuous monitoring during all transitions of the cure reaction. It is possible to determine the extent of reaction, end of cure, and fluctuations in viscosity with DDA.

A dielectric is an insulating material. Dielectric dispersion is the phenomenon which occurs when the dielectric is placed between the parallel plates of a capacitor and subjected to an alternating electric field. Peter Debye demonstrated that a relationship exists between the movement of dipoles and an alternating electric current.¹ Our laboratory measures dielectric properties over a frequency range of six decades. The goal for using DDA is to relate the chemistry of the cure cycle to the dielectric properties of the polymer system by correlating the time, temperature, and frequency dependent dielectric measurements with chemical characterization measurements.²

Dielectric studies have been reported on the aromatic thermosetting polyimide and on similar resin systems.^{3,4} The objective of this section is to report the work I completed using DDA.

Dipole Moments

It is necessary to first review some basic physical chemistry and electronic concepts which apply to DDA before analyzing data. Excellent physical chemistry developments for DDA theory have been reported.^{2,5,6,7,8} A good electronic development for DDA theory has been reported.⁹ My theoretical development will be similar to the references.

A dipole moment in a molecule is the sum of the distances (d) separating all positive and negative charges (+q,-q) multiplied by the charge. A molecule which has a point charge representing all the positive charges located in a different place than the point charge representing all the negative charges is said to have a permanent dipole. A nonpolar molecule has the positive and negative point charges located in the same place. The dipole moment can be represented by,

$$\mu = q \cdot d$$

where,

μ =the dipole moment

q =the charge

d =the distance between charges

The dipole moment of a polymer is the vector sum of the moments of the monomer units,

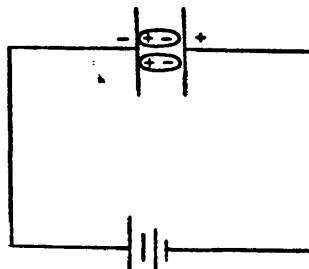
$$\vec{\mu} = q \cdot \vec{d}$$

Only an average moment for a polymer can be determined. The configuration of the molecule is dependent on temperature and molecular environment.⁵

Polarization

Polarization is the process of moving charges a short distance apart within a molecule. This operation is performed by placing the dielectric between the plates of capacitor and applying an electric current. All charges in the capacitor attempt to align themselves with the field created by the current. Positive charges line up on the negatively charged plate and negative charges line up on the positively charged plate. Figure DDA 1 illustrates the phenomena.

Fig. DDA 1



There are three types of polarizations that are experienced by a dielectric. Electronic Polarization (P_e) is introduced when the electrons in a molecule are moved

toward the positive plate of a capacitor. Atomic Polarization (P_a) involves displacement of nuclei and is characterized by bond angles and bond lengths being altered. Orientation Polarization (P_o) is the result of a permanent dipole in the chemical structure of the molecule favoring orientations parallel to the applied field.

The total polarization (P) of a molecule equals the sum of the three polarizations,

$$P = P_e + P_a + P_o.$$

P_e and P_a are referred to as distortion polarizations because they involve a distortion of the normal molecular structure. Temperature has little effect on distortion polarizations. P_o is temperature dependent. An increase in thermal energy causes molecules to move and resist alignment with the electric field.

When a dielectric is viscous, charges can move freely to the oppositely charged plates. When a polymer is cured or "set", charges can move only a short distance. Movement of charges from one side of the capacitor to the other is termed the "ionic response". Charges constrained to move only a short distance are equivalent to creating a dipole and are therefore termed a "dipolar response".

Permittivity

Continuing with the idea of a capacitor and the dielectric being the media between the plates, consider

the consequences of a potential difference. When a potential (V) is applied across the plates of an empty capacitor, the capacitance is,

$$C_o = \frac{Q}{V}$$

where, Q = the charge on the plates

If a dielectric is present the polarization adds to the charge. The capacitance now is,

$$C = (Q + P)/V$$

The static relative permittivity also known as the dielectric constant is the ratio of the capacitances.

$$\epsilon_o = \frac{C}{C_o}$$

The dielectric constant can be related to the total induced polarization,⁵

$$\epsilon_o = 1 + 4\pi P/\epsilon E$$

where ϵ is a constant which depends on units.

Each molecule in the material has its own set of polarizabilities which are directly related to the electronic, atomic, and dipolar contributions. The total polarizability is related to its components in the same way the total polarization is,

$$\alpha_T = \alpha_e + \alpha_a + \alpha_d$$

The polarizabilities of a molecule are a function of the applied field.⁵ As a field changes sinusoidally, the orientation and distortion polarizations try to follow the field in terms of orientation. At low frequencies, the molecule can flip and vibrate back and forth as the plates

charge changes from positive to negative. If the frequency is increased to around 10^{12} cycles per second permanent dipoles cannot orient themselves fast enough. The orientation polarizability factor ϵ' appears thus decreasing the permittivity. The atomic polarization ceases to be a factor in the infrared region of the spectrum and the electronic polarization drops out in the X-ray region of the spectrum. The fall in permittivity is called dielectric dispersion. Our measurements are made in the Hz to MHz region where orientation dispersions for polymers usually occur.

We are concerned with the relationships of $V(t)$, $Q(t)$, and $I(t)$ for different materials in sinusoidal fields. "It is a feature of dielectric relaxation that these relationships obey the same mathematical formalism as the relationship of $V(t)$, $Q(t)$, and $I(t)$ for electric circuits".⁹ Circuits composed of resistors and capacitors can be used to represent or model the dielectric material.

The theory of dielectric relaxation relates the lag in dipole orientation to the changing direction of the alternating electric field. When the frequency of the field is large the polarization acquires a loss component out of phase with the field and a conductance component in phase with the field. The loss component is the thermal dissipation of energy. The permittivity of a material is therefore a complex variable and is indicated by,

$$\epsilon^* = \epsilon' - i\epsilon''$$

Basic Electronics to Solve Complex Variable Components

Our experiment is composed of a dielectric placed between the plates of a capacitor. We want to report data on the intrinsic property of the material known as complex permittivity. To accomplish this task we use the theories proposed by Debye.

Peter Debye demonstrated that there is a relationship between the movement of dipoles with an alternating current and the electrical responses which can be measured from a series circuit consisting of a capacitor and a resistor.



Electric current results from movement of electric charge. Alternating current refers to a current which varies sinusoidally with time.

$$\epsilon = \epsilon_0 \sin \omega t = \epsilon_0 \sin 2\pi f t$$

where, ω = angular frequency in radians.

Radians and degrees can be quickly interconverted by the relation,

$$1 \text{ Radian} = \frac{360^\circ}{2\pi}$$

A Resistor has a potential difference (V) and a current (I) which are "in phase".

$$V = V_m \sin(\omega t + \theta)$$

$$I = I_m \sin(\omega t + \theta)$$

Figure DDA 2 shows a graphical demonstration of the "in phase" relationship. Here θ is the starting point and is assumed to be zero. Figure DDA 3 is a resistive circuit.

Fig. DDA 2

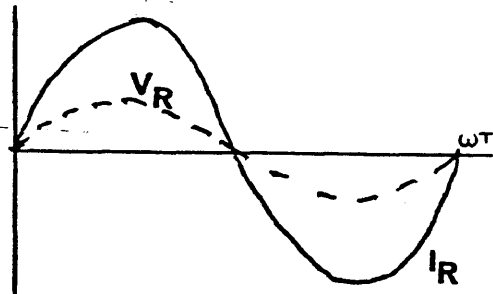
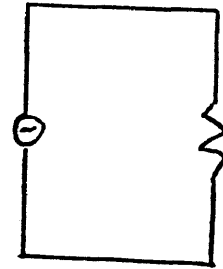


Fig. DDA 3



If,

$$V = \epsilon_0 \sin \omega t$$

and,

$$V = I \cdot R \quad (\text{Ohm's Law})$$

Then,

$$I = \frac{\epsilon_0}{R} \sin \omega t$$

A capacitor will have V and I ninety degrees "out of phase".

$$V = \epsilon_0 \sin \omega t$$

where the voltage across a capacitor is,

$$V = \frac{q}{C}$$

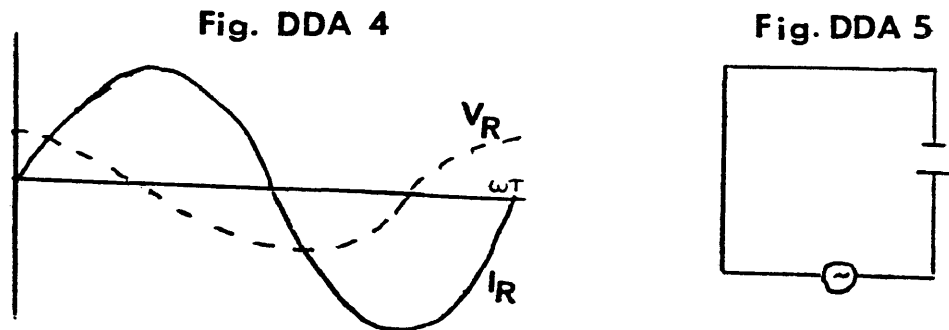
where,

$$q = \epsilon_0 C \sin \omega t$$

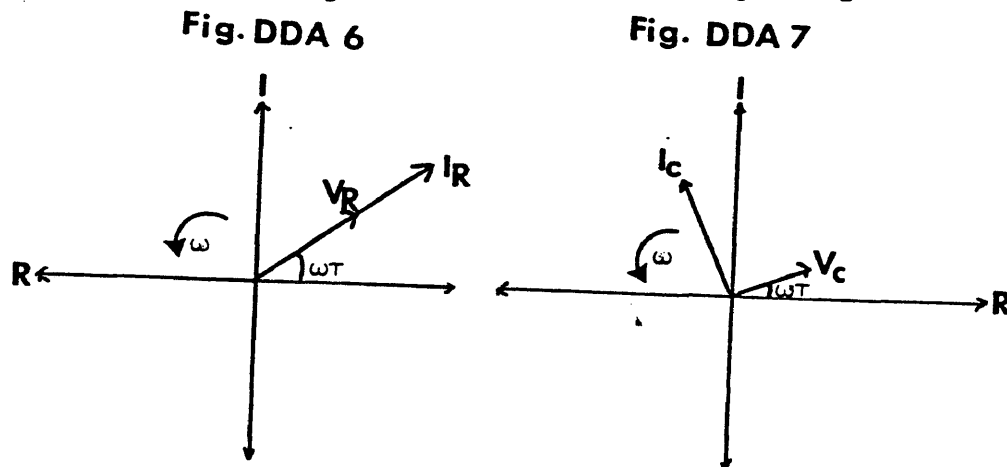
therefore,

$$I = \frac{dq}{dt} = \omega \epsilon_0 C \cos \omega t$$

Figure DDA 4 is a graphical representation of the "out of phase" relationship. Figure DDA 5 is a capacitive circuit.



It is easiest to analyze a circuit in the frequency domain instead of the time domain because only complex algebra is required for interpretation. We can represent the sinusoidal V and I as a "Phasor" diagram in the complex plane. Figure DDA 6 is a phasor diagram of a resistor and figure DDA 7 is a phasor diagram of a capacitor. Both diagrams are in the complex plane.



In the above diagrams,

$$V_R = V_C = \epsilon_0$$

$$I_R = \epsilon_0 / R$$

$$I_C = \omega \epsilon_0 C$$

It is important to note from the diagrams that the vectors V_R , V_C , I_R , and I_C are the maximum values from the sinusoidal curves and that ωt is the phase angle. It is also shown that I_C is ninety degrees out of phase from V_C .

We do not measure the voltage and current of a resistor and a capacitor. This is merely a mathematical representation or equivalent model of our material which was stated earlier. We measure an input current phasor I and an input voltage phasor V . From V and I an impedance (Z) is calculated in ohms.

$$Z = \frac{V}{I}$$

I am going to introduce the term "reactance" (X_C).

$$X_C = \frac{1}{C}$$

Therefore,

$$I_C = \left(\frac{E_0}{X_C} \right)$$

and,

$$V_C = I_C \cdot X_C$$

For all circuits,

$$Z = R + iX$$

Where R equals the the real part and is the resistance part of the circuit, and X equals the imaginary part and is the reactance part of the circuit. The impedance can be expressed in polar form,

$$Z = \sqrt{R^2 + X^2} \angle \tan^{-1} \left(\frac{X}{R} \right)$$

$|Z|$ =the magnitude of impedance

$$\tan^{-1}\left(\frac{X}{R}\right) = \text{the angle of impedance}$$

The reactance determines the angle by which the voltage leads the current. A negative angle is a capacitive circuit.

We also measure admittance (Y).

$$Y = \frac{1}{Z}$$

where,

$$I = YV$$

The admittance of a resistor is related by ,

$$Y = \frac{1}{R}$$

The admittance of a capacitor is related by,

$$Y = i\omega C$$

Considering conductance and susceptance,

$$Y = G + iB$$

where, G =conductance

B =susceptance

Admittance can be represented in polar form.

$$Y = \sqrt{G^2 + B^2} \angle \tan^{-1}\left(\frac{B}{G}\right)$$

Solving for Complex Components .

For a series circuit containing a true resistance and a true capacitance,

$$Z^* = R + iX$$

or,

$$Z^* = R + \frac{1}{i\omega C_0}$$

But for a capacitive circuit,

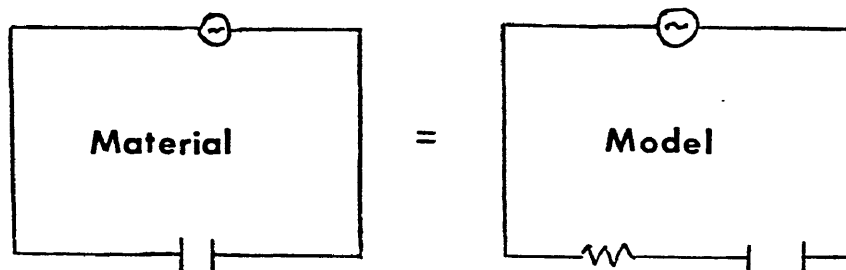
$$Z^* = \frac{1}{i\omega C_0}$$

Where ϵ^* is a complex number composed of resistive and capacitive elements.

$$\epsilon^* = \epsilon' - i\epsilon''$$

If the two circuits are equated as suggested by figure DDA 8 we can solve for the resistive and capacitive components.

Fig. DDA 8



For impedance of capacitor,

$$V = \frac{1}{i\omega(\epsilon' + i\epsilon'')C_0} \cdot I$$

For impedance of a series circuit of a true resistance and a true capacitive element,

$$V = \left(R + \frac{1}{i\omega C} \right) \cdot I$$

We can now solve for the complex equation components,

$$R + \frac{1}{i\omega C} = \frac{1}{i\omega C(\epsilon' - i\epsilon'')}$$

$$\frac{i\omega CR + 1}{i\omega C} = \frac{\epsilon' + i\epsilon''}{i\omega C(\epsilon'^2 + \epsilon''^2)}$$

$$\frac{\epsilon'}{\epsilon'^2 + \epsilon''^2} = 1, \text{ and } \frac{\epsilon''}{\epsilon'^2 + \epsilon''^2} = R\omega C$$

$$\frac{\epsilon''}{\epsilon'} = R\omega C$$

$$\frac{\epsilon'}{\epsilon'^2 \left(1 + \left(\frac{\epsilon''}{\epsilon'} \right)^2 \right)} = \frac{1}{\epsilon' (1 + R^2 \omega^2 C^2)} = 1$$

$$\epsilon' = \frac{1}{1 + R^2 \omega^2 C^2}$$

$$\frac{\epsilon'}{\epsilon''} = \frac{1}{R\omega C}$$

$$\frac{\epsilon''}{\epsilon''^2 \left(1 + \left(\frac{\epsilon'}{\epsilon''} \right)^2 \right)} = \frac{1}{\epsilon'' \left(1 + \frac{1}{R^2 \omega^2 C^2} \right)} = R\omega C$$

$$\epsilon'' = \frac{R\omega C}{1 + R^2 \omega^2 C^2}$$

The above is the electric circuit equivalent of Peter Debye's equations for the real and imaginary components.

ϵ' and ϵ'' can be put into useful electronic terms by inverting the relationship of the complex capacitor to the series circuit of a true resistance and a true capacitance.

$$\frac{1}{R} + i\omega C = i\omega(\epsilon' + i\epsilon'')C_0$$

Remembering conductance is equal to reciprocal resistance.

$$G + i\omega C = i\omega\epsilon' C_0 + i\omega\epsilon'' C_0$$

Therefore,

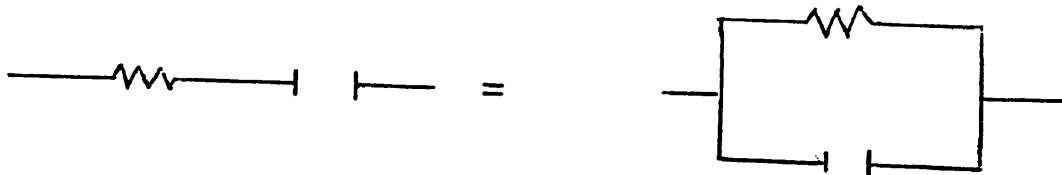
$$\epsilon' = \frac{C}{C_0}$$

and,

$$\epsilon'' = \frac{G}{\omega C_0}$$

Our measurements for impedance and admittance are made on a parallel resistor and capacitor circuit. Debye's equations still apply because a series resistor/capacitor circuit can be equated to a parallel resistor/capacitor circuit. Figure DDA 9 shows the circuit and mathematical equivalency. Our bridge is able to make more sensitive measurements when operating in a parallel mode.

Fig. DDA 9



$$Z = R + iX$$

$$Y = \frac{1}{R+iX} = G + iB$$

The phase angle is the ratio of the capacitive imaginary part of the circuit to the resistive real part.

$$\frac{\epsilon''}{\epsilon'} = \tan\phi$$

This is easily corroborated by remembering,

$$I_R = I_m \sin(\omega t + \phi)$$

$$I_C = I_m \cos(\omega t + \phi)$$

When the resistive component is at time zero,

$$R = A \sin\phi$$

When the capacitive component is at time zero,

$$C = A \cos\phi$$

where,

$$R^2 + C^2 = A^2$$

and,

$$\frac{R}{C} = \tan \phi$$

An important feature of Debye's work is that he found that the components of the complex permittivity were related to dielectric relaxation. It was found that,

$$\epsilon' = \frac{\epsilon_0 \epsilon_\infty}{(1 + \omega^2 \tau^2)} + \epsilon_\infty$$

$$\epsilon'' = \frac{(\epsilon_0 - \epsilon_\infty) \omega \tau}{1 + \omega^2 \tau^2}$$

$$\tan \phi = \frac{\epsilon_0 \epsilon_\infty \omega \tau}{\epsilon_0 \epsilon_\infty \omega^2 \tau^2}$$

where, τ = the dielectric relaxation time
 ϵ_0 = the limiting low frequency value
 ϵ_∞ = the limiting high frequency value

These equations are referred to as the Debye equations. Herbert Frohlich presents an excellent derivation of these equations in Theory of Dielectrics.⁶

The primary assumption is that polarization decreases exponentially with time after an electric field is removed from a dielectric. The relaxation time is the time necessary for the polarization to decay to (1/e) times the polarization equilibrium. It can be said that, "The rate of rotational diffusion of the polar moments is characterized by the relaxation time τ ".² Except in the

pure systems of small molecules, a distribution of relaxation times exists because different polar groups have different relaxation times and intermolecular forces which can effect motion of dipoles.

A Cole-Davidson distribution parameter is added to the complex permittivity components because the polymer has a mixture of relaxation times. Remember different molecules have different dipoles and therefore different relaxation times. The distribution parameter also reflects the extent to which the motion of dipoles are correlated with one another and is therefore a function of intermolecular forces.²

$$\begin{aligned} \epsilon' &= \frac{\epsilon_0 - \epsilon_\infty}{(1 + \omega^2 \tau^2)^\beta} + \epsilon_\infty \\ \epsilon'' &= \frac{(\epsilon_0 - \epsilon_\infty) (\omega \tau)^\beta}{(1 + \omega^2 \tau^2)^\beta} \end{aligned} \quad 0 < \beta < 1$$

One can see from figure DDA 10 that the β parameter broadens the dielectric dispersion region. Note from figure DDA 10 that the inflection of ϵ' and the maximum of ϵ'' occur when $\omega = \frac{1}{\tau}$. The area around $\omega = \frac{1}{\tau}$ is the dielectric dispersion region. The permittivity decreases in the dielectric dispersion region.

Actually, the real and the imaginary components of the complex permittivity have a dipolar and an ionic component.⁵

$$\epsilon'' = \epsilon''_d + \epsilon''_i$$

$$\epsilon' = \epsilon'_d + \epsilon'_i$$

The dipolar components are given by the Cole-Davidson adjusted Debye equations.

$$\epsilon'_d = \frac{\epsilon_0 - \epsilon_\infty}{(1 + \omega^2 \tau^2)^\beta} + \epsilon_\infty$$

$$\epsilon''_d = \frac{(\epsilon_0 - \epsilon_\infty) (\omega \tau)^\beta}{(1 + \omega^2 \tau^2)^\beta}$$

Johnson and Cole derived empirical equations for the ionic contribution to complex permittivity.¹⁰

$$\epsilon'_i = C_o Z_o \sin\left(\frac{n\pi}{2}\right) \omega^{-(n+1)} \left(\frac{\sigma}{8.85 \cdot 10^{-14}}\right)$$

$$\epsilon''_i = \frac{\sigma}{8.85 \cdot 10^{-14} \omega} - C_o Z_o \cos\left(\frac{n\pi}{2}\right) \omega^{-(n+1)} \left(\frac{\sigma}{8.85 \cdot 10^{-14}}\right)^2$$

where, σ = conductivity in $\text{ohm}^{-1} \text{cm}^{-1}$

Z^* = electrode impedance induced by ions

$$0 \leq n \leq 1$$

"The first term in ϵ'_i is due to the conductance of ions translating through the medium. The second term is due to electrode polarization effects. The second term becomes increasingly significant as the frequency of measurement is decreased."¹¹

DDA Experimental

Dr. Kranbuehl's laboratory has assembled the equipment necessary to conduct dielectric experiments. They developed and published the method used to acquire and analyze data which I used for this report.

"Dynamic dielectric measurements were made using a HewlettPackard 4192A LF Impedance Analyzer controlled by a 9826 HewlettPackard computer. The resin was cured in a 3" mold placed between thermostated heating plates. The time-temperature profile of the mold was controlled by a program in the computer. The lay-up consisted of a number of layers of Kapton to insulate the probe from the metal mold, a probe which can be inserted directly between layers of polymer resin and further layers of Kapton between this and the mold top. An iron constantan thermocouple was attached directly to the mold and the temperature measured by a Keithley 179 TRMS Digital Multimeter. Measurements of capacitance (C) and conductance (G) at frequencies from 5 to $5 \cdot 10^6$ Hz were taken at regular intervals during the cure cycle and stored on a computer disk. The complex permittivity was calculated for each of these measurements. The temperature was also recorded for each measurement. Plots of the results were prepared from the stored data and were plotted using a HewlettPackard 7475A 6 pen plotter."²

Figure DDA 11 illustrates the equipment. Figure DDA 12 illustrates the lay up in the mold. The bleeder plies indicated in figure DDA 12 are providing space for the polymer when it becomes viscous. Thus, the polymer does not ooze out of the mold.

A feathered capacitor developed in Dr. Kranbuehl's laboratory, which is gold sputtered on a low loss

dielectric substrate, is used to make the measurements. The glass, polymer, or ceramic substrate also contributes to the measurements. Because of this effect, we determine gauge constants for each type of probe before they are used in order that the properties of the sensor can be subtracted from the sample data. A constant is determined by scanning the frequencies in air and in CCl_4 . The permittivity of air and CCl_4 are known quantities and from a subtraction the gauge permittivity can be determined.

The bridge measures impedance and admittance. From these measurements the capacitance and conductance can be determined. The capacitance and conductance are used to calculate the complex permittivity.

$$\epsilon^* = \epsilon' - i\epsilon''$$

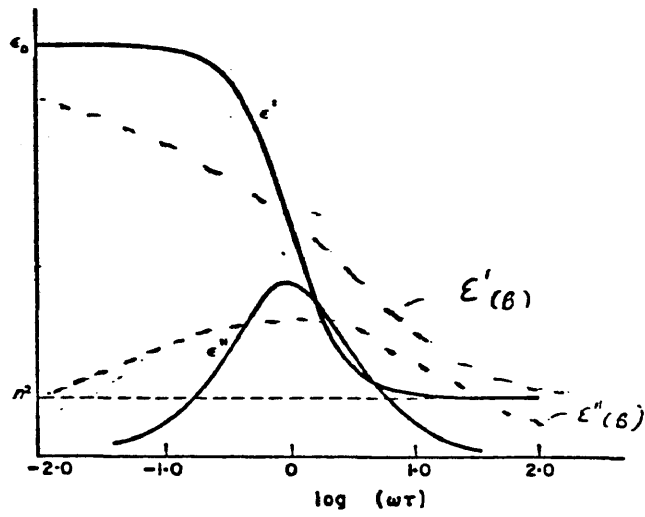
where,

$$\epsilon' = \frac{C}{C_0}$$

$$\epsilon'' = \frac{G}{C_0 2\pi f}$$

and C_0 is the effective air replaceable capacitance of the probe.

Figure DDA 10



ϵ' = Real

ϵ'' = Imaginary

β = Cole-Davidson

Figure DDA 11

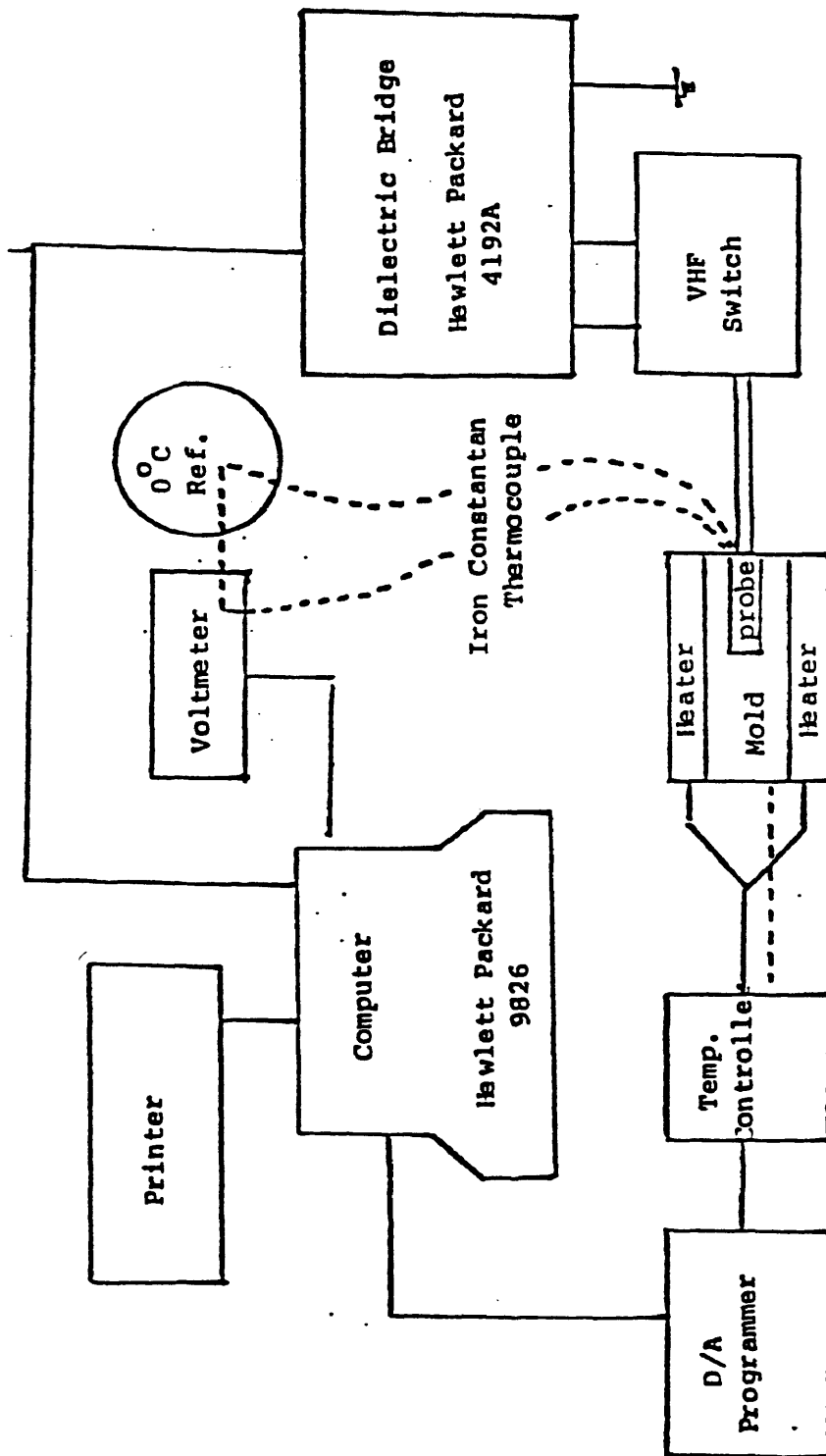
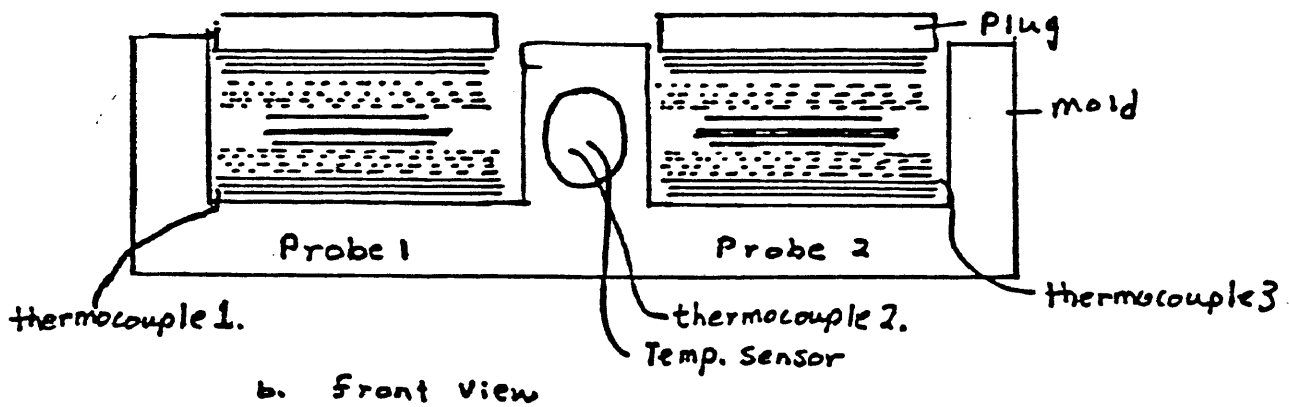
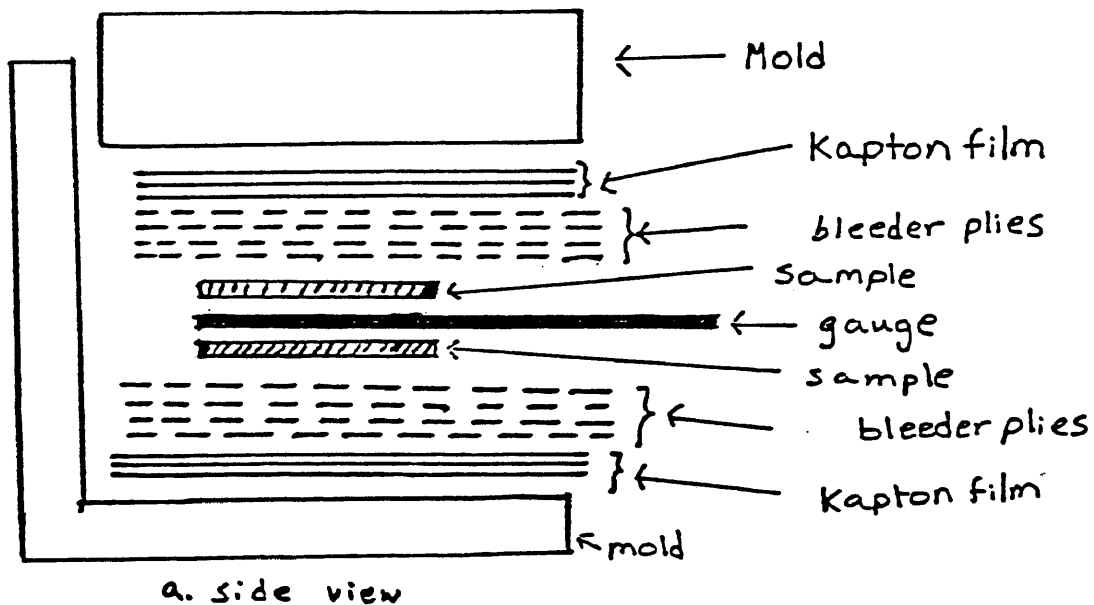


Figure DDA 12



Reproduced from Yi

NOTES FOR CHAPTER II

1. Peter Debye, "Polar Molecules," The Chemical Catalogue Company, Inc., New York, N.Y., 1929.
2. D. Kranbuehl, S. Delos, E. Yi, J. Mayer, and T. Jarvie, Proc. of the Soc. of Plastics Eng., (ANTEC) 311(1985).
3. D. E. Kranbuehl, S. E. Delos, and P. K. Jue, SAMPE J., July/August, 18(1983).
4. D. E. Kranbuehl, S. E. Delos, E. C. Yi, and J. T. Mayer, Proc. of 2nd Intl. Conf. on Polyimides, 469(1985).
5. Nora E. Hill, et al, "Dielectric Properties and Molecular Behavior," Van Nostrand Reinhold Co., New York, N.Y., 1969.
6. Herbert Frohlich, "Theory of Dielectrics," Oxford at Clarendon Press, Great Britian, 1958.
7. Eun C. Yi, Undergraduate Honors Thesis, College of William and Mary, 1985.
8. Patricia K. Jue, Undergraduate Honors Thesis, College of William and Mary, 1983.
9. Vera V. Daniel, "Dielectric Relaxation," Academic Press, New York, 1967.
10. J. F. Johnson and R. H. Cole, J. Am. Chem. Soc., 73, 4563(1951).
11. D. Kranbuehl, S. Delos, M.Hoff, and L. Weller, ACS: PMSE, April, 535(1986).

CHAPTER III

Analysis of a Polyimide Cure

The "fresh" polyimide is a sample of the monomer reactant mixture which has been stored in the freezer. The mixture was dried using a rotovap and a vacuum pump to remove excess methanol. The mixture was placed directly on the probe and run on a preprogrammed cure cycle consisting of ramps and holds. A cure cycle which was developed for molding parts which contain the aromatic thermosetting polyimide was used for the dielectric analysis. The cure cycle is a 1.5 C/min. ramp from room temperature to 80 C, a hold at 80 C for 60 minutes, a 1.5 C/min. ramp to 205 C, a hold at 205 C for 40 minutes, a 1.5 C/min. ramp to 255 C, a hold at 254 C for 40 minutes, and finally a 1.5 C/min. ramp to 320 C and a hold at 320 C for 2 hours. Dielectric and temperature data is taken every two and a half minutes.

Plots of $\log \epsilon'$ and $\log \epsilon''$ versus time are shown on figures DDA 15 and DDA 16. The temperature ramp is indicated and it has four plateaus for the holds. The frequencies measured are 5 Hz, 50 Hz, 125 Hz, 250 Hz, 500 Hz, 5 kHz, 25 kHz, 50 kHz, 250 kHz, 500 kHz, 1000 kHz, and 5000 kHz. Figures DDA 15 and DDA 16 show the frequencies

50 Hz, 500 Hz, 5 kHz, 50 kHz, and 500 kHz.

Examination of figures DDA 15 and DDA 16 reveals the frequency dependence is very large at the beginning of the cure cycle, narrows at the gel point ($\gt 100$ C), and remains narrow through the completion of the cure cycle. The fluidity of the system at the start of the cure is reflected in the higher values of ϵ' and ϵ'' at lower frequencies. The values are a measure that shows how well the ions and dipoles can keep up with the alternating current. Higher values imply they can alternate more easily with the current and it is a characteristic of the fluidity of the system.

As the temperature is increased to 80 C the values for ϵ^* increase. The response is expected because the thermal energy put into the system increases the mobility of the ions and dipoles. The values for ϵ' and ϵ'' begin to fall before the 80 C hold. Remembering the visual experiment, this is the point where any excess methanol in the mixture is boiled off. The drop in ϵ' and ϵ'' results from the fact that the mixture becomes less fluid as methanol evaporates.

During the hour hold at 80 C a shoulder appears around the 40 minute mark. This point indicates that the rapid fall of ϵ^* caused by methanol evaporation has ended, and the more moderate decline in ϵ' and ϵ'' due to the formation of nadic imide and bisnadimide has begun. The moderate decline indicates the imidization between NE and

MDA occurs slowly at 80 C.

When the hold at 80 C has ended the values for ϵ' and ϵ'' increase due to an increase in temperature. At about 100 C the values for ϵ' and ϵ'' drop precipitously. At this temperature the BTDE is able to imidize with MDA. The rapid chain extension forms polymers which drastically reduce the mobility of ions and dipoles. The immediate increase in viscosity due to polymer formation is called the gel point. From the visual experiment we know the resin never becomes a liquid at temperatures higher than the gel temperature. All dielectric measurements made after the gel point represent movement of ions and dipoles in the solid or rubbery state.

After the gel point it can be seen that very little information can be obtained from ϵ' . However, ϵ'' does show some frequency dependence at elevated temperatures. During the holds at 205 C, 255 C, and 320 C the dielectric response increases at the beginning of the hold and decreases gradually during the hold. This response is related to the increased mobility of ions and dipoles caused by temperature at the beginning of the hold and decreased mobility caused by imidization reactions in the matrix and by crosslinking of the matrix occurring throughout each hold.

From the above interpretation it can be said that the dielectric method can give useful information. It

describes qualitatively how the resin system is changing during a cure cycle. Dielectric measurements are one of only a few methods of observing the course of a reaction through a liquid and a solid state.

To determine if the dielectric response is ionic or dipolar, plots of $\log \epsilon'$ versus \log frequency ($\log f$) and $\log \epsilon''$ versus $\log f$ are examined. If the dielectric response of the material were due only to dipoles a plot similar to DDA 10 would result. In the purely dipolar Debye response, ϵ' decreases with increasing frequency while ϵ'' goes through a maximum. Figures DDA 17 and DDA 18 exhibit $\log \epsilon'$ versus $\log f$ and $\log \epsilon''$ versus $\log f$ respectively through the imidization reaction. Figures DDA 19 and DDA 20 exhibit $\log \epsilon'$ versus $\log f$ and $\log \epsilon''$ versus $\log f$ respectively at the elevated temperatures. It is important to note that each curve on the figures represents the frequency dependence at a specific time and temperature point during the cure cycle.

Examination of figure DDA 17 shows portions of curves 1-4 have slopes of -1.5. This slope is indicative of diffusion controlled ion migration.¹ As the temperature is increased, the migrating ion effect is displaced to lower frequencies because the formation of nadic amide and bisnadimide make the solution more viscous. Curves 5 and 6 occur at the end of the 80 C hold which is the gel point of the polymer. No diffusion controlled ion migration is

observed in curves 5 and 6, nor at any point in the cure cycle at a higher temperature.

Examination of figure DDA 18 shows portions of all six curves have slopes of -1. This type of slope is indicative of the phenomenon known as ionic transport. Sometimes ionic transport is called d.c. conductivity. The phenomenon occurs when the conductance of a material is independent of frequency. Remember,

$$\epsilon'' = \frac{G}{\omega C_0}$$

therefore,

$$\log \epsilon'' = -1 \cdot \log \omega + \log \frac{G}{C_0}$$

As the resin gels, the ionic transport effect is displaced to lower frequencies or longer times because the ions are slowed by an increasingly viscous medium. Deviations from linearity at the higher frequencies in curves 4-6 are also due to the inability to translate freely in a viscous medium. Beyond the gel point ions are confined to localized motions.

Curves 1-3 have deviations from a slope of -1 at low frequencies due to electrode polarization effects.² At these temperatures the resin is fluid enough to allow build up of ions at the electrodes within the measurement time. This phenomenon has also been called the double layer effect for obvious reasons.

Figures DDA 19 and DDA 20 illustrate the log-log plots at elevated temperatures. Curves 1 and 2 occur at the

beginning and end of the first hold. Curves 3 and 4 occur at the beginning and end of the second hold. Curves 5 and 6 occur at the beginning and end of the last hold.

Examination of figure DDA 19 leads to the conclusion that ϵ' for the polyimide is not very frequency dependent at elevated temperatures. Examination of figure DDA 20 demonstrates the dielectric signal is larger at lower frequencies for higher temperatures.

The dispersions at elevated temperatures could be the result of dipoles in the resin matrix. The dispersions at elevated temperatures could be due to localized "hole hopping" which occurs in solid state matrixes.³

Master curves for the aromatic thermosetting polyimide using $\log \epsilon'$ versus $\log f$ and $\log \epsilon''$ versus $\log f$ have been constructed from the dielectric data for the entire cure cycle. The plots provide dielectric information over an effective frequency range much broader than any single instrument can provide in the time or frequency domain alone.⁴ It can be assumed that the dielectric response during all stages of the cure is caused by the same processes, because all the curves are superimposeable. Figures DDA 21 and DDA 22 illustrate the curves.

Figure DDA 15

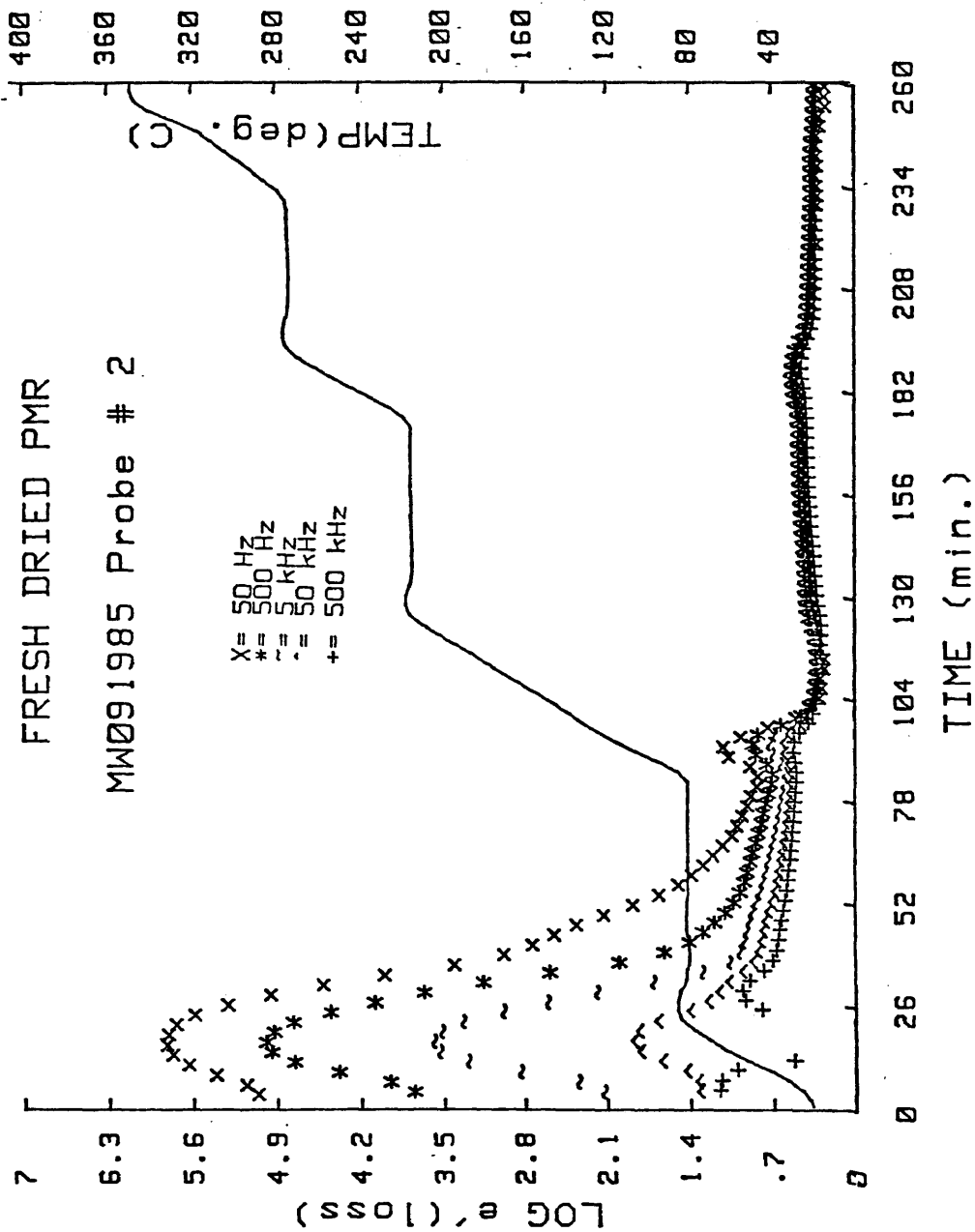


Figure DDA 16

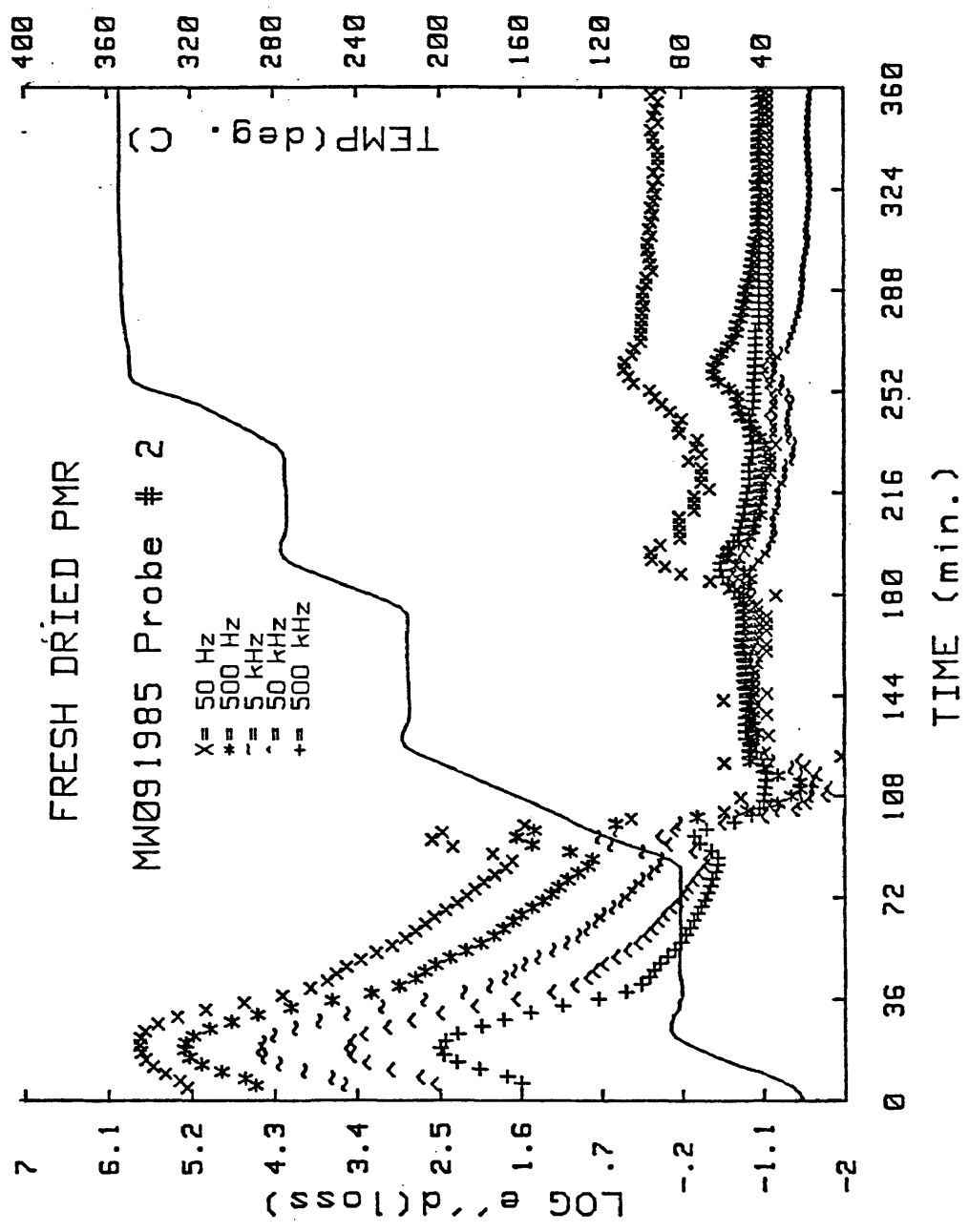


Figure DDA 17.

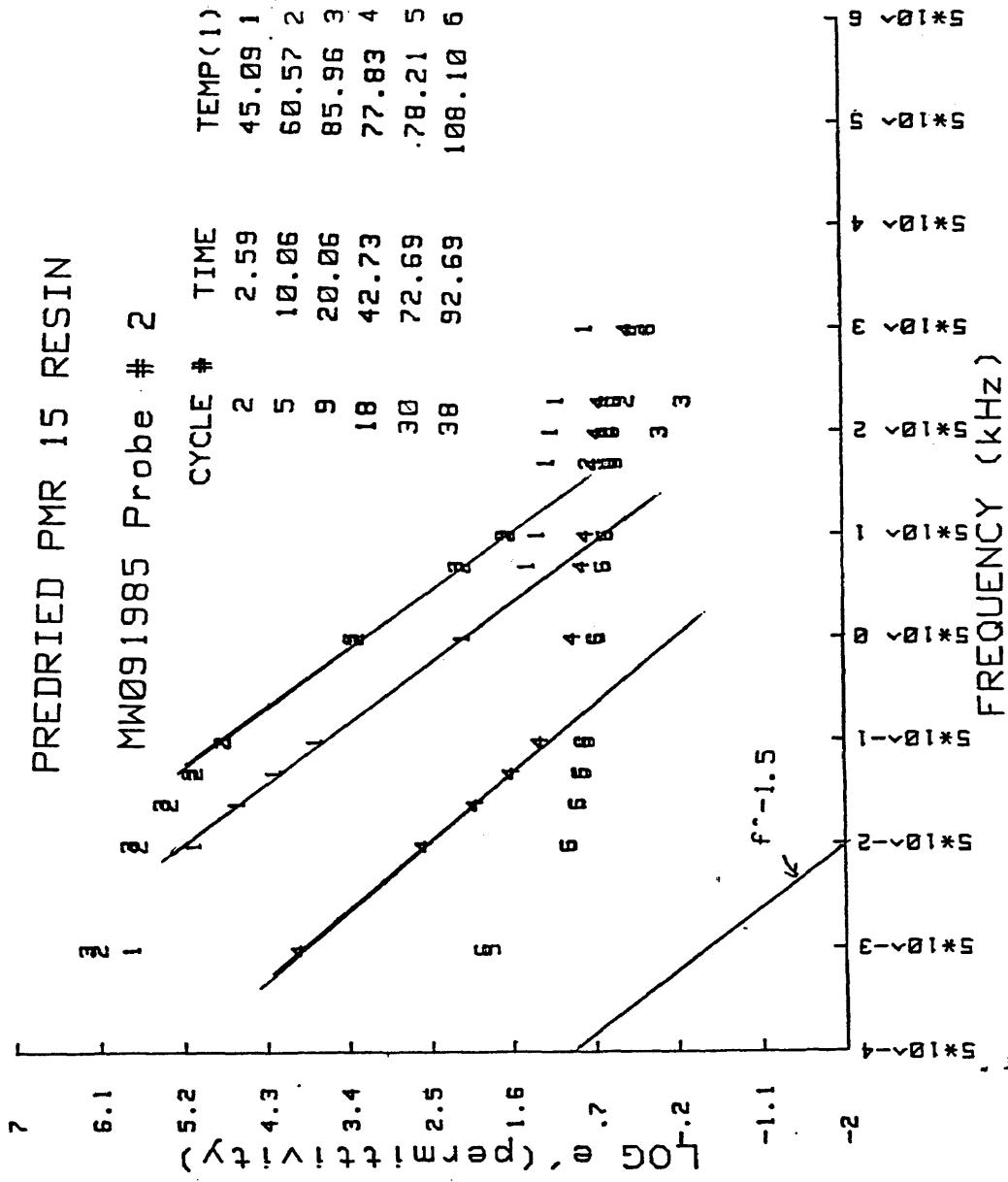


Figure DDA 18

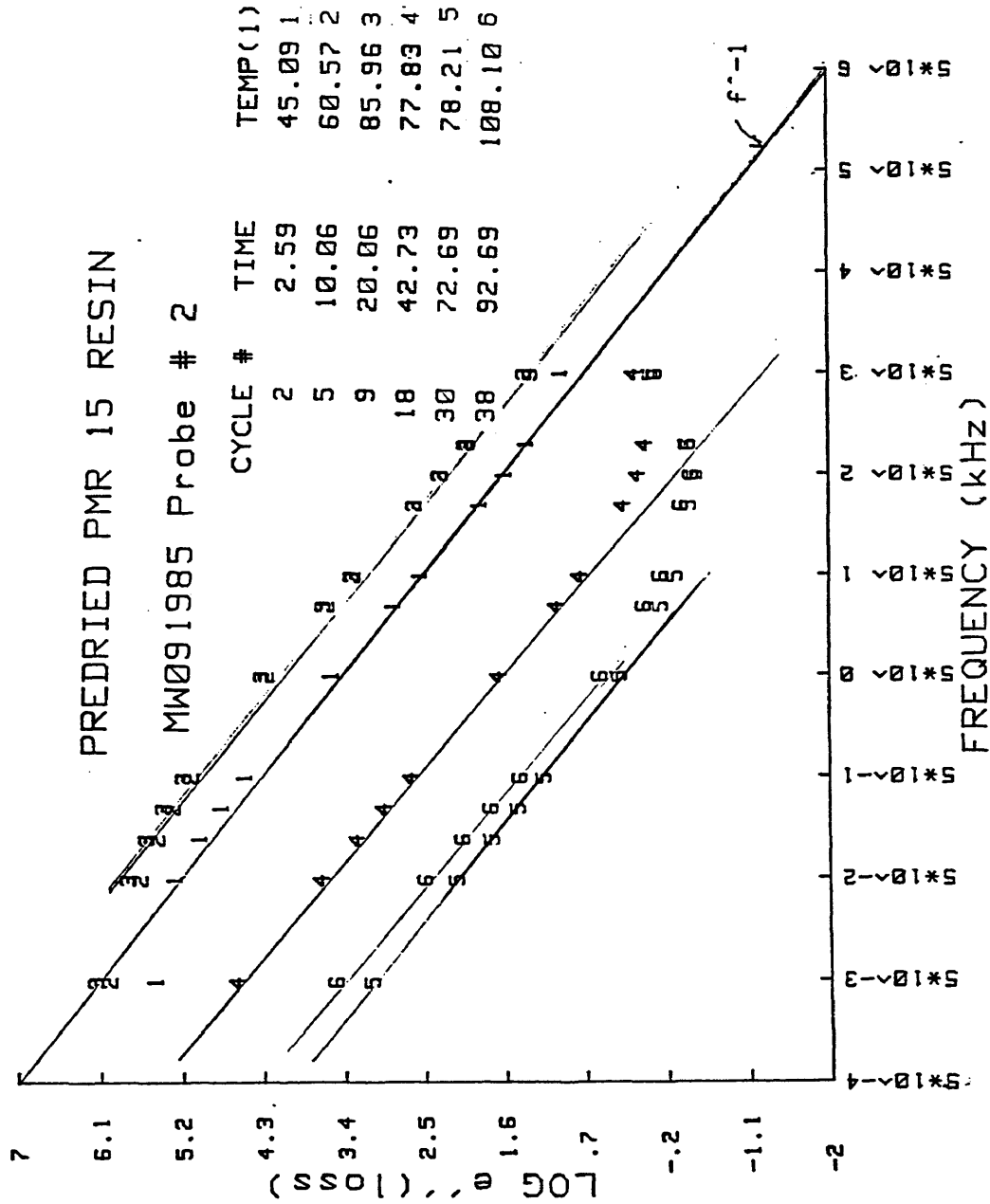


Figure DBA 19

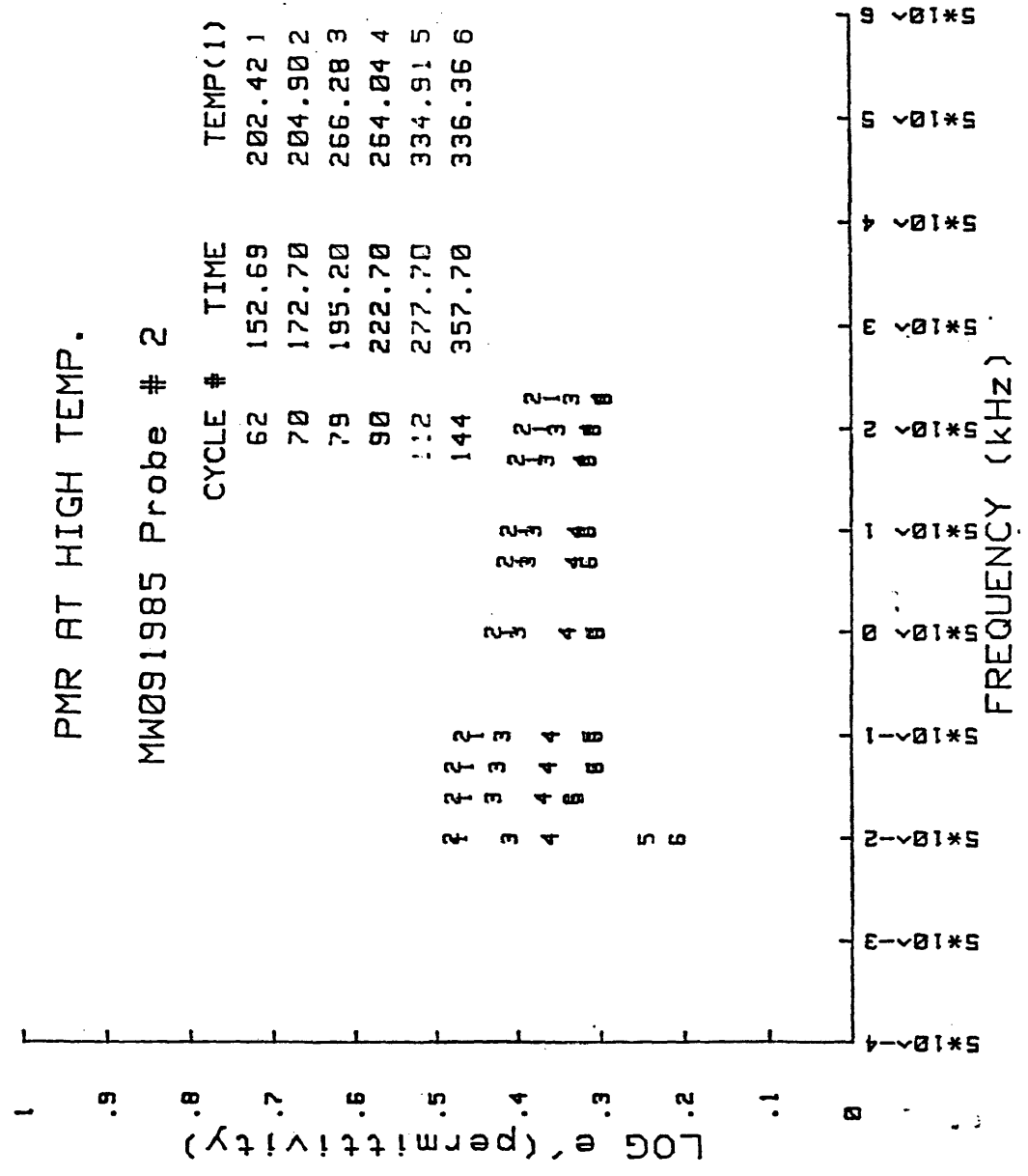


Figure DDA 20

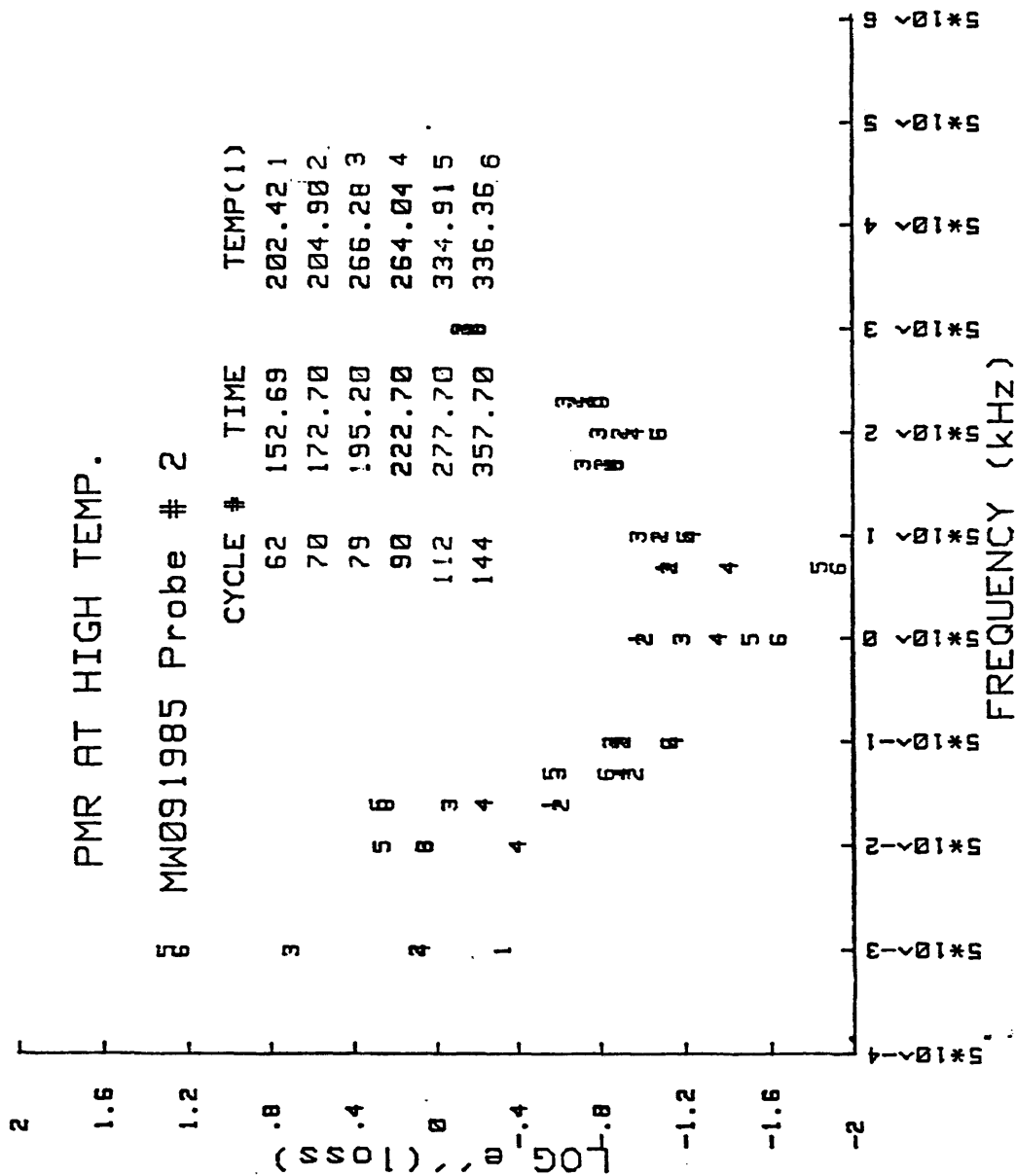
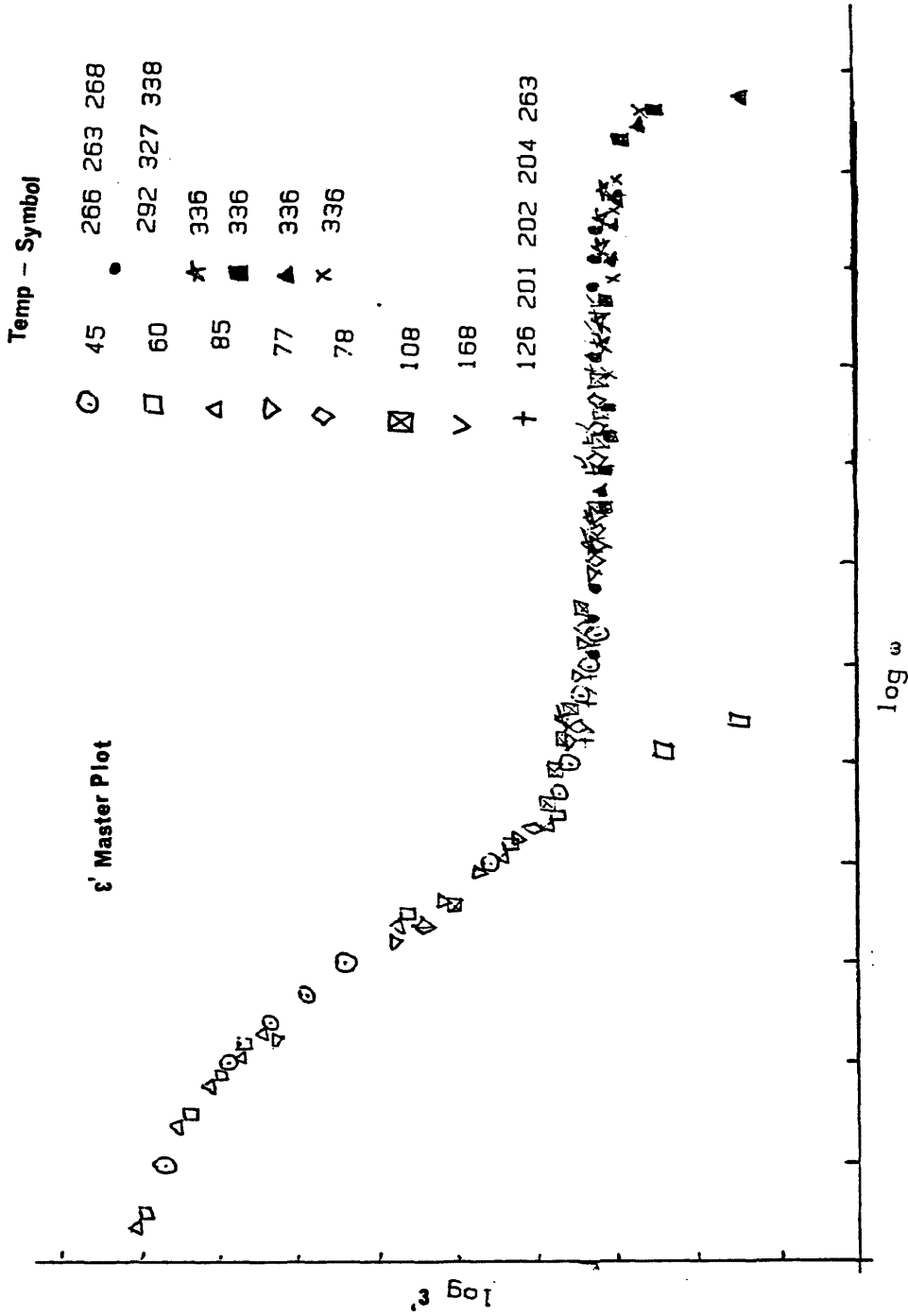
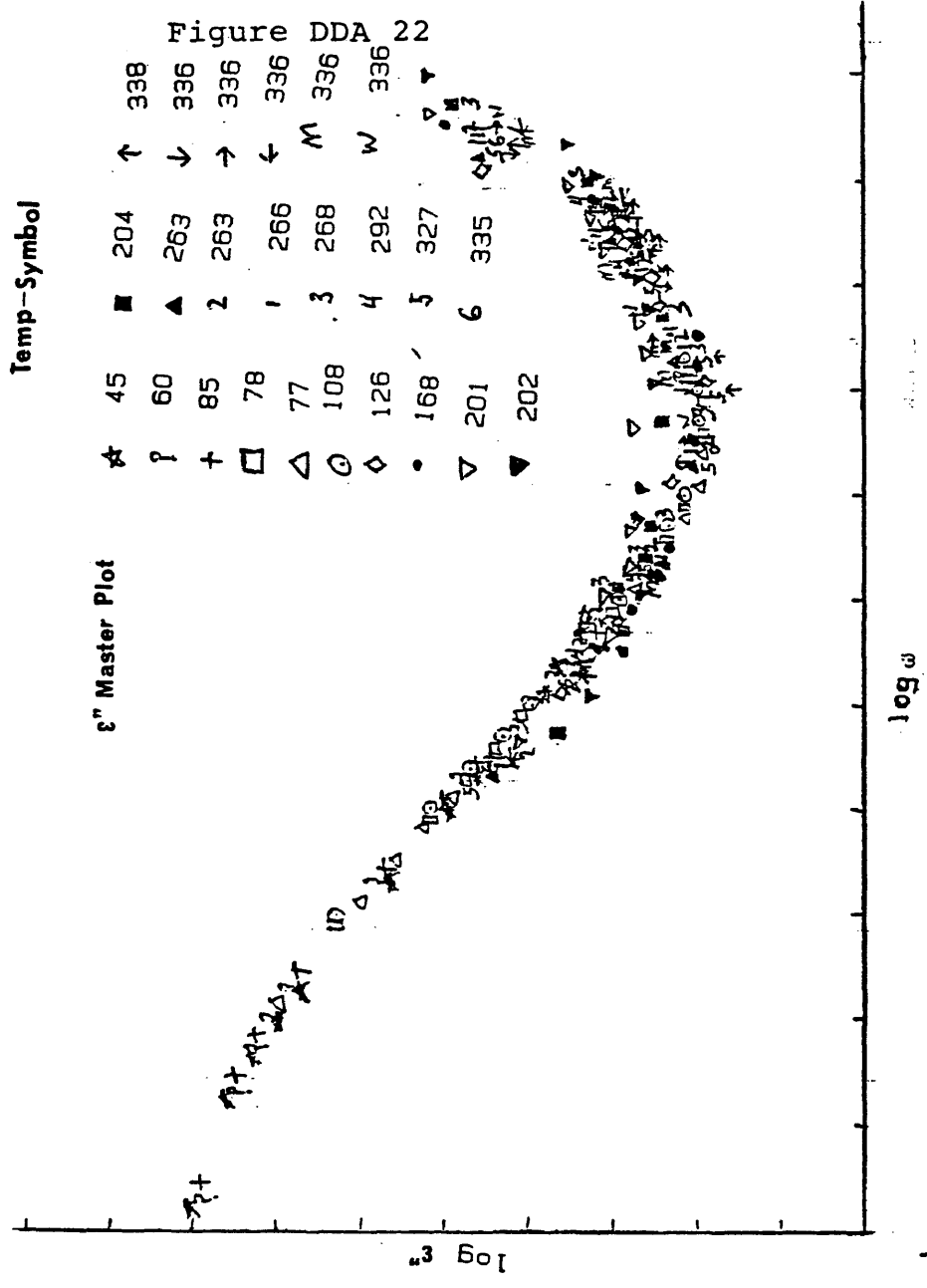


Figure DDA 21





NOTES FOR CHAPTER III

1. S. Uemura, J. Pol. Sci., Pol. Phys. Ed., 12,
1177(1974).
2. D. E. Kranbuehl, S. E. Delos, E. C. Yi, and J. T. Mayer,
Proc. of 2nd Intl. Conf. on Polyimides, 469(1985).
3. T. J. Lewis, "The Dielectric Behavior of Non-crystalline
Solids." in Dielectric and Related Molecular Processes,
V3, Ch. 7, The Chemical Society, London, U.K. (1977).
4. D. Kranbuehl, S. Delos, M. Hoff, and L. Weller,
ACS: PMSE, April, 535(1986).

CHAPTER IV

Ageing Study at 0% and 90% Humidity

Dielectric phenomena are distinctly different for samples of the aromatic thermosetting polyimide which have been exposed to different atmospheric conditions for varying lengths of time. Figures DDA 23 and DDA 24 show the effects of age on the real, ϵ' , response of the resin stored at room temperature with relative humidities of 0% and 90% respectively. Figures DDA 25 and DDA 26 show the effects of age on the complex, ϵ'' , response of the resin stored under the same conditions. All comments to be made in this section will be directed at the imidization region of the reaction. Useful information is difficult to interpret at higher temperatures because of the noise associated with the fresh resin run on Day 0 of the study.

The sample exposed to 0% RH was stored in a dessicator which contained CaCl_2 . The sample exposed to 90% RH was stored in a dessicator which contained a saturated solution of ZnSO_4 . Both dessicators were stored in the lab at room temperature.

The samples stored at 0% RH and 90% RH exhibited visual differences with time. The 0% RH sample became a

lighter brown color with time while the 90% RH sample became a darker brown. The 0% RH solution became powdery and granular resembling sand while the 90% RH sample became hard and brittle resembling a candy stick.

An increase in the viscosity of a sample can be monitored by the decrease with age of the initial values of both ϵ' and ϵ'' .¹ Examination of figures DDA 23-→26 demonstrate that the sample stored at 0% RH becomes more viscous with age than the sample stored at 90% RH. We can expect this result because methanol can be removed from solution by the CaCl_2 drying agent thus causing the 0% RH sample to become much more viscous. CaCl_2 may also remove methanol from the diesters to form anhydrides.

Notice that the point of maximum ϵ' and ϵ'' for the 90% RH sample shifts from occurring before the 80 C hold to occurring during the 80 C hold. It is believed that water replaces methanol as the solvent.¹

The dielectric response of the 90% RH sample is distinctly larger than the dielectric response of the 0% RH sample during the 80 C hold after the fifth day of ageing. This difference is expected because the water in the 90% RH solution makes it more fluid.

During the 80 C hold, the ϵ' and ϵ'' values for the 90% RH increase for the first seven days of exposure while the ϵ' and ϵ'' values for the 0% RH sample decrease for the first seven days of exposure. This dielectric response during

the 80 C hold indicates that the resin increases the amount of water it incorporates as a solvent for at least a week. In the 90% RH sample the frequency plots for days 7, 11, and 19 virtually overlap one another. This dielectric response suggests that there is a maximum amount of water which the resin can incorporate.

At the end of the 80 C hold a distinct difference can be seen in the peak shape for ϵ' and ϵ'' for the two samples. Remember the peak is caused by first an increase in ion mobility due to increased temperature then a decrease due to the BTDE-MDA chain lengthening polymerization. In the 90% RH sample, at later days, the peak appears only as a shoulder. In the 0% RH the peak appears sharp and distinct throughout the length of the study. These results can be attributed to solvent differences. The 90% RH sample has a high dielectric response before the temperature ramp to 205° C because of its fluidity and therefore would not experience a sharp increase due to increased temperature. A similar argument can be made for why the 0% RH sample has a sharp increase. If at later days very little solvent is present, the ion mobility can be expected to be greatly influenced by temperature.

A much sharper drop in the dielectric response of is seen for the sample stored at 90% RH. This can be related to the fact that tetra-acids react faster with MDA than diesters. Earlier in this report it was shown that

BTDE can interact with water to form a tetra-acid.

An interesting sidelight to my ageing study occurred on September 26th, 1985. The reader may recall hurricane Gloria passed through the Tidewater area on that day. Figures DDA 27 and DDA 28 show the dielectric response of ϵ' and ϵ'' for identical ageing studies at 0% RH on day 7. The graphs indicate that moisture from the air may have been incorporated in the resin which was run during the hurricane. Notice that the dielectric response during the 80 C hold is greater for the hurricane day.

Figure DDA 23
 0% PMR AGEING

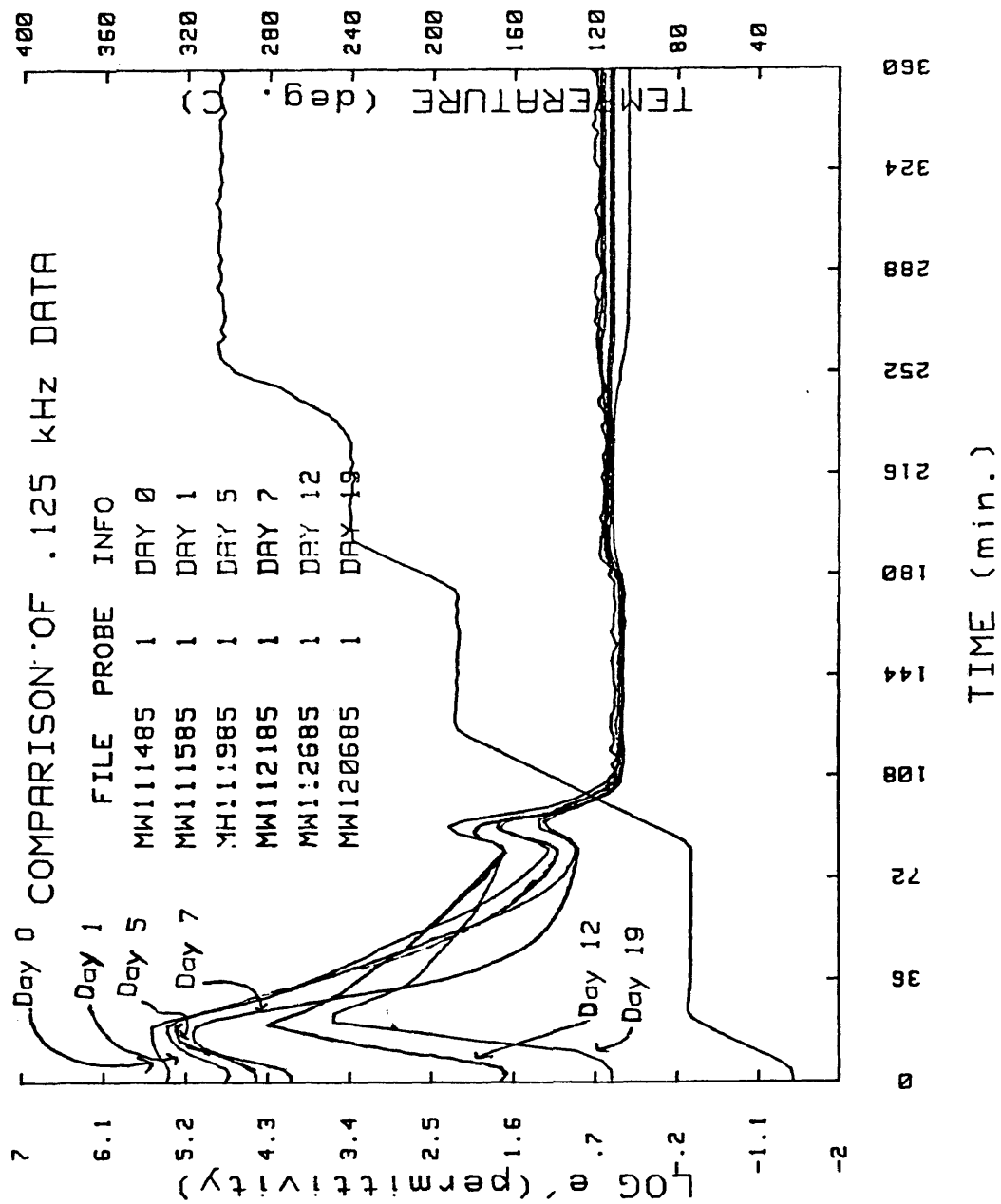


Figure DDA 24

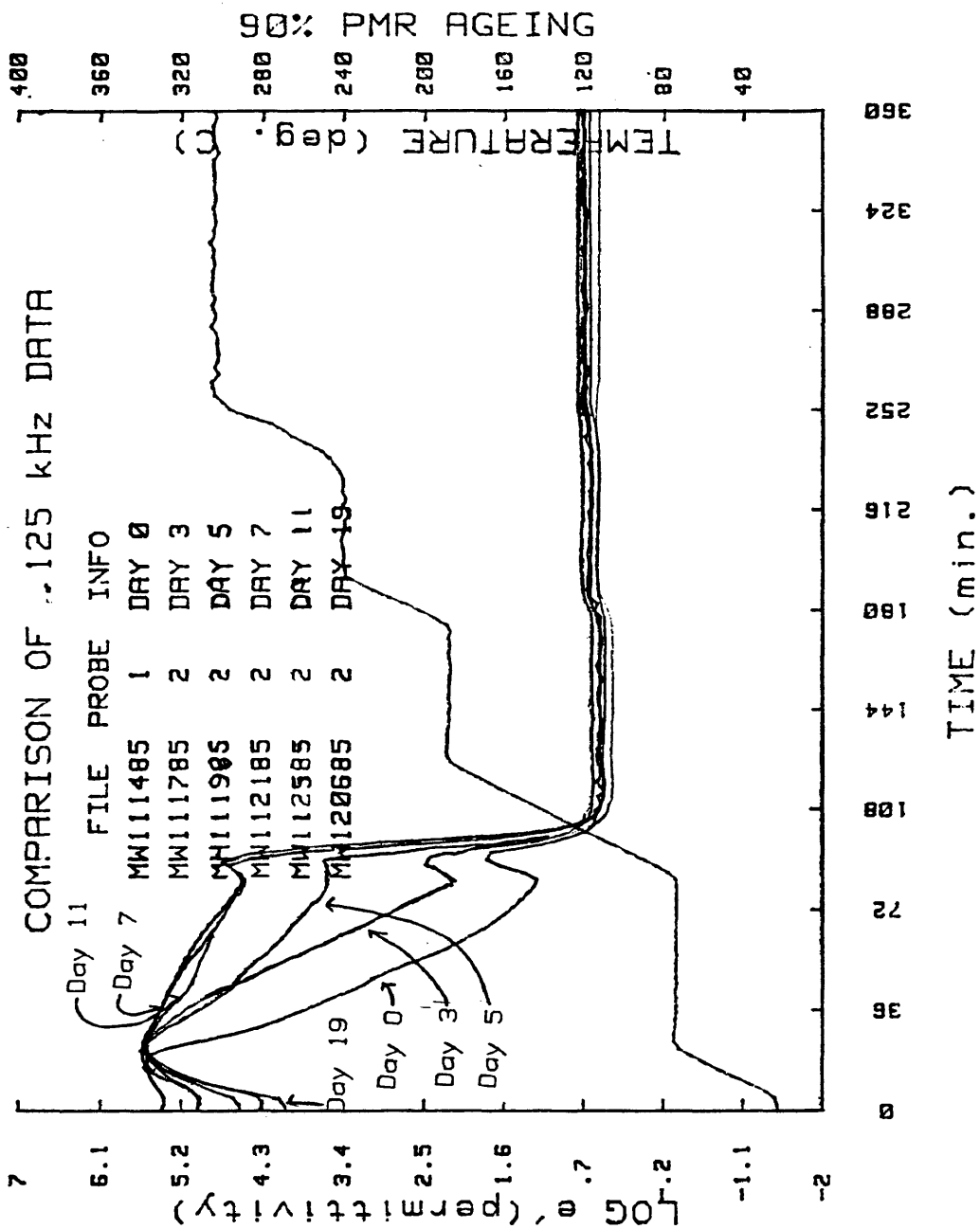


Figure DDA 25

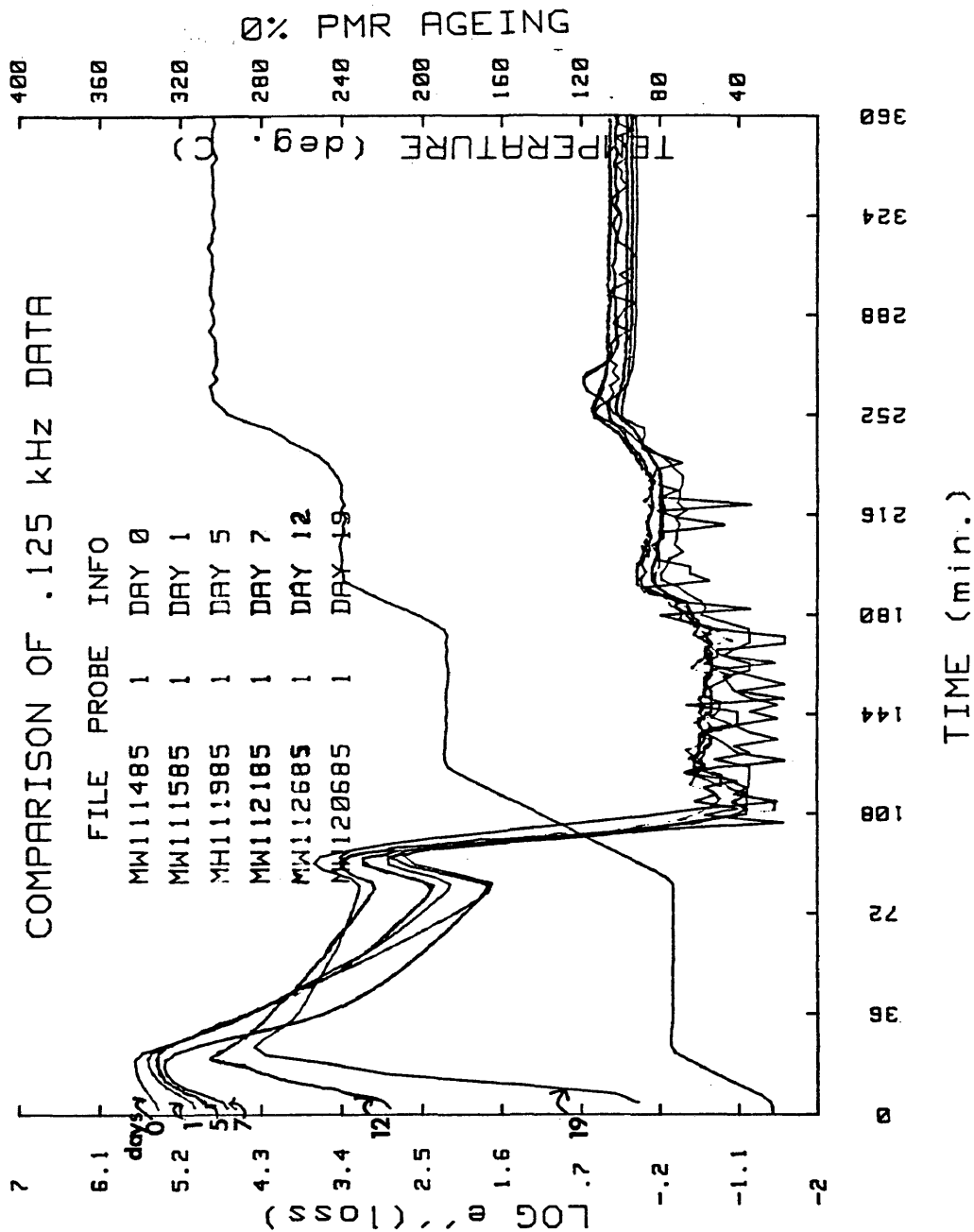


Figure DDA 26

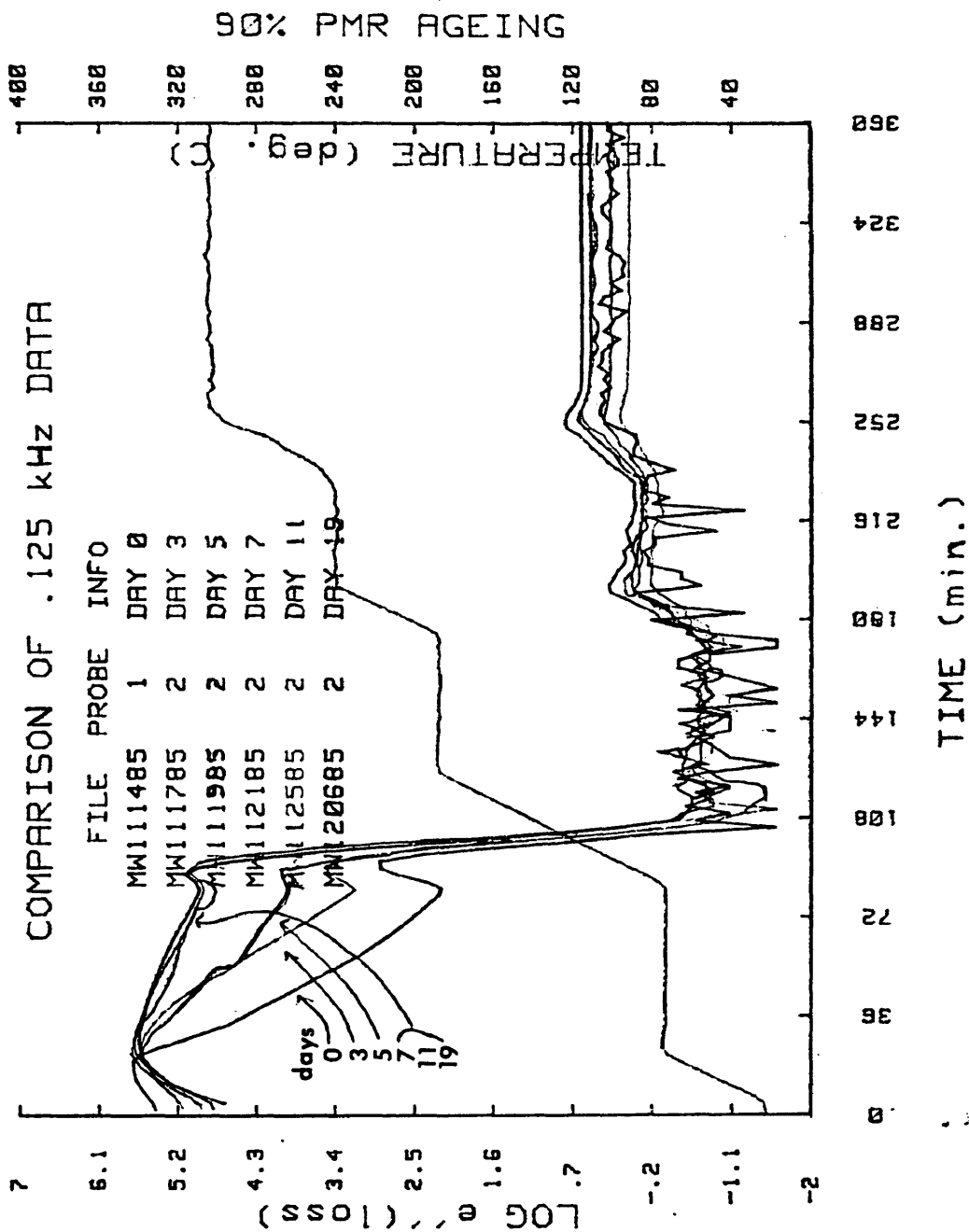


Figure DDA 27

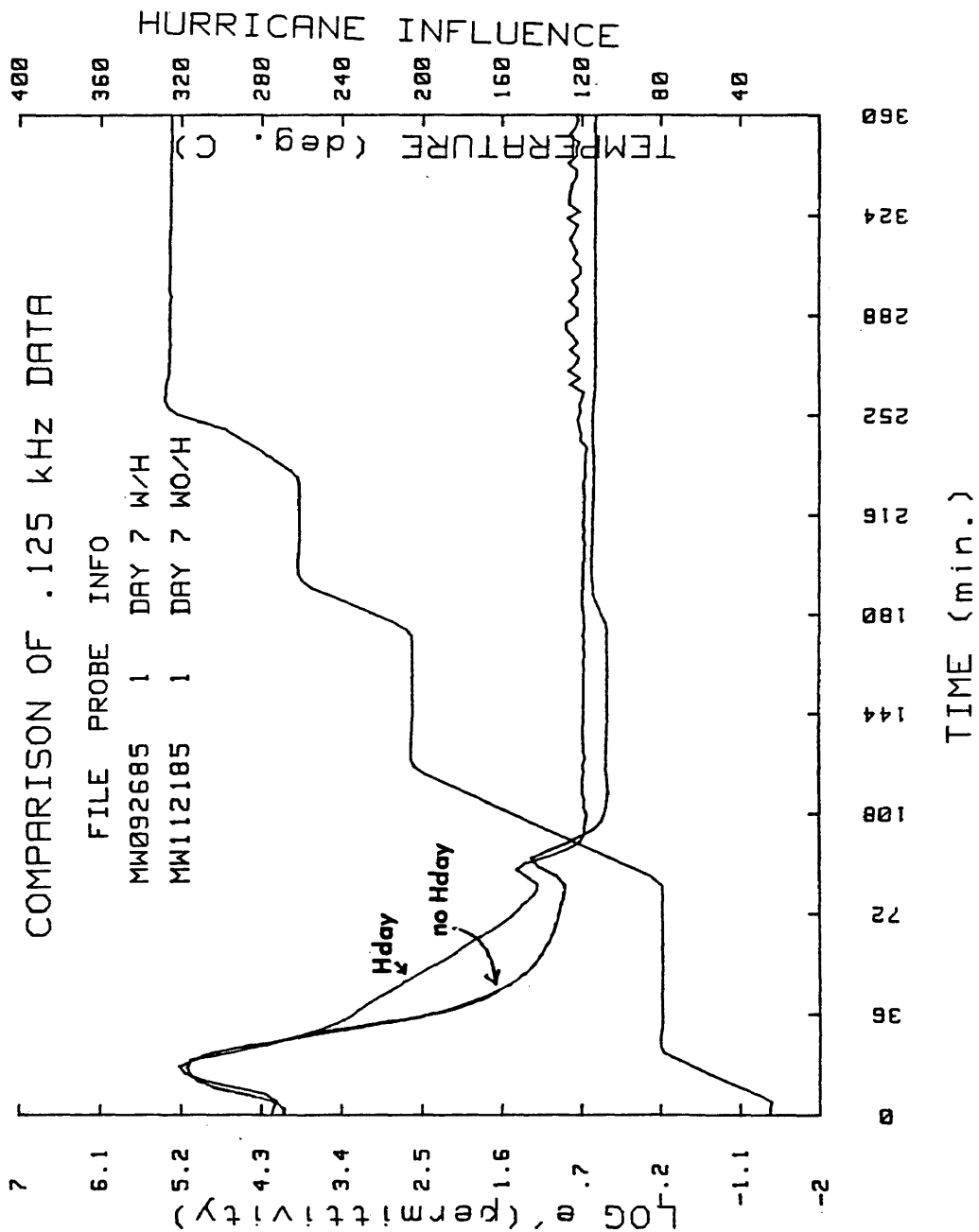
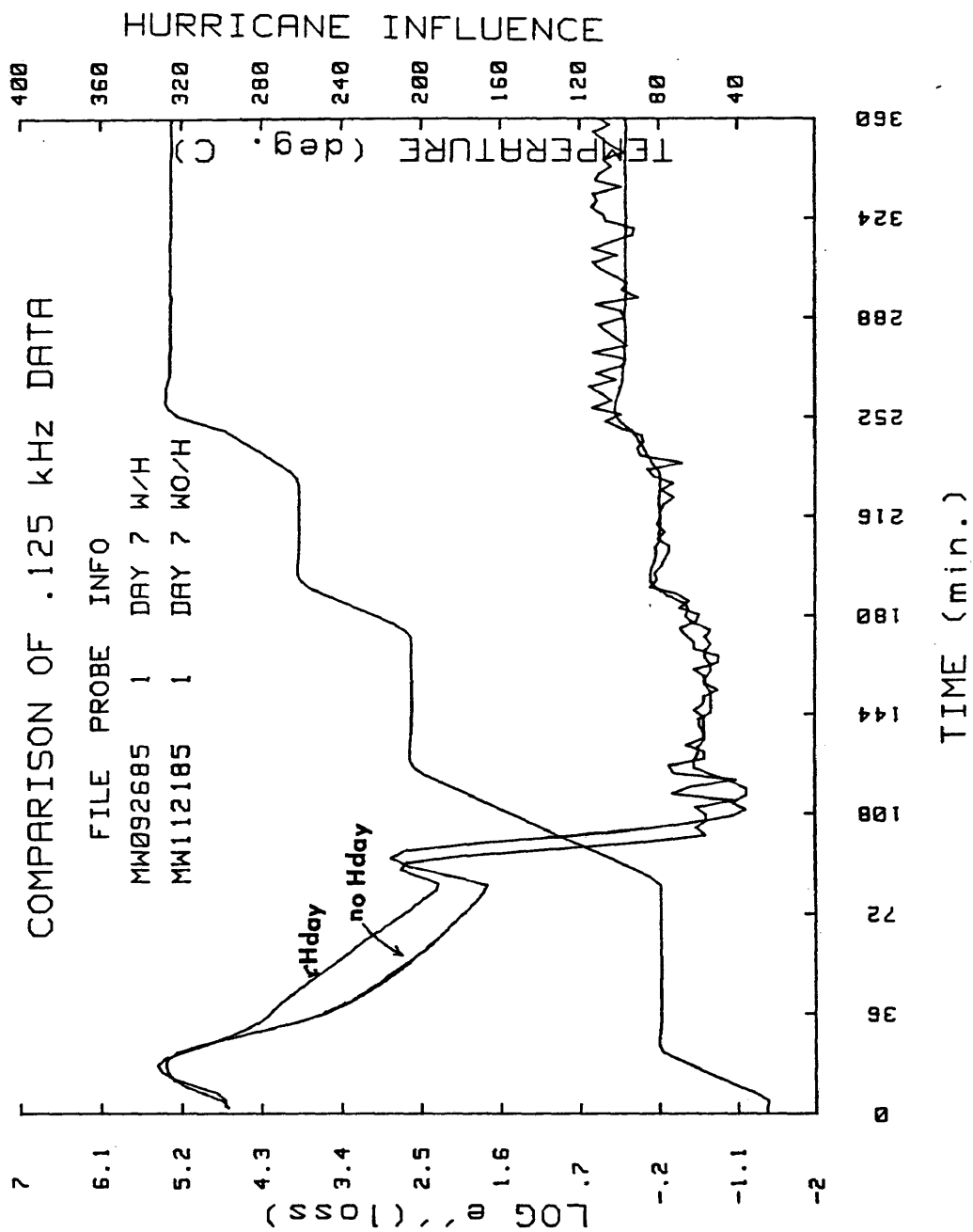


Figure DDA 28



NOTES FOR CHAPTER IV

1. D. E. Kranbuehl, S. E. Delos, E. C. Yi, and J. T. Mayer, Proc. of 2nd Intl. Conf. on Polyimides, 469(1985).

CHAPTER V

What is a Differential Scanning Calorimeter?

The ICTA Nomenclature Committee defined differential scanning calorimetry to be 'A technique for recording the energy necessary to establish a zero temperature difference between a substance and a reference material against either time or temperature, as the two specimens are subjected to identical temperature regimes in an environment heated or cooled at a controlled rate'.¹ The Perkin-Elmer Corporation coined the term differential scanning calorimetry (DSC) to describe the method by which their original scanning calorimeter, the DSC-1, performed thermal analysis. It is the null-balance principle which distinguishes DSC from other thermal analysis devices.

Our laboratory uses a Perkin-Elmer DSC-7 thermal analysis system. The system includes a DSC-7 instrument, a 32 bit minicomputer, an instrument controller, a printer, and a graphics plotter. With the TAS-7 software library, the PE-7500 Professional Computer is capable of controlling the DSC-7 to make direct calorimetric measurements for the characterization and analysis of the thermal properties of materials.² The DSC-7 can be programmed to scan a

temperature range between -170°C and 725°C . On a temperature ramp the DSC-7 can be used to determine endothermic and exothermic reactions. The DSC-7 can also be programmed to run isothermally, permitting the operator to obtain kinetic information.

The principle innovation of DSC is the capability for direct, convenient, and precise quantitative measurement of transition energy.³ E. S. Watson et al demonstrated that quantitative performance of the instrument is independent of specific heat of the sample, sample geometry, and temperature scanning rate. Analysis is performed on samples that weigh between 5 and 20 milligrams. The energy put into the system is reported in milliwatts.

How does a DSC Work?

The null-balance principle described by Perkin-Elmer is an idea in which a sample and a reference are kept at the same temperature during either a heating ramp, a cooling ramp, or an isotherm. Because thermal properties of materials are temperature dependent, this principle necessitates the use of separate furnaces and temperature sensors for the sample and the reference. If the sample undergoes an endothermic reaction additional power can be added to the sample furnace to adjust the temperature to that of the reference or the reverse process can be performed, taking power away from the reference. If the

sample experiences an exothermic reaction the reverse of both processes is observed. If the sample and reference have the same specific heat no adjustment is necessary. The amount of electrical energy which is added or subtracted from the furnaces is directly related to the thermal behavior of the material.

The schematic diagram presented on figure DSC 1 shows the control loops which are used to accomplish the temperature balance. The DSC-7 sample and reference holders are made of platinum and iridium and each has a furnace with a platinum resistance heater and a platinum temperature sensor mounted directly underneath the holders. Two control loops are used during a scan.⁴ The first loop, average temperature loop, is to output a signal proportional to the desired temperature for the sample and reference holders. This is where the operator sends the machine on an indicated ramp or isothermal hold. The power sent for the desired temperature is the same because the furnaces are identical. After the furnaces are adjusted to the desired temperature, the thermometers sense the temperature in the furnaces and send the temperature in an electrical signal to the second control loop, the differential temperature loop. The difference in power is calculated from the signals sent from the thermometers and is recorded on the CRT of the PE 7500. The differential power amplifier then adjusts the temperature of the

furnaces to be equal, which means the energy signal for the furnace temperature is equal and thus the procedure is back to the first control loop.

The difference in power which is recorded on the CRT of the PE 7500 represents the thermal behavior of the material. It is reported as dH/dt on the ordinate axis with temperature or time on the abscissa. The area under an endotherm or above an exotherm is equal to the delta H or enthalpy for the transition. This can be seen by considering some basic physical chemistry.

If,

Total Energy=Kinetic Energy+Potential Energy+Internal Energy

$$E = K + P + U$$

For a stationary system resting in a furnace,

$$K \text{ and } P = 0$$

Therefore,

$$E = U$$

From thermodynamics,

$$H = U + PV$$

H is enthalpy

P and V define work energy

Levine offers a simple proof in his physical chemistry text demonstrating the heat absorbed or released at constant pressure is equal to the change in enthalpy.⁶

$$U_2 - U_1 = q + w = q - \int_{V_1}^{V_2} P dV = q_P - P \int_{V_1}^{V_2} dV = q_P - P(V_2 - V_1)$$

$$q_P = (U_2 + PV_2) - (U_1 + PV_1) = H_2 - H_1$$

$$\Delta H = q_P \quad \text{const. } P, \text{ closed syst., } P\text{-}V \text{ work only}$$

A negative value for q represents an exothermic process and a positive value represents an endothermic process.

In experiments that involve solid to solid transitions or solid to liquid transitions the change in enthalpy is equal to the change in internal energy. This is true because the volume has minimal change in these transitions and therefore the PV work term can be neglected. However, in vaporization experiments the work term cannot be neglected because a large change in volume is encountered.

$$\Delta V = (\text{vol. of ideal gas} - \text{vol. of liquid})$$

$$\Delta V = ((nRT/P) - (\text{mass}/\text{density}))$$

The DSC-7 instrument accomplishes the null-balance by splitting the adjustment signal in half. The difference in furnace temperature is compensated by adding or subtracting half the energy needed for the sample furnace, and the reverse is done to the reference furnace. The furnaces are encased in large heat sinks. In the heating mode power is provided over and above that which is necessary to compensate the heat loss to the sink, in the cooling mode power is reduced below the loss to the heat sink.⁷

A DSC run is performed by encapsulating a sample in an aluminum pan and placing an empty pan in the reference holder. To obtain reproducible results the thermal resistance between the sample and pan, R_s , and the thermal

resistance between pan and holder, R_o , must be kept constant and to a minimum. R_s and R_o affect peak shape but not peak area. The slope of a leading edge of an endotherm of a very pure sample such as indium will be equal to $(1/R_o)(dT_p/dt)$.⁸ Mortimer and McNaughton have summarized some simple precautions to obtain accurate results.⁸

- 1) Standardize the pan position in the holders.
- 2) Use nitrogen as a flushing gas.
- 3) Small and constant sample weights should be used during a study.
- 4) Standardize the sample geometry. It has been shown that a granular sample will give a different shaped peak than a thin disc. This is related to the heat transport through the sample. However, it has also been shown that the area of the peak remains unchanged and therefore, enthalpy will be the same for different sample geometries.

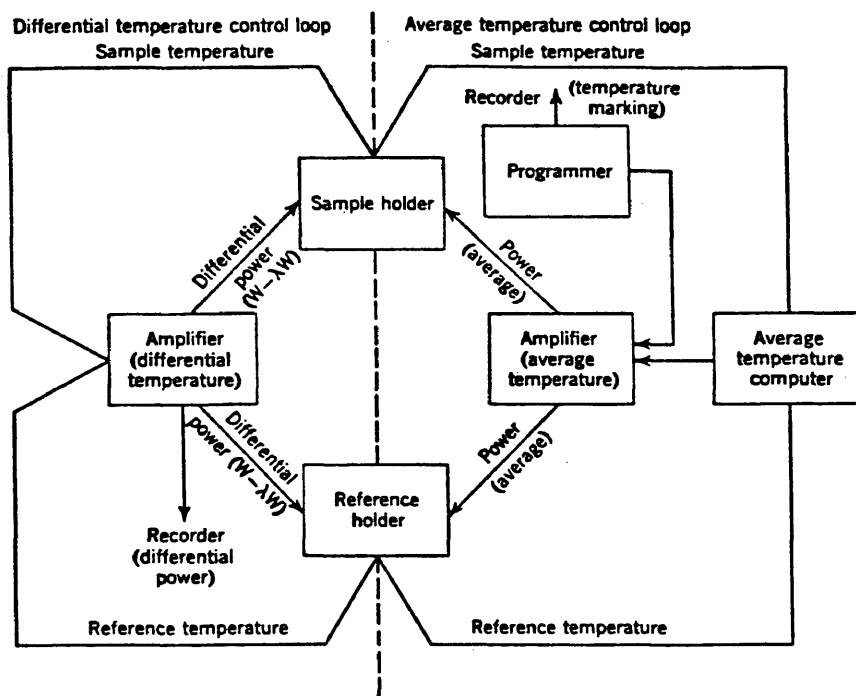


Fig. DSC 1

Reproduced from Wendlandt.

NOTES FOR CHAPTER V

1. M. I. Pope and M. D. Judd, "Differential Thermal Analysis," Heyden and Sons Ltd., New York, N.Y., 1977.
2. PE DSC 7 Operators Manual.
3. E. S. Watson, M. J. O'Neill, J. Justin, and N. Brenner, Analytical Chemistry, 36, No. 7 June, 1235(1964).
4. Wesley Wendlandt, "Thermal Methods of Analysis," in Chemical Analysis, 19, John Wiley and Sons, London, U.K., 1973.
5. Perkin Elmer Thermal Analysis Newsletter, 9, 1970.
6. Ira N. Levine, "Physical Chemistry," McGraw-Hill Book Co., New York, N. Y., 1978.
7. Henry T. Gaud, Comprehensive Analytical Chemistry, 12 B, (1982).
8. J. L. McNaughton and C. T. Mortimer, "Differential Scanning Calorimetry," Butterworths, London, U.K., 1975.

CHAPTER VI
Measurement of Heat Capacity by Differential
Scanning Calorimetry

It is possible to calculate the heat capacity of a material at any point during a cure cycle directly from DSC data. When a sample is subjected to a linear temperature program and the heat flow into the sample is continuously monitored, the heat flow rate is proportional to the instantaneous specific heat of the sample.¹ Knowledge of the heat capacity is important for the determination of a heat transport model for a resin. The CRC Handbook of Chemistry and Physics defines heat capacity as 'The quantity of heat required to increase the temperature of a system or substance one degree of temperature'.² The heat capacities I have determined will be expressed in calories per gram per degree kelvin.

The instrument must be calibrated before it is used. This task is accomplished by running a high purity standard which has a known melting point and latent heat of fusion. The instruments controls are then adjusted to the standard. Our laboratory uses a sample of Indium which is 99.99% pure and is provided by the Perkin-Elmer corporation.

To check the accuracy and precision of our instrument I ran a sample of indium at different heating rates and different samples of indium at one heating rate. The known value of the melting point for indium is 156.6 C. The known value of the latent heat of fusion for indium is 28.45 joules per gram (J/g). The results of the experiment are shown on table 1 and table 2. It can be seen that the 'onset', which is the melting point for a high purity metal, is accurate within less than one degree. The latent heat of fusion is low for all the runs performed possibly because the calibration is low, however, the calibration was performed according to a set procedure and these results are from the best calibration I could obtain. None of the runs is more than .4 J/g from the expected value. The precision seen on the latent heat of fusion is excellent. All values are within .2 J/g. An example of a DSC calibration run can be seen on figure Cp 1. Notice that the onset is indicated in minutes and not temperature. I computed the temperature from the minutes by knowing the run has a 2 minute isothermal hold at thirty degrees at the beginning and is scanned at 20 degrees a minute.

TABLE 1
Different Scanning Speeds for 24.5 mg. of Indium.

Rate	Onset	J./g.
10 C/min.	156.34	28.082
20 C/min.	156.56	28.214
30 C/min.	156.84	28.142
40 C/min.	156.96	28.191

TABLE 2
Different Masses of Indium at 20 C/min.

Mass	Onset	J./g.
4.84 mg.	157.50	28.078
10.86 mg.	156.36	28.328
24.50 mg.	156.36	28.214

In order to calculate the heat capacity of a sample a baseline and a sample run must be performed. A 'run' is a programmed series of ramps and holds input into the computer using TAS 7 software. To determine heat capacities the procedure is to program a short isothermal hold at the beginning and end of a scan with a designated temperature ramp in between the isotherms. The isotherms provide a check that the sample is starting and ending at the preset temperatures. Plus, the isotherms are unaffected by the sample because it has no influence on the power dissipation of the sample holder.¹ The baseline is optimized before it is used as a line for the sample run. Curvature of the baseline results from holders not being precisely matched.³ If one of the holders is a better thermal radiator some of the power which is monitored by the differential comparator will be to equilibrate the holders. This adjustment is compensated in the optimization process by adjusting two control knobs, the slope and the balance, in order to

provide a programmed offset which equals the discrepancy between the holders. The purpose of the optimization is to get the ramp part of the scan as flat as possible and on as small a scale as possible.

The baseline is optimized with an aluminum sample capsule in each furnace. When a baseline with a relatively flat ramp is obtained, the aluminum sample capsule in the sample furnace can be removed from the DSC and filled with a weighed amount of sample material. The sample is then run under the same preprogrammed temperature ramp as the capsule.

A transient is observed just after the beginning isotherm and just before the ending isotherm. This transient results from the fact that the temperature is advanced before it is compared. Initially there is a slight difference in the temperatures of the holders but this difference is very quickly compensated. We are not concerned with any calculations in the transient region.

The PE-7500 computer automatically rescales every run to a value of zero on the ordinate axis. The result of this operation is that the values for dH/dt on the ordinate axis cannot be used directly for comparison purposes. We draw a line between the isothermal holds and measure the deflection from this line with a ruler at selected temperatures. This measurement is the dH/dt used in the C_p calculation.

In order to calculate C_p the following information must be obtained. The baseline run and the sample run must be plotted on the same scale. The deflection dH/dt 's must be determined in millimeters at the desired temperatures. The mass of the sample must be known. The programmed heating rate must be known. C_p is calculated from the following expression,

$$C_p = (\text{the change in } dH/dt) / (m \cdot q)$$

$\Delta \frac{dH}{dt}$ = difference in deflection heights of baseline and sample.

m = mass of the sample.

q = programmed heating rate.

To test this method for calculating heat capacity the heat capacity of indium and zinc were determined. I used indium to test the low temperature region and zinc to calculate the high temperature region. The literature values I compared my data with were determined from the CRC handbook. The reported calculation for C_p is,

$$C_p = a + (b \cdot 0.001)T + (c \cdot 0.000001)T^2 + (d \cdot 10000)/T^2$$

Values for a , b , c , and d are experimentally or theoretically determined and the temperature, T , is treated as the independent variable.² Only the values of a and b are reported for indium and zinc, therefore I assumed the other values went to zero. The results are presented in tables 3 and 4.

Table 3

Determination of the Cp of Indium

Sample	Date of Run	Temp in C	Cp in cal/(g*K)	%Error
56.46 mg.	4/10/85	40	.059328	3.3
		60	.058494	1.9
		80	.059260	1.7
		100	.060804	3.5
		120	.061266	4.3
		140	.062046	4.9
20.54 mg.	4/10/85	40	.059262	3.2
		60	.056280	2.7
		80	.055428	4.9
		100	.056706	3.1
		120	.059062	0.2
		140	.062250	4.8

Table 4

Determination of the Cp of Zinc

Sample	Date of Run	Temp in C	Cp in cal/(g*K)	%Error
5.65 mg	7/28/85	210	.0964	0.3
		230	.0912	9.9
		250	.0920	9.8
		270	.0956	6.4
		290	.0974	5.2
		310	.0959	7.6
		330	.0965	7.7
		350	.1007	3.9
		370	.1007	5.7
		14.13 mg	8/6/85	210
230	.0966			4.0
250	.0976			3.5
270	.0995			2.2
290	.1024			.06
310	.1045			2.0
330	.1103			5.7
370	.1092			4.0

We can conclude from these results that our system of calculating Cp is successful for obtaining data with an average error of less than 5% and a maximum error of 10%. In fact, Perkin-Elmer's third newsletter predicts an

accuracy of five percent. The reason for the error is that the temperature ramp is not strictly linear and the calibration constant is somewhat dependent on temperature.³ This dependence stems from the fact that a thermal resistance exists in the sample itself and a thermal resistance exists between the pan and a sample. They propose that a pure sample of known heat capacity should be run before the sample is run. The calculation can then be performed,

$$C_p = (sdH/dt * m' * C_p') / (kdH/dt * m)$$

where,

sdH/dt = sample ordinate deflection

kdH/dt = known pure compound ordinate deflection

m' = mass of known pure compound

m = mass of sample

C_p' = heat capacity of pure compound

Our results from this method of computation were about the same as before. Data are shown in table 5. This method has the disadvantages of having to use a pure compound heavier than the sample we intend to measure and the problem of having to perform an extra run for a C_p workup.

Table 5

Here Zinc is the unknown sample.

Samples	Date	Temp in C	C_p	%Error
56.46 mg of Indium	4/15/85	50	.0999	6.6
13.80 mg of Zinc		70	.0976	3.3
		90	.1015	5.8
		110	.1039	8.0

We use the first method for obtaining heat capacity.

We applied this technique to a scan of a sample of the aromatic thermosetting polyimide and a scan of the cured polyimide.⁴ To make calculations on the uncured sample it was necessary to assume that the weight loss occurred all at once at the end of the imidization. This assumption is based on the fact that water is lost during imidization and nothing is lost during crosslinking. Faults can be found in the fact that the polyimide loses weight throughout the imidization and not all at once at the end.

The workup consists of a baseline run, a sample run of 8.79 mg. of the polyimide, and a 5.92 mg. sample of the cured polyimide. I assumed that the imidization was finished at 200 degrees and at that point the weight of the sample was 5.92 mg. Table 6 shows the results for the Cp of the aromatic polyimide during a cure and after a cure.

Table 6

Temp in C	Cp of Curing sample	Cp of Cured sample
35.4	.44833	.13868
48.9	.51372	.23576
67.8	.56976	.22189
88.1	.81260	.22189
108.4	.90601	.20803
128.6	1.21424	.22189
147.6	1.22358	.20803
169.2	1.98318	.19415
188.1	2.78755	.19415
207.0	1.65034	.19415
228.6	1.30363	.20803
248.9	.59634	.19415
267.8	.47153	.20803
289.5	.42992	.23576
309.7	.40218	.23576
330.0	.48539	.24963
348.9	.33284	.26350
369.2	.30510	.29123
388.1	.37448	.34671
409.7	.42992	.37448
430.0	.45765	.41605
450.3	.42992	.45765

I cannot compare these values of Cp to a known number since none has been reported. Most Cp values of organic compounds are around .3 cal./(gram*deg).³ It is easy to see that the Cp value is strongly influenced by the imidization reaction seen between 88 and 230 degrees celsius. We can also see that the cured resin has different values for Cp at lower temperatures. After 388 degrees notice that the Cp values are similar suggesting the reaction is completed.

Figures Cp2 to Cp8 are examples of workups used to determine heat capacities. Figure Cp2 is the scan of 56.46 mg of indium and figure Cp3 is its baseline. Figure Cp4 is

the scan of 14.13 mg of zinc and Cp5 is its baseline. A computer program has been written which performs the subtraction point for point by the method which has been described previously. The zinc data were analyzed by this program. Figure Cp6 is the scan of the curing polyimide, and figure Cp7 is the scan of the cured polyimide, and figure Cp8 is their baseline.

Figure Cp1

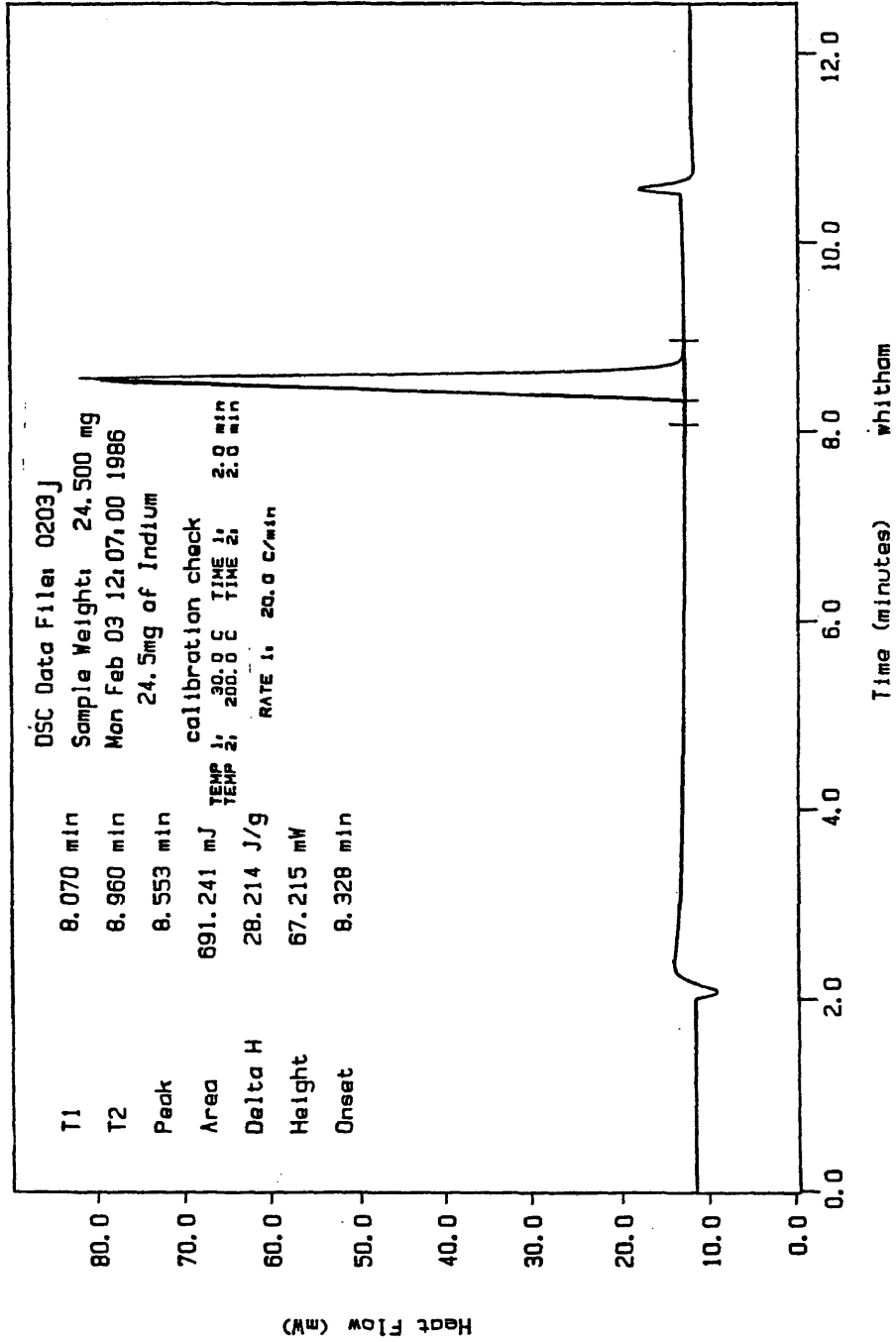


Figure Cp2

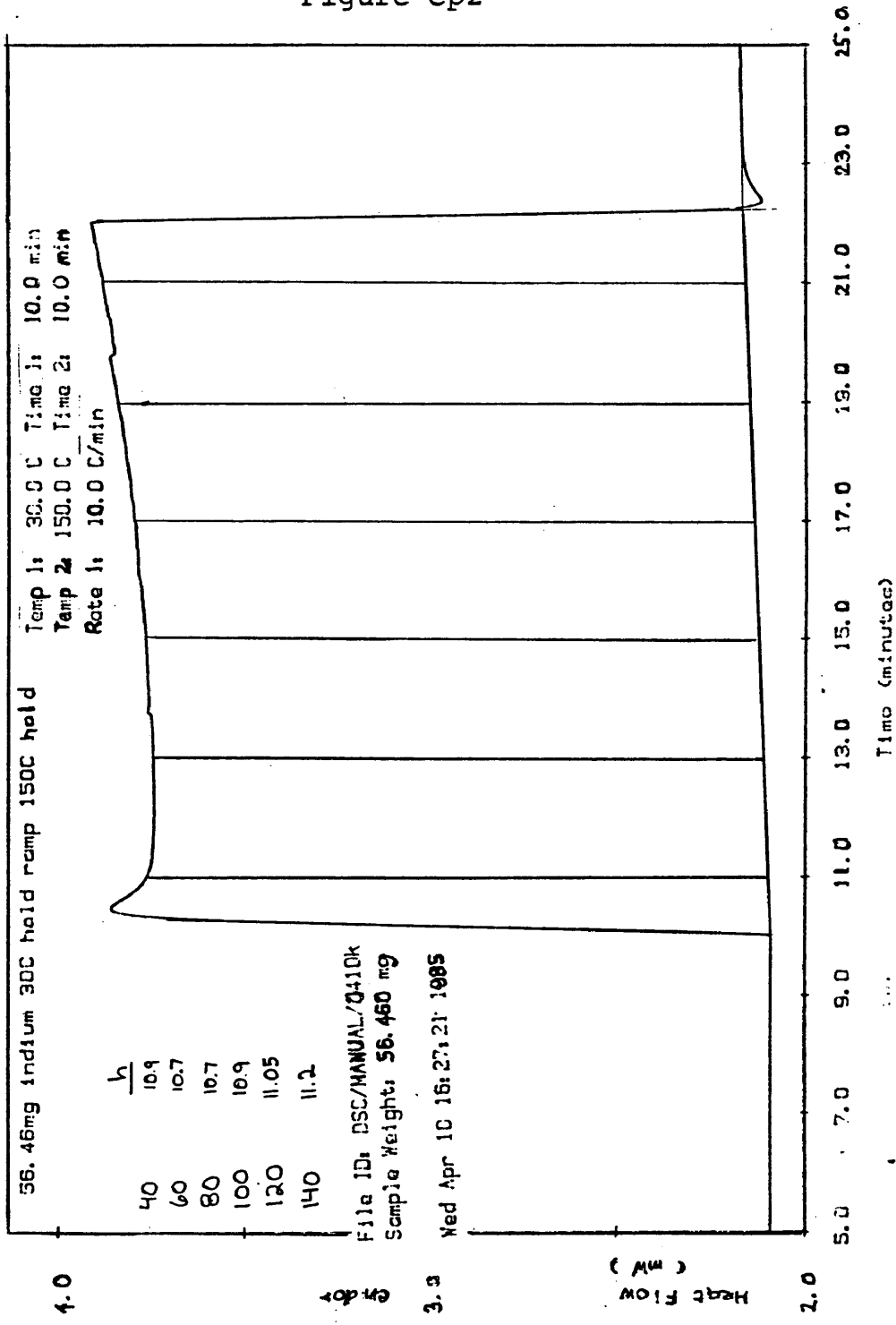


Figure Cp3

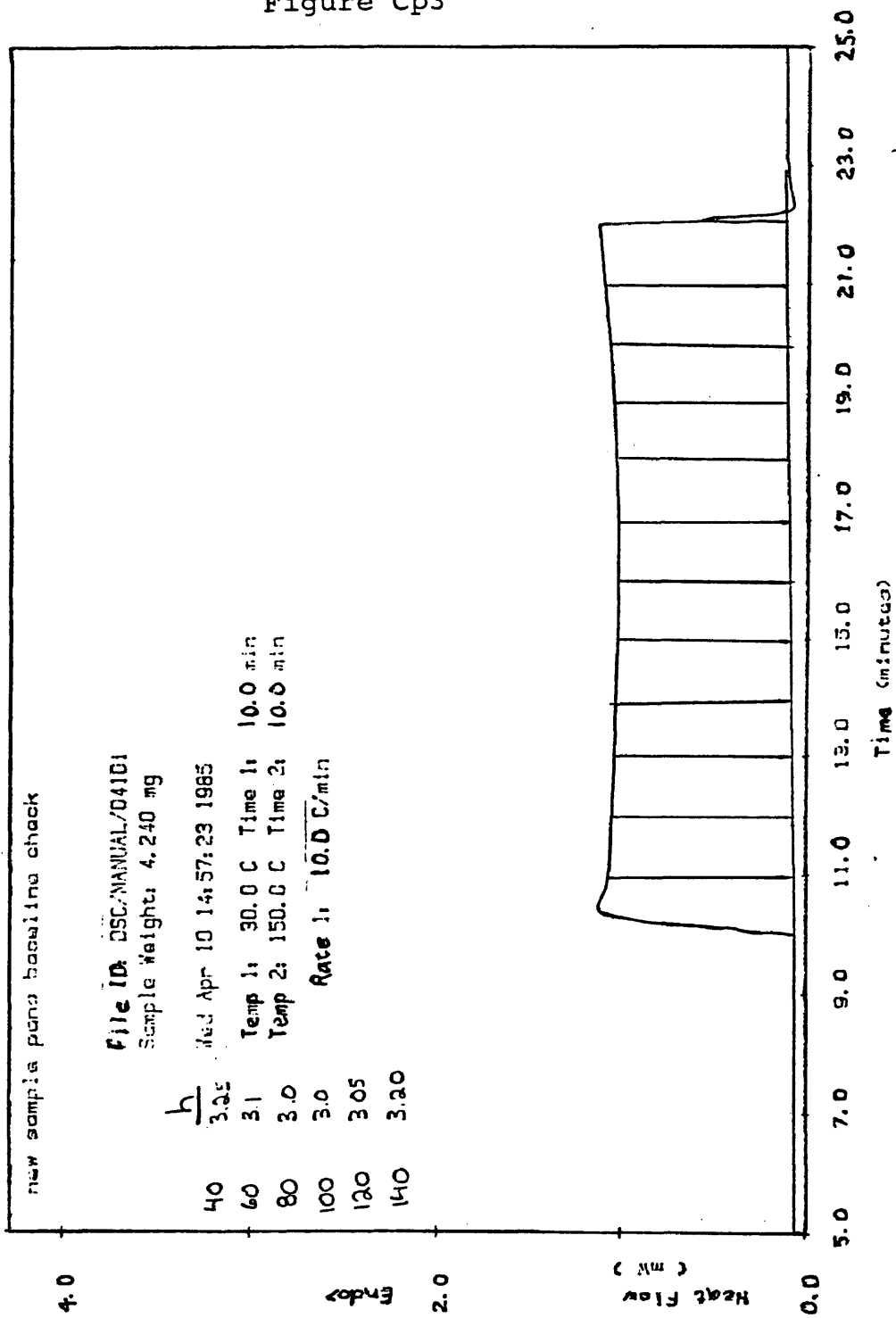


Figure Cp4

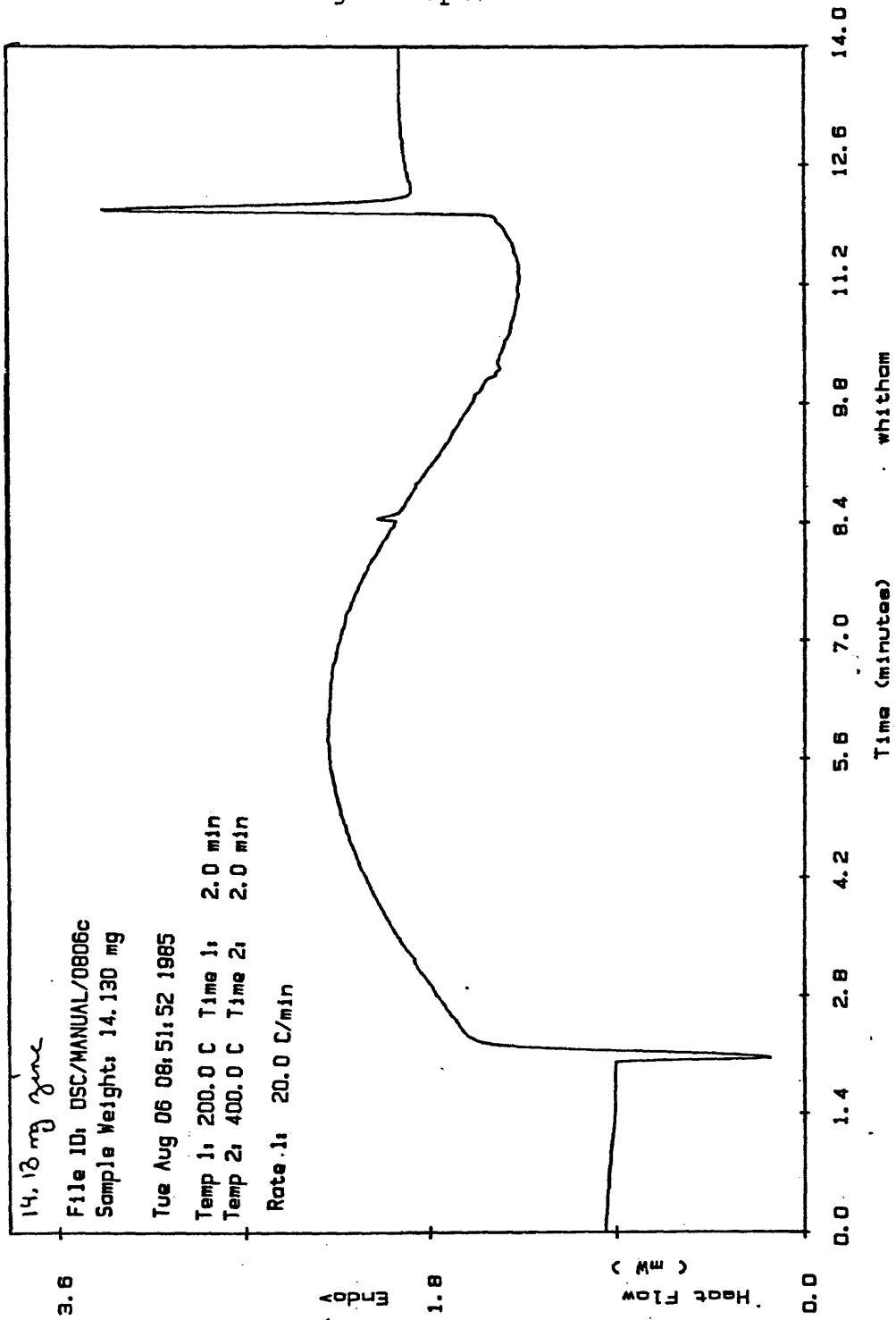


Figure Cp5

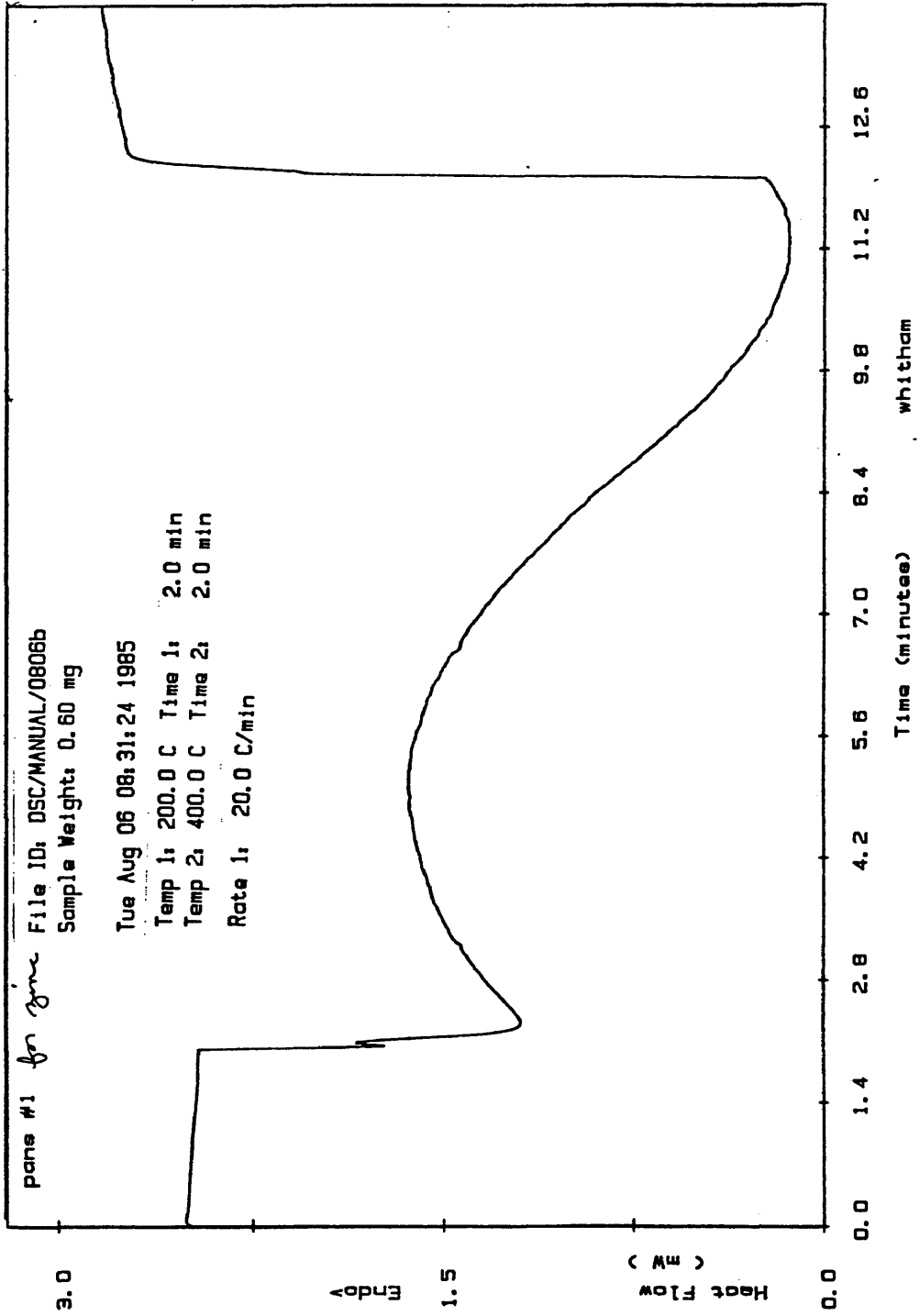


Figure Cp6

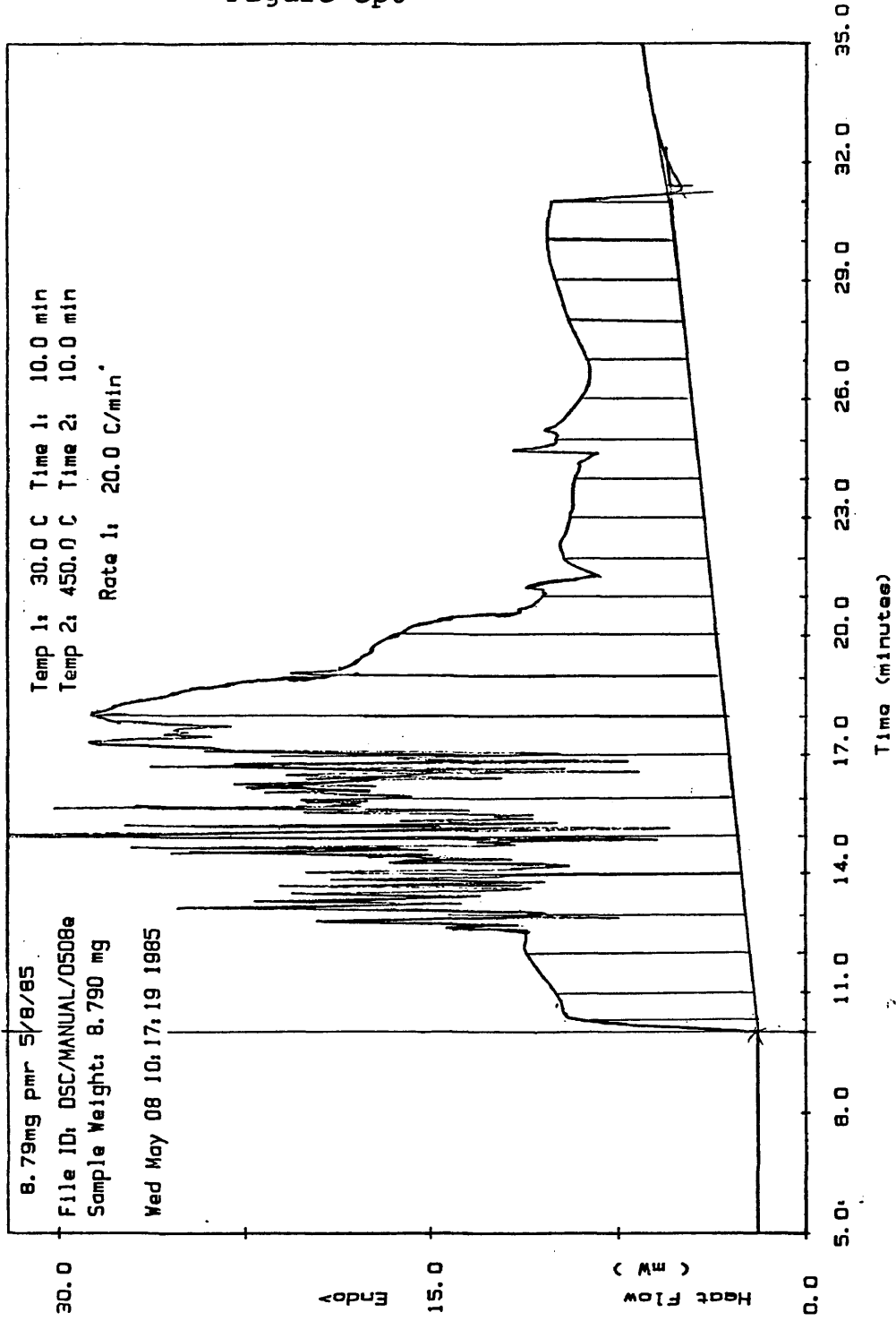


Figure Cp7

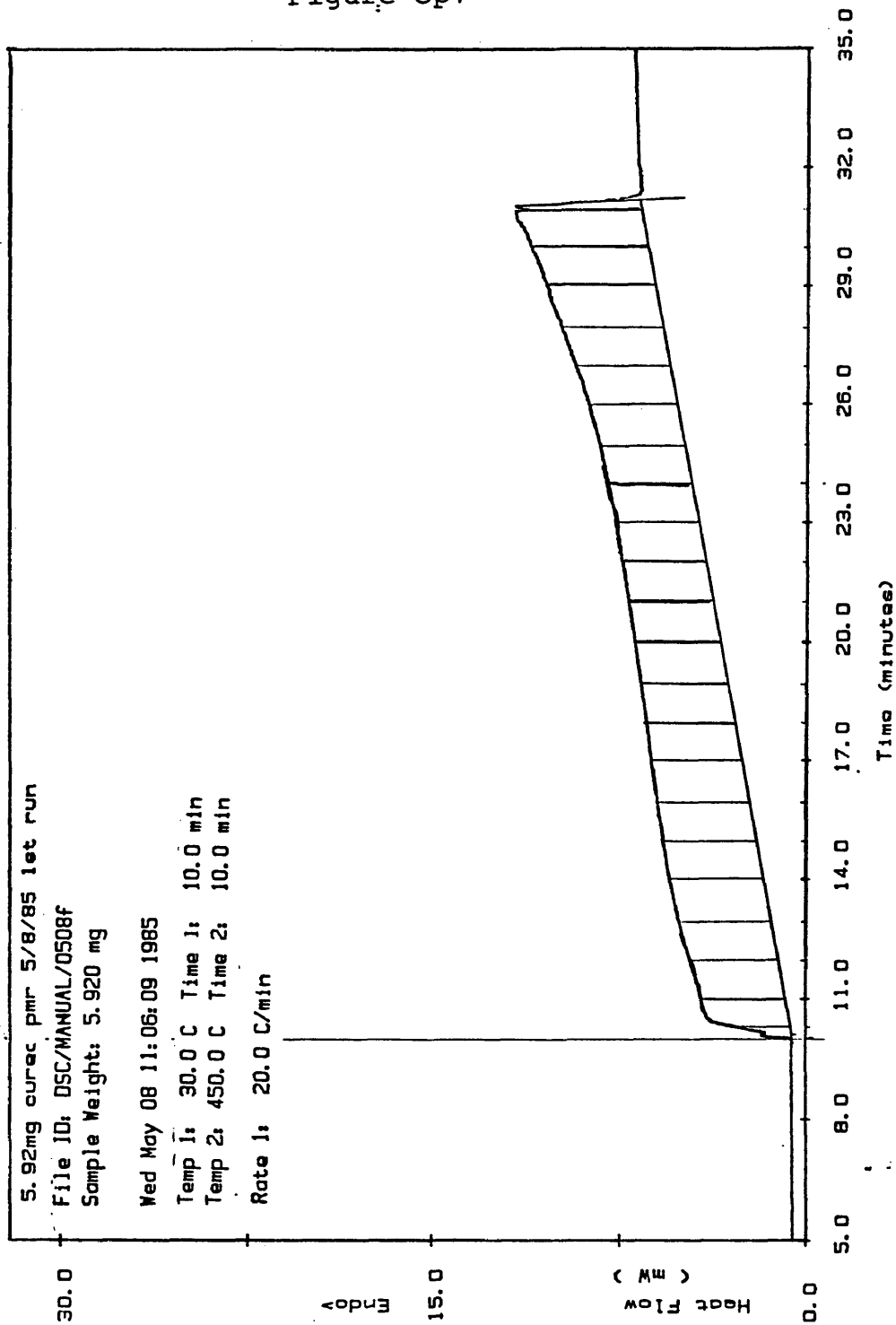
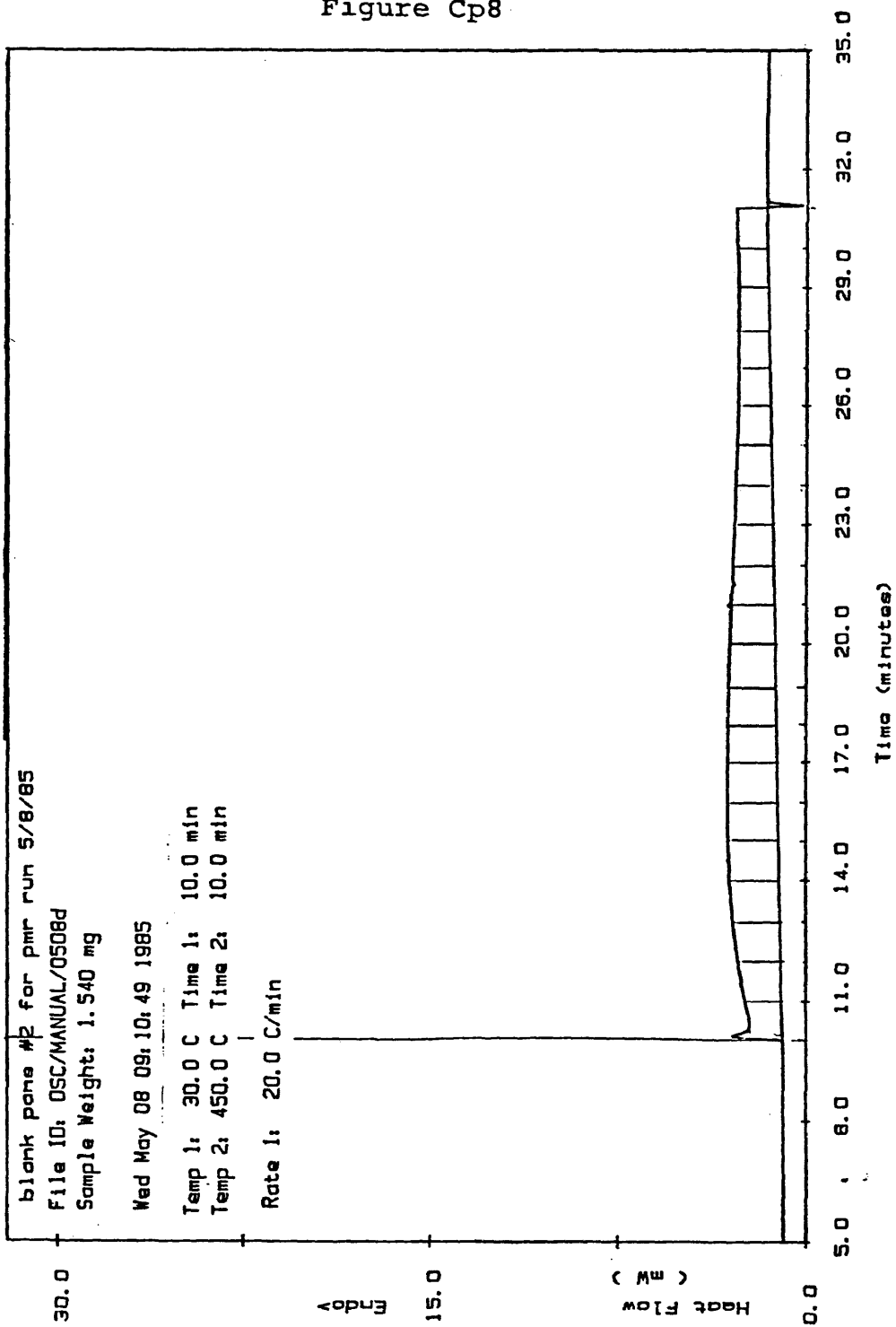


Figure Cp8



NOTES FOR CHAPTER VI

1. M. J. O'Neill, Analytical Chemistry, 38, No. 10, 1331(1966).
2. 59th edition of the CRC handbook of Chemistry and Physics.
3. Perkin Elmer Newsletter No. 9 (1970).
4. D. Kranbuehl, M. Hoff, S. Delos, and M. Whitham, "Progress Report to General Electric," 1985.

CHAPTER VII

Analysis of DSC Scans

The objective of this chapter is to examine and label some of the thermochemistry which can be observed for the aromatic thermosetting polyimide.

Figure A-1 is a scan from 30°C to 400°C at 20°C/min.. It includes the overall cure reaction for the polyimide. A melt-imidization region can be observed between 75°C and 180°C. The crosslinking can be seen between 275°C and 350 C. The melt-imidization region exhibits thermal noise because of the water and methanol which are released during the imidization, and because of excess methanol evaporation from the dried resin system.

The melt-imidization region can be examined better from figure A-2 which illustrates a scan from 30°C to 250°C at 5°C/min. Three thermal transitions appear to be observed. The endothermic region from 75°C to 90°C comes from a melt of the monomers. The region from 90°C to 120°C is the reaction between NE and MDA. Dielectrically we know the NE-MDA imidization is a slow reaction which occurs before the BTDE-MDA imidization. The third endothermic region begins at 120°C. Examination of figure A-1 tells

the reader this region extends past 250°C. This region has been called the melt-flow region by Dr. Lauver, because it corresponds to a softening of the pre-polymers during processing. It is most likely the BTDE-MDA imidization and an imidization of anhydrides formed at these elevated temperatures.

Figure A-3 is a scan from 30 C to 400 C at 20 C/min. of a 1:1 molar mix of BTDE and MDA. It can be seen that after a melt below 100 C the mixture doesn't show a reaction until 120 C. It becomes more endothermic between 130 C and 230 C. This observation corresponds to my theory that the "melt-flow" region is really part of the BTDE-MDA imidization.

Figure A-4 is a scan from 30 C to 400 C at 20 C/min. of a 2:1 molar mix of NE and MDA. The double melt peak below 100 C is probably caused by sample orientation in the pan. I put two separate chunks of material in the pan. One of dry NE and one of dry MDA. I am including this scan because it gives better results than a scan I performed on the mixture after it was pulverized with a mortar and pestle. The exotherm at 130 C followed by an endotherm may be caused by a combination of methanol evaporation and the formation of the imide. A bond to the nitrogen is formed (exotherm) first and water plus methanol are later released (endotherm). The exotherm which occurs between 280 C and 350 C is the crosslinking reaction which involves the nadic

endcappers of the NE-MDA-NE chains. The unusual shape of the exotherm, which includes an endotherm in the middle, can be explained by the release and capture of cyclopentadiene. As cyclopentadiene is released, bonds break and energy is released, thus causing an exotherm. As cyclopentadiene is captured, bonds form and energy is absorbed, thus causing an endotherm. As a free radical reaction progresses, bonds break and then reform with other endcappers, thus causing a final exotherm-endotherm. The mechanism is explained further in chapter IX. The crosslinking reaction in the model compound helps to pinpoint the crosslinking reaction in the aromatic thermosetting polyimide.

Scans A-5 through A-9 are from heat ramps of the monomer units plus the anhydrides of NE and BTDE.

Figure A-5 is a scan of NE and figure A-6 is a scan of its anhydride, NA. A clean melt in A-6 is observed while the melt in A-5 is much broader. Possibly NE melts at lower temperatures and as it is heated some anhydride is formed which melts at higher temperatures. The crosslinking reaction for NE and NA appear similar. Differences can be attributed to the geometry of the sample which was discussed at the end of chapter V. Notice that the crosslinking occurs at lower temperatures for NE and NA than for the polyimide or model compound. Possibly longer chains restrict the movement of the endcapper, thus

requiring more energy to be put into the system in order that the crosslinking reaction can occur between neighboring endcappers.

Figure A-7 is a scan of BTDE and figure A-8 is a scan of its anhydride, BTDA. The melt occurs at 100 C for BTDE while the melt occurs at 220 C for BTDA. The noise and second endotherm in figure A-7 is probably caused by the release of alcohol and slow formation of BTDA.

Figure A-9 is a scan of MDA. A melt can be observed at 90 C and decomposition is seen at 330 C.

Figure A-1

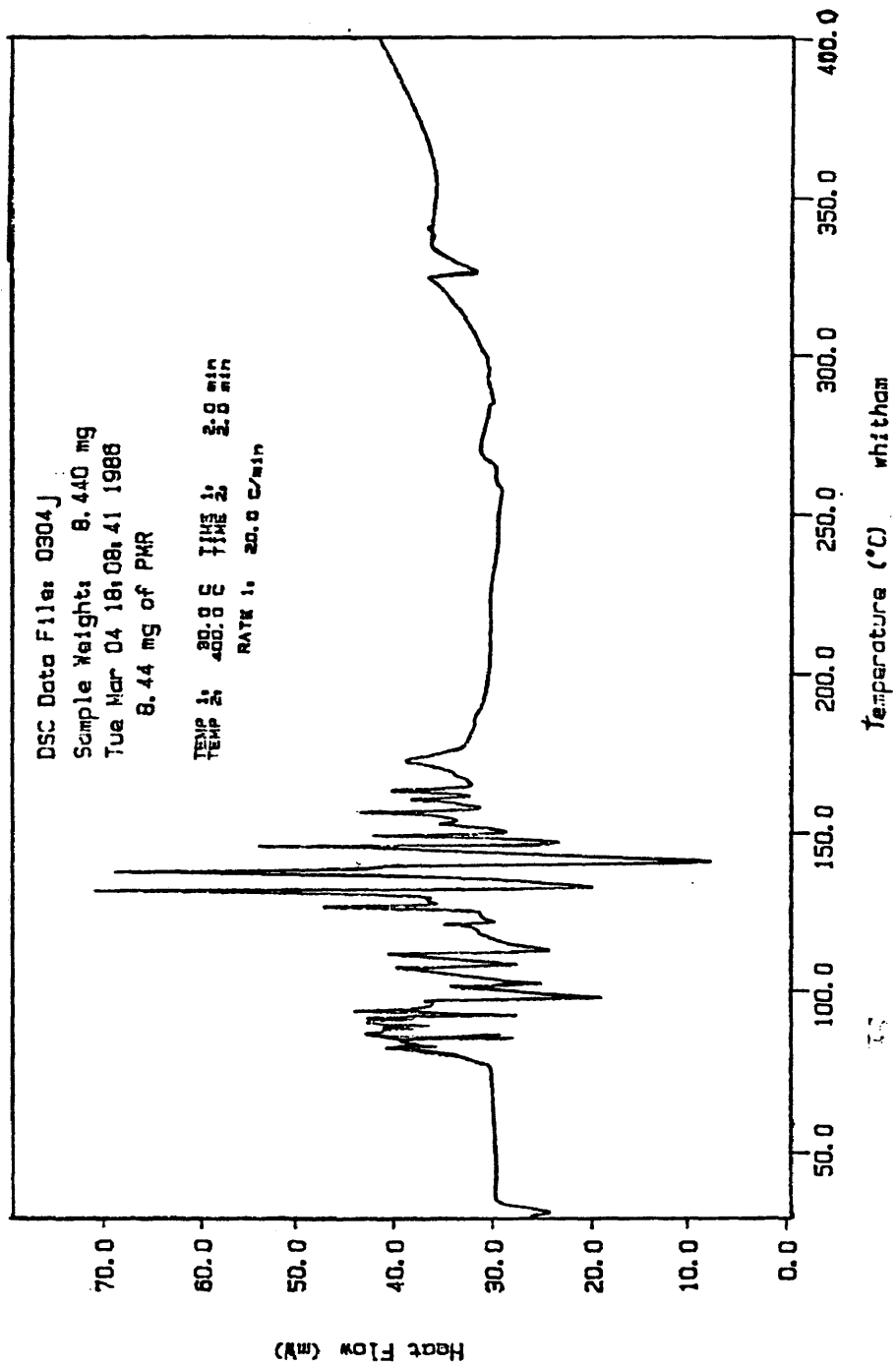


Figure A-2

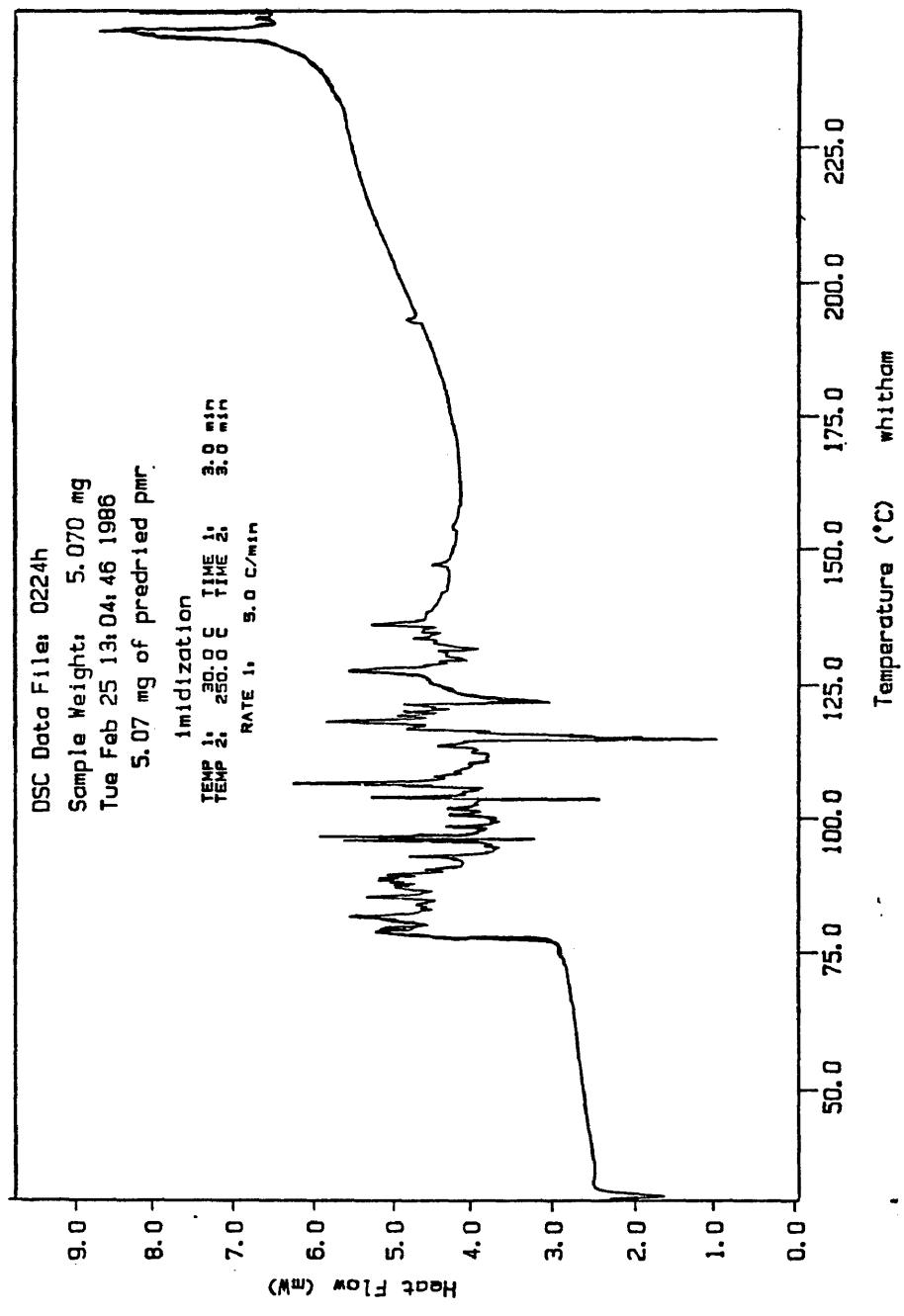


Figure A-3

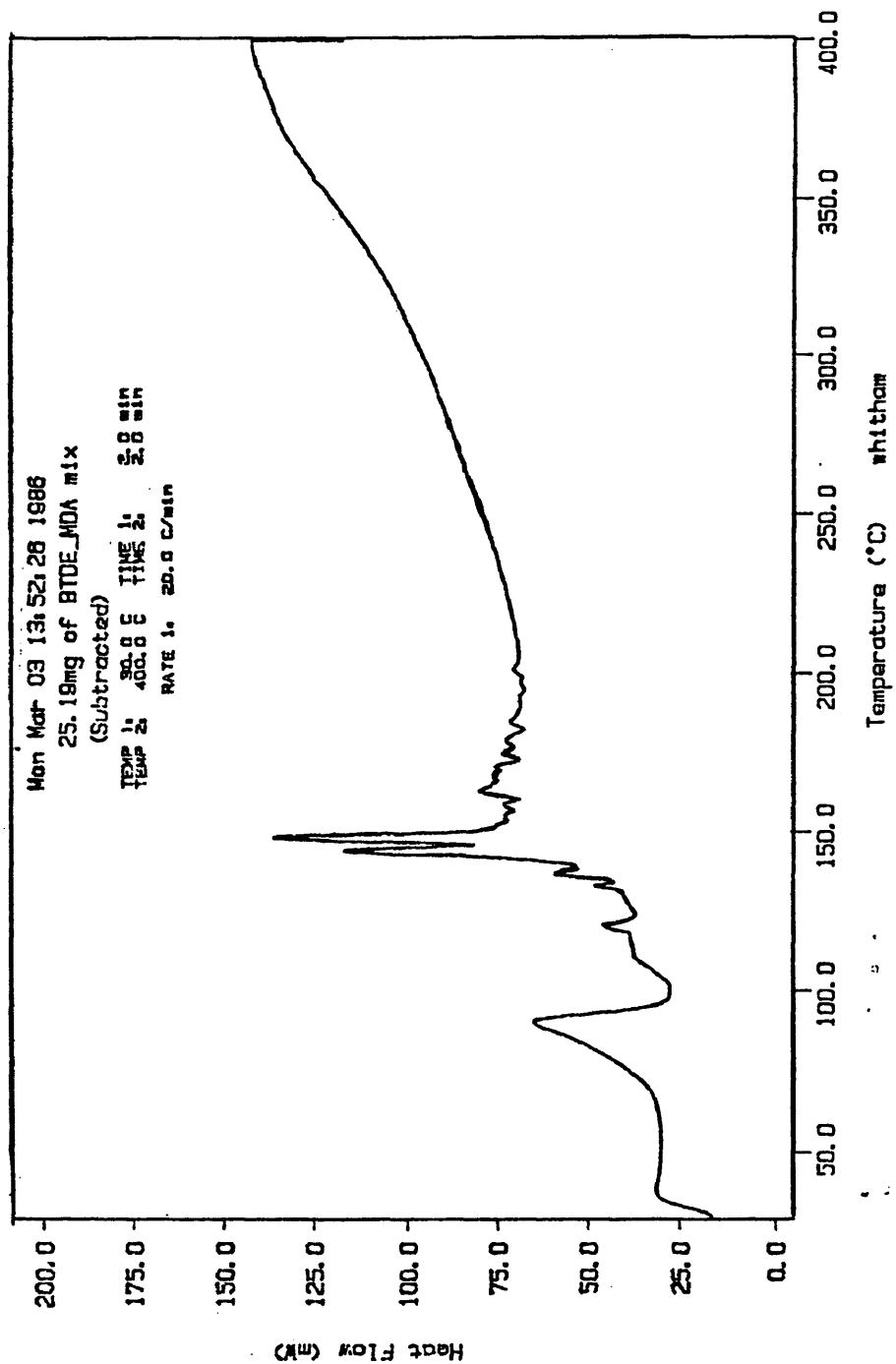


Figure A-4

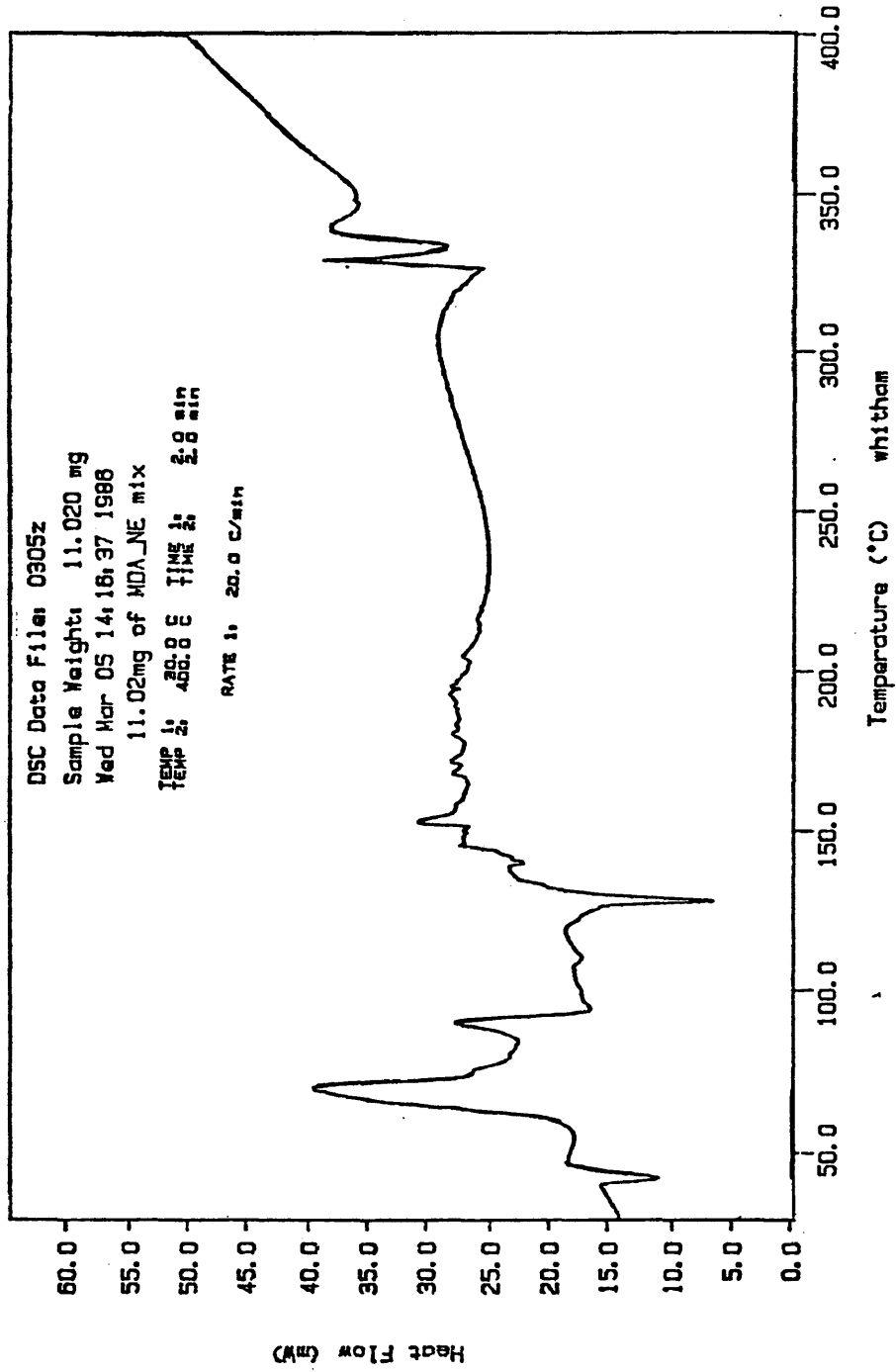


Figure A-5

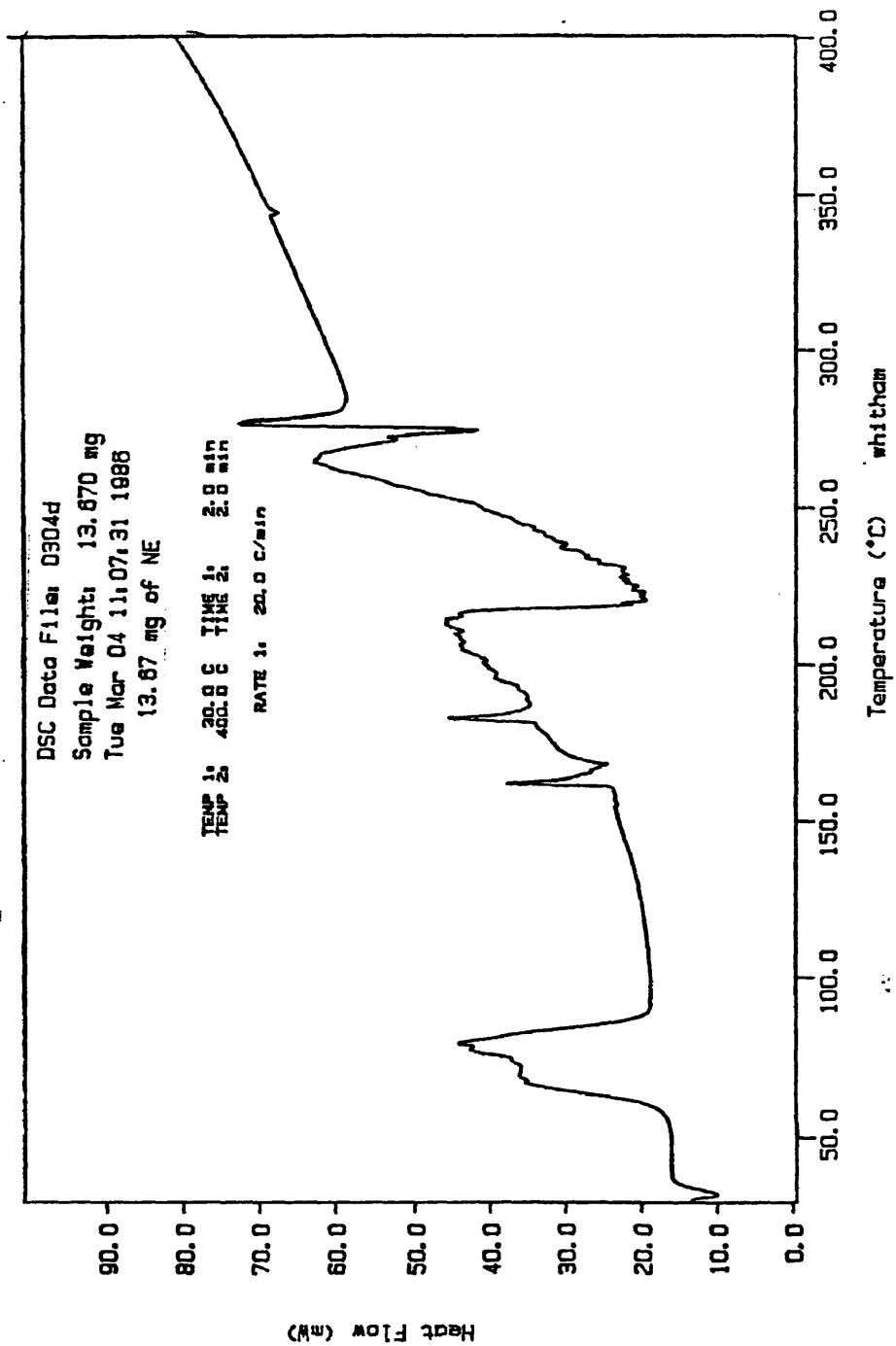


Figure A-6

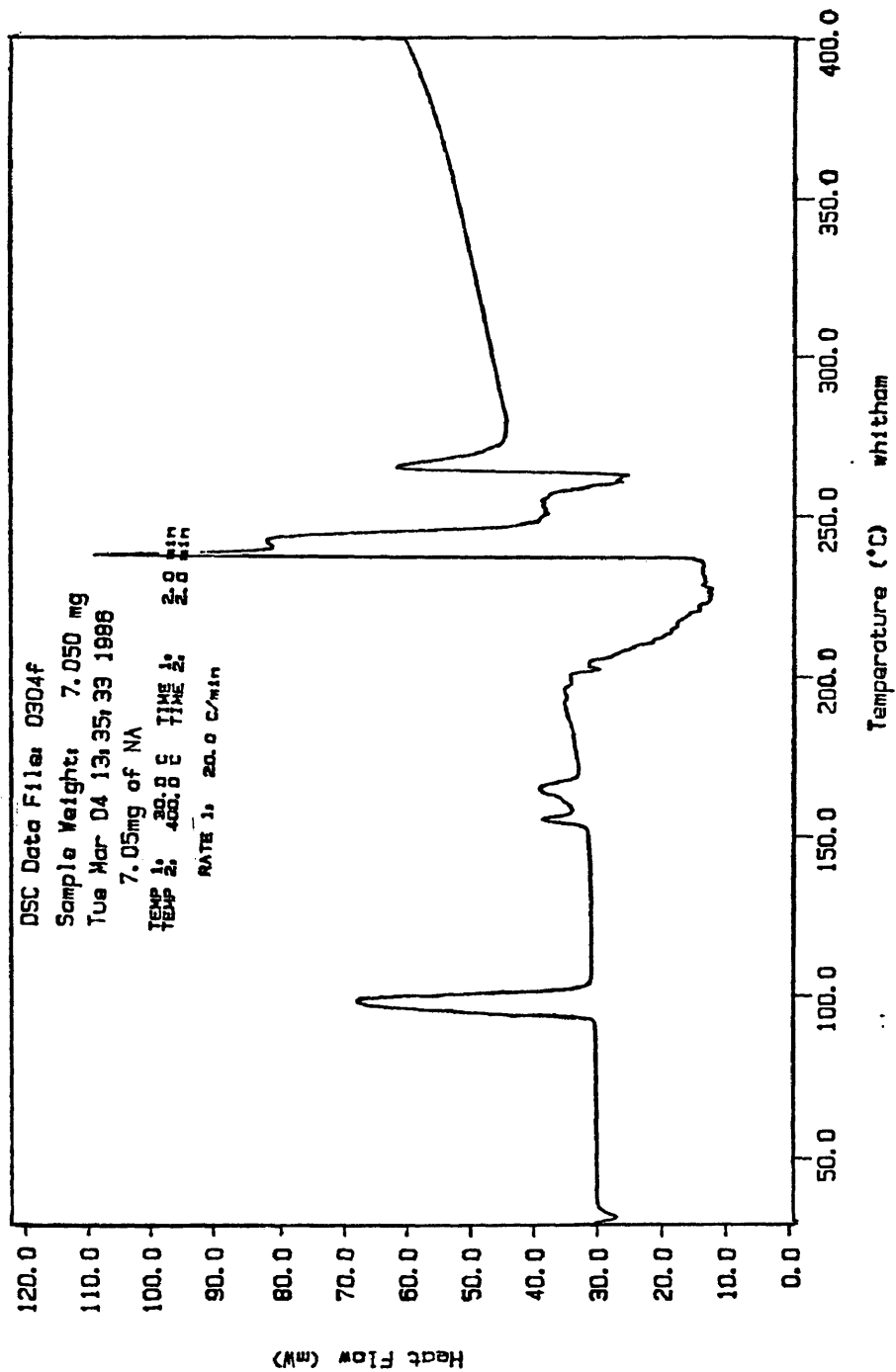


Figure A-7

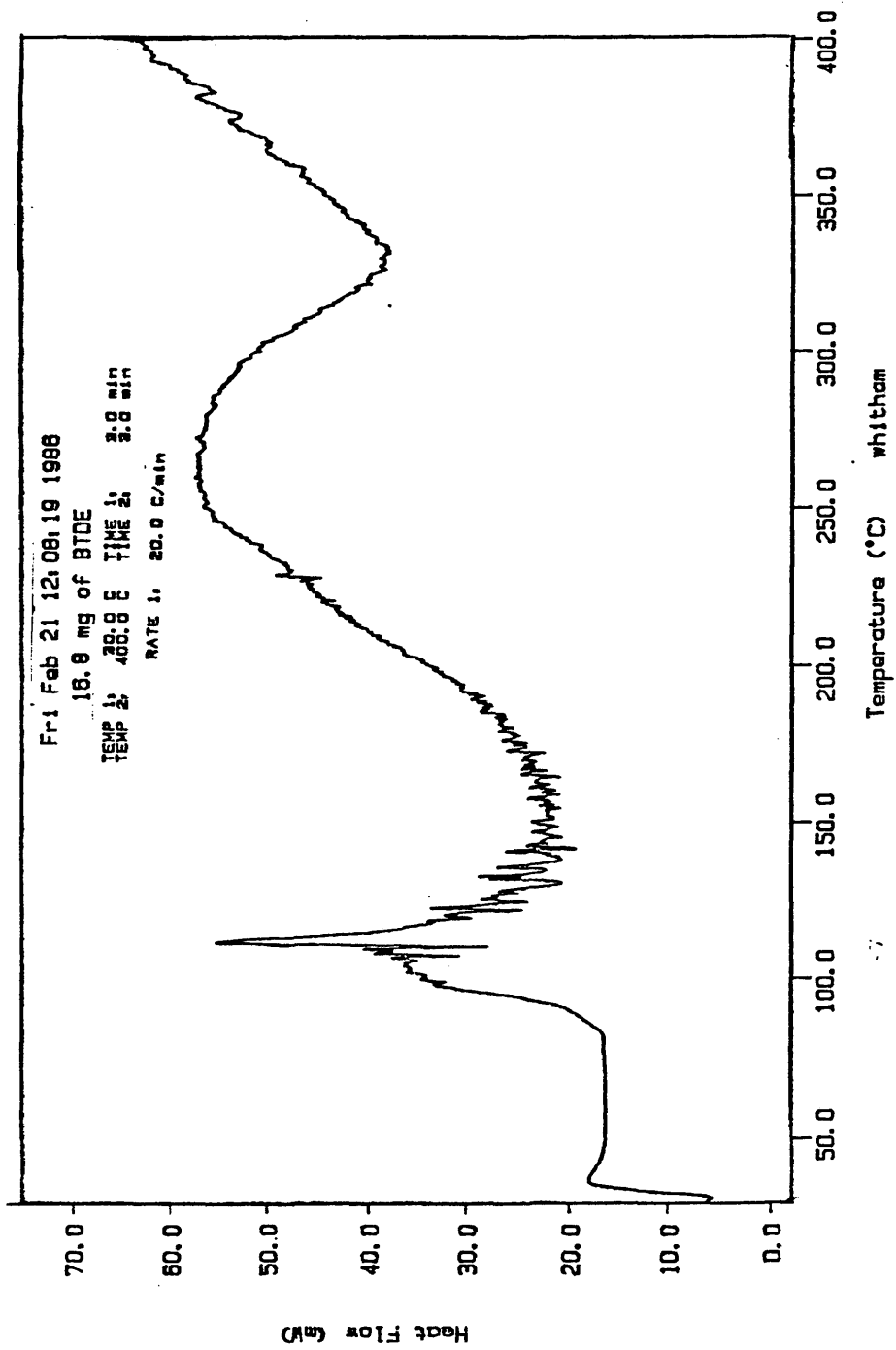


Figure A-8

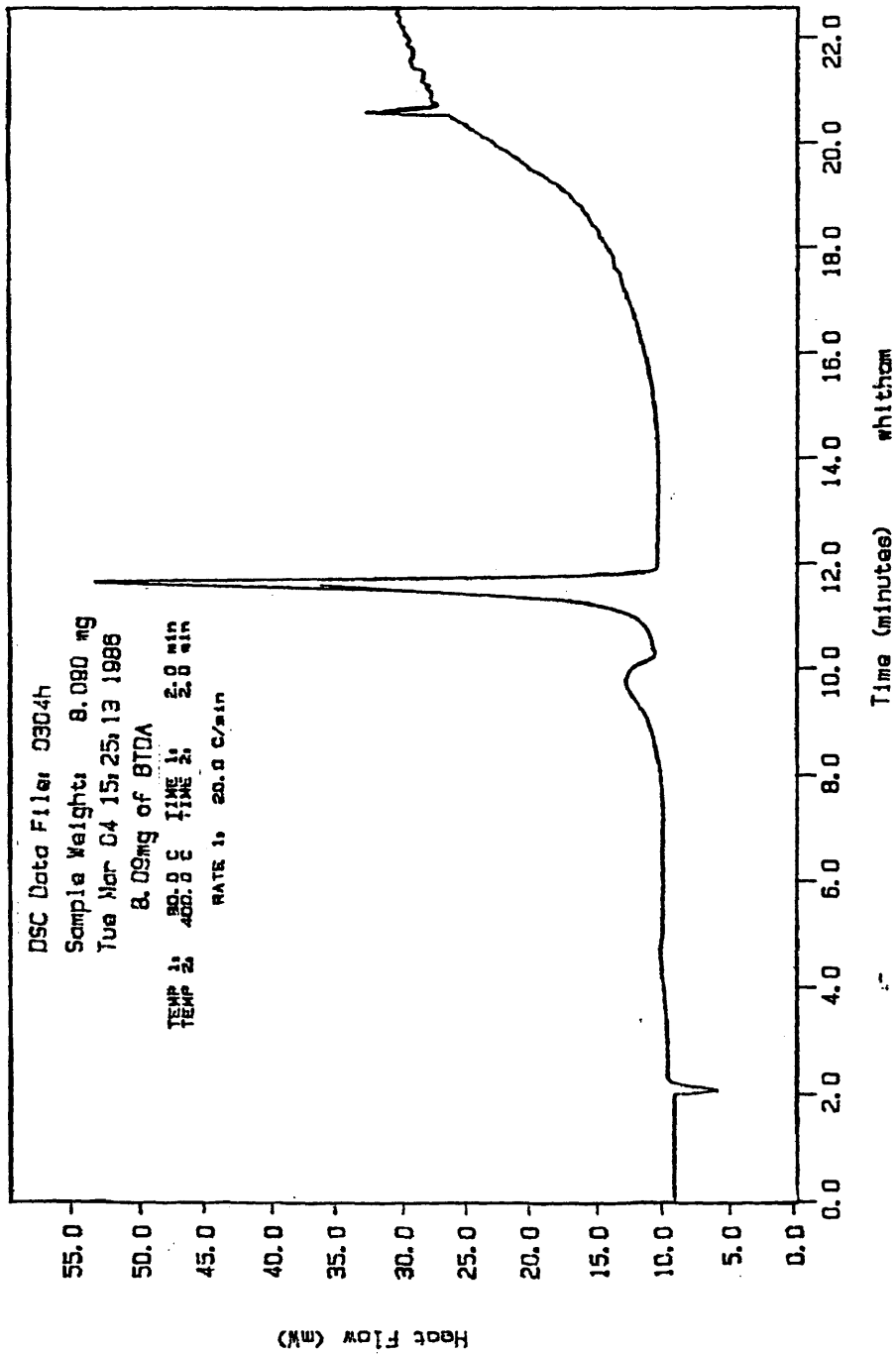
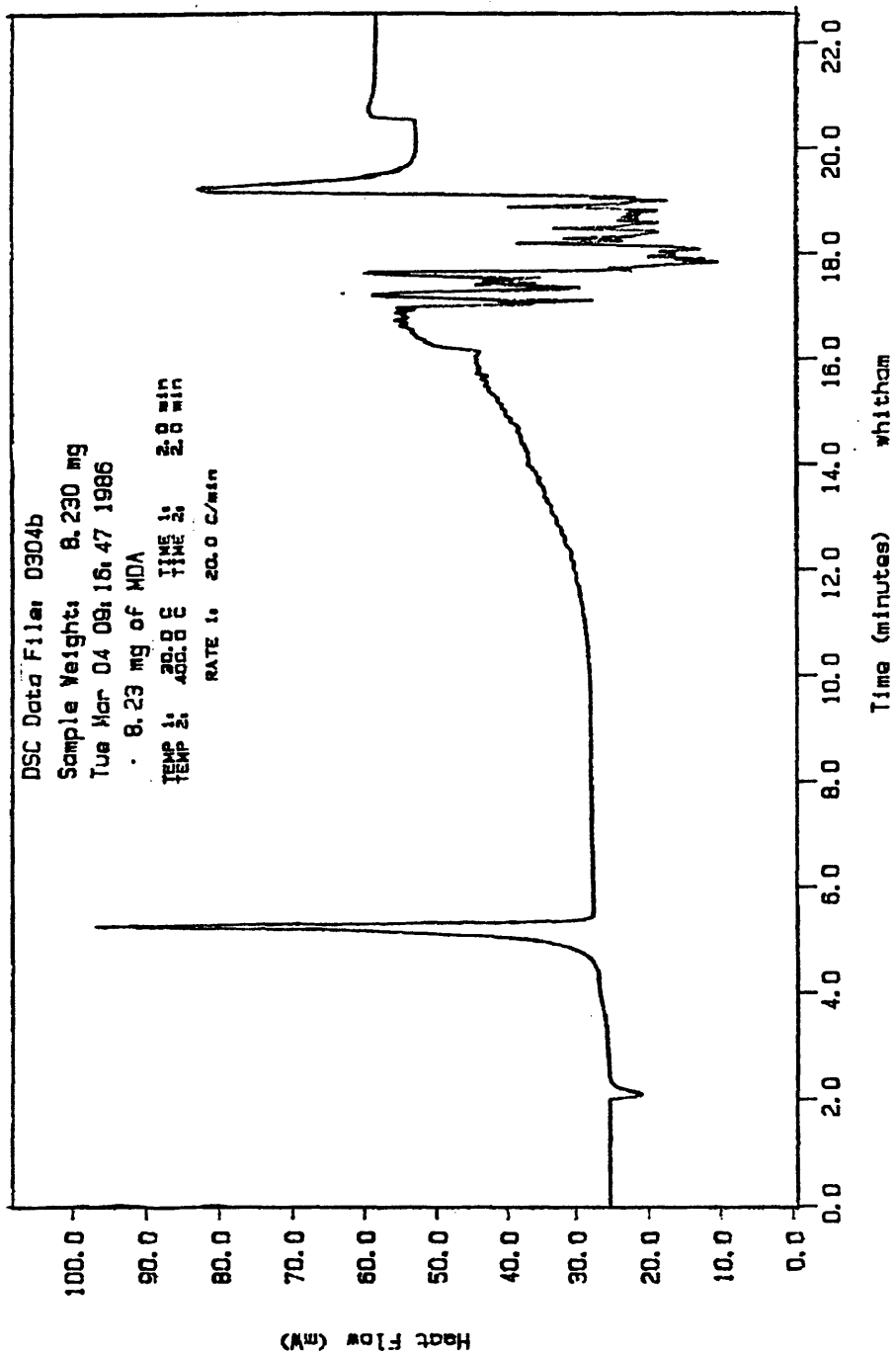


Figure A-9

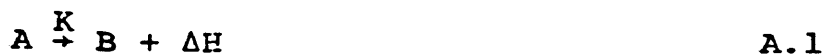


CHAPTER VIII

Activation Energy by DSC

It is possible to determine kinetic properties of a reaction or transition using the DSC. The Perkin-Elmer DSC 7 manual offers an excellent review of kinetic formulas which I will use to help demonstrate how an activation energy is determined.¹

When a material A is converted to B with a heat of physical transition or heat of chemical reaction ΔH , the reaction rate is indicated by K.



Often the rate equation has the general form,

$$\frac{d\alpha}{dt} = K(1-\alpha)^n \quad \text{A.2}$$

In equation A.2 α is the percent of chemical conversion, and n is the order of the reaction. Taking the natural log of both sides of A.2,

$$\ln \frac{d\alpha}{dt} = n \ln(1-\alpha) + \ln K \quad \text{A.3}$$

A plot of $\ln(d\alpha/dt)$ versus $\ln(1-\alpha)$ yields a slope equal to n . For a first order reaction,

$$\ln(1-\alpha) = - \left(K_0 \exp \left(\frac{-E_A}{RT} \right) \right) t \quad \text{A.4}$$

The reaction rate is dependent on temperature by,

$$K = K_0 \exp\left(\frac{-E_A}{RT}\right)$$

where, K_0 =the preexponential constant
 E_A =the activation energy
 R =the gas constant
 T =the absolute temperature
 t =time

A plot of $\ln(1-\alpha)$ versus time yields a slope equal to $-K$. Taking the natural log of both sides of A.5,

$$\ln K = \frac{-E_A}{RT} + \ln K_0$$

A plot of $\ln K$ versus $1/T$ yields a slope equal to E_A/R . The activation energy and the preexponential constant can then be easily calculated.

Several scans must be performed to obtain an activation energy. I will demonstrate how I determined the activation energy for the crosslinking reaction in the aromatic thermosetting polyimide under a pressure of 100 psi as an example.

The first scan which needs to be run is a straight ramp which includes the reaction of interest. Figure E_A1 is a graph of the polyimide from 200 C to 400 C after the sample pans have been subtracted. The immediate features of the graph are the endotherm peak at 250 C and the exotherm peak at 360 C. The endotherm can be attributed to a melt or "softening" and the exotherm can be considered the crosslinking.

In order to calculate the activation energy the K

value must be determined for several different temperatures. Isothermal holds are selected at temperatures after the crosslinking reaction has started. The crosslinking reaction can go to completion if the polyimide is held for a long enough period of time at a temperature where the reaction has already been initiated. Isotherm runs were made at 300 C, 310 C, 320 C, 325 C, and 330 C.

The method for performing an isothermal run involves holding the material at a designated initial temperature, ramping to the prescribed isotherm temperature, and holding at the isotherm for a specified amount of time. A baseline run of empty pans must be run on the same programmed ramp as the sample run. The baseline run should have a flat line at the isotherm because no transition is occurring which requires power compensation to the sample holder. In line with the null balance principle, the crosslinking reaction is exothermic and would require less energy to keep in balance with the reference until the reaction is completed. This implies that the sample run will have a curve which slopes upward and levels off at the completion of the reaction.

A program has been written which will subtract the data from a sample and a baseline run point for point during the isotherm. Figures E_A2 through E_A5 are examples of subtracted curves. Remembering that a reaction is

assumed to be complete when the isotherm becomes flat, we can conclude that the area underneath the line which is extended from the flat portion of the curve and above the subtracted curve represents the α of complete conversion. From figure E_A2 it can be seen that I marked several time intervals in this area. Each time interval represents a percentage of the total area and is considered to be $d\alpha/dt$ in the mathematical calculations.

It is important to notice that the total area becomes smaller as the temperature is increased in figures E_A2 to E_A5. Table 7 indicates the enthalpies calculated from the areas. The enthalpy for 310 C is much higher than the enthalpies at the other temperatures. This may be attributed to some of the reaction occurring before the isothermal hold temperature is reached. I tried an isotherm at 300 C but was unsuccessful in getting a reaction in four hours time. This may imply that not enough energy is added to the sample to start a free radical crosslinking polymerization at 300 C.

Table 7
Delta H in J/g for the temperatures measured.

310	320	325	330
48.16	28.29	25.9	21.56
	34.9	22.5	31.8
		36.16	

From the mathematics included at the beginning of this section we know that the order of the reaction can be determined by a plot of $\ln\left(\frac{d\alpha}{dt}\right)$ versus $\ln(1-\alpha)$. I

determined the n value for a run at 310 C, 320 C, and 330 C. One can see from table 8 that it is reasonable to conclude that the crosslinking is a first order reaction. Figure E_A6 shows the curve for the 330 isotherm.

Table 8
The Determination of the Reaction Order.

Isotherm Temperature	n
310	.93
320	1.08
330	.93

Knowing that the reaction is first order it is then possible to determine the K for the reaction. Remembering the mathematics, a plot of $\ln(1-\alpha)$ versus time will yield a slope equal to K. Table 9 shows a compilation of all the K's determined for this study. Figure E_A7 shows the curve for the 330 isotherm.

Table 9
The Determination of Reaction Rate

T (°C)	1/T (°C ⁻¹)	K (min ⁻¹)	ln K
310	3.23*10 ⁻³	.055	-2.89
320	3.13*10 ⁻³	.078	-2.55
320	3.13*10 ⁻³	.142	-1.95
325	3.07*10 ⁻³	.178	-1.72
325	3.07*10 ⁻³	.312	-1.16
325	3.07*10 ⁻³	.343	-1.07
330	3.03*10 ⁻³	.281	-1.27
330	3.03*10 ⁻³	.426	-0.85

Figure E_A8 is a plot of $\ln K$ versus $1/T \cdot 10^{-3}$. The slope of a line through the indicated points yields the activation energy. The intercept yields the preexponential factor. The data points from table 8 were submitted to a $y = mx + b$ curve fit program. The values determined were,

$m = 1.08 \cdot 10^4$ with a slope deviation of 1044

$b = 31.7$

We can conclude that the activation energy and the \log of the preexponential factor can be determined with a 10% error for the aromatic thermosetting polyimide at 100 psi. Here,

$$E_A = 21.4 \text{ Kcal}$$

$$K_0 = 5.85 \cdot 10^{13} \text{ sec}^{-1}$$

Figure E_A1

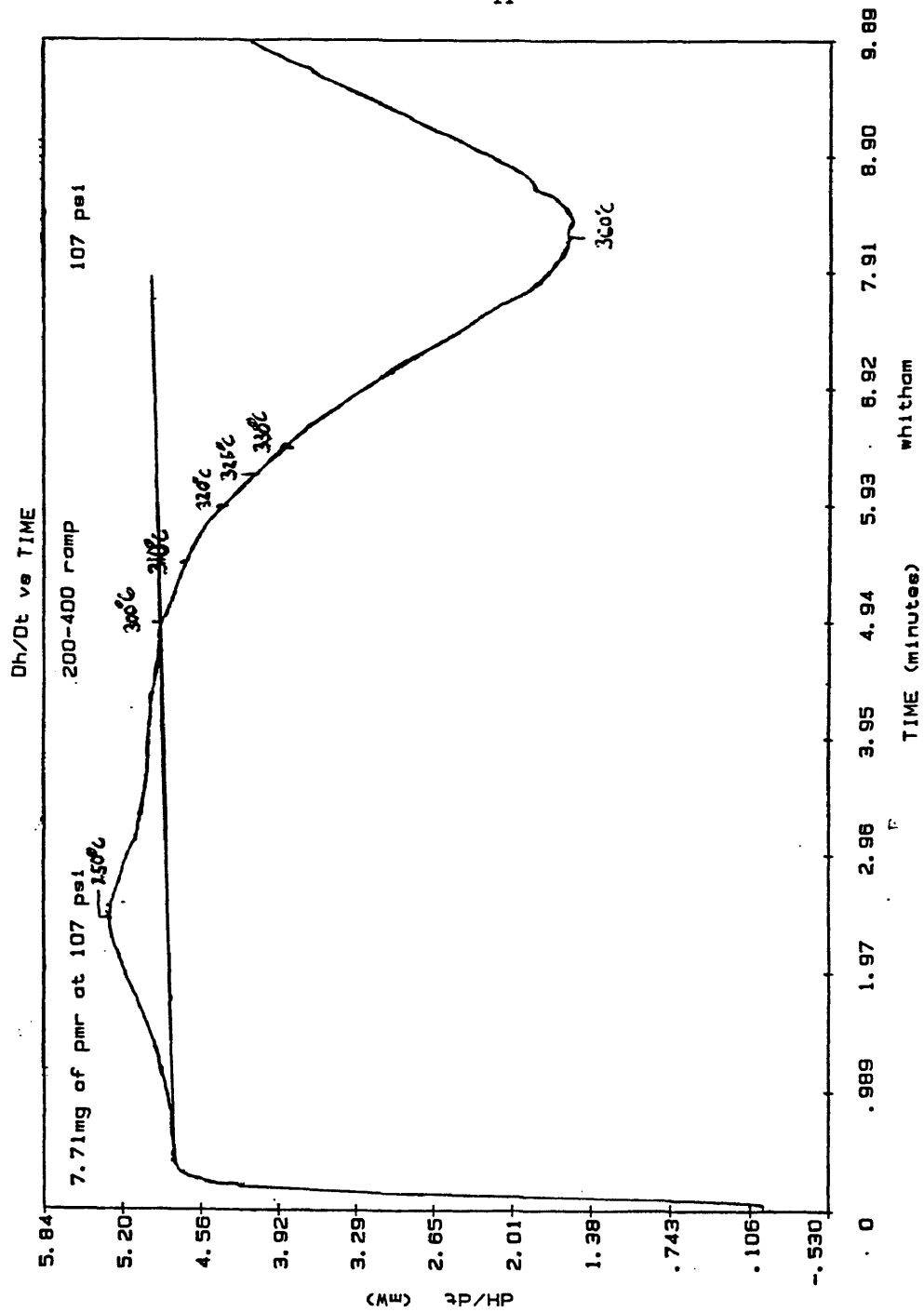


Figure E_A2

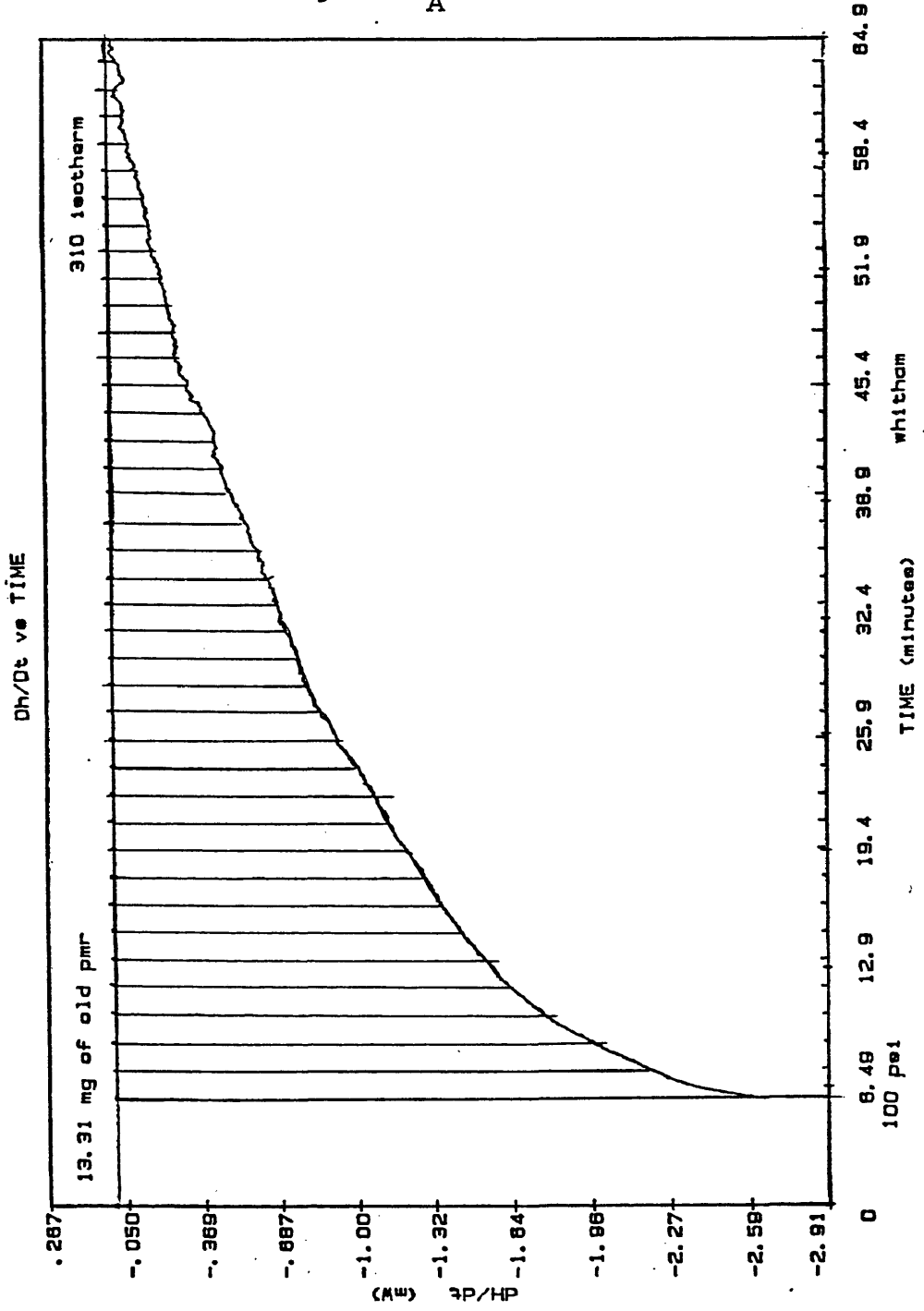


Figure E_A3

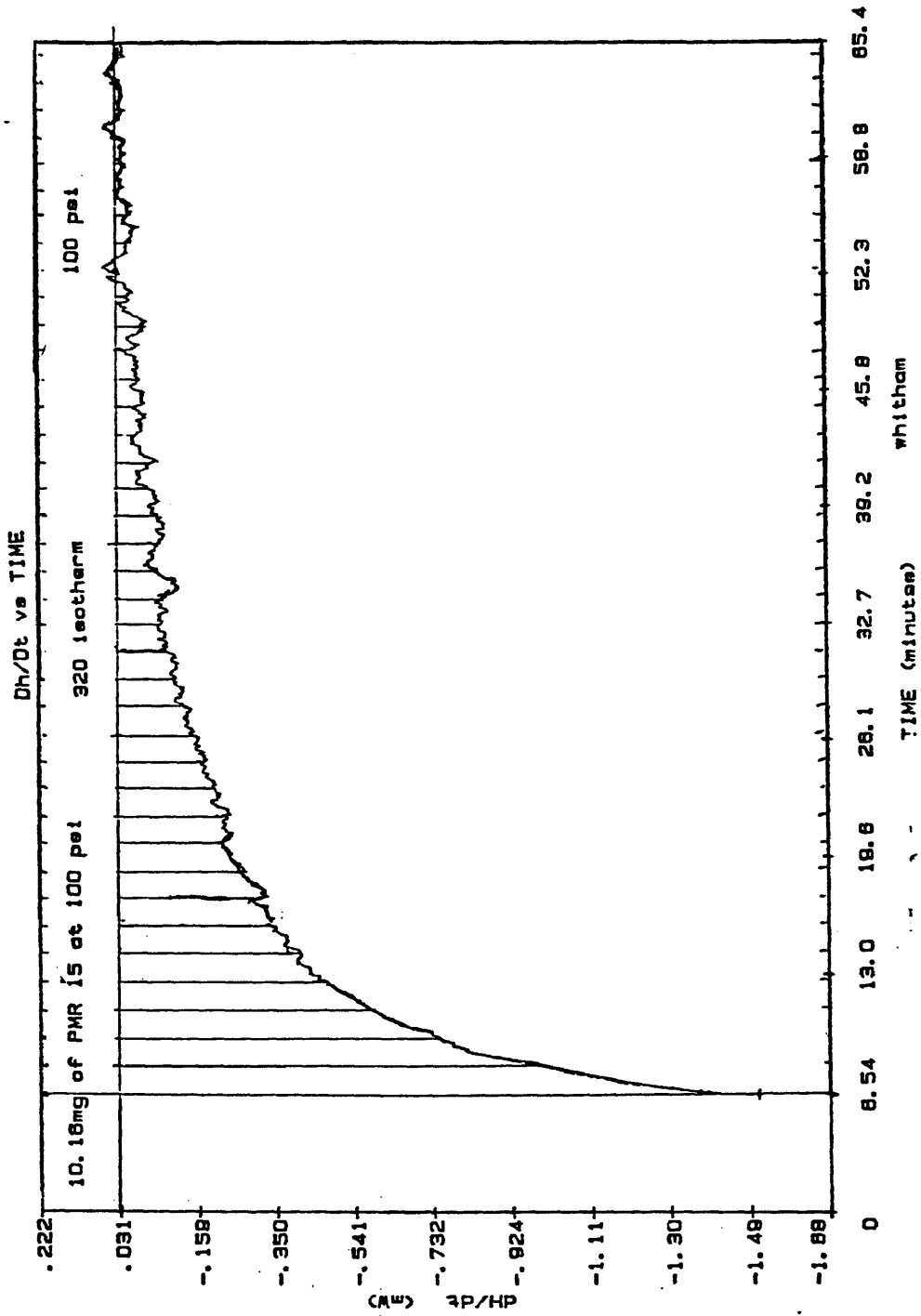


Figure E_A 4

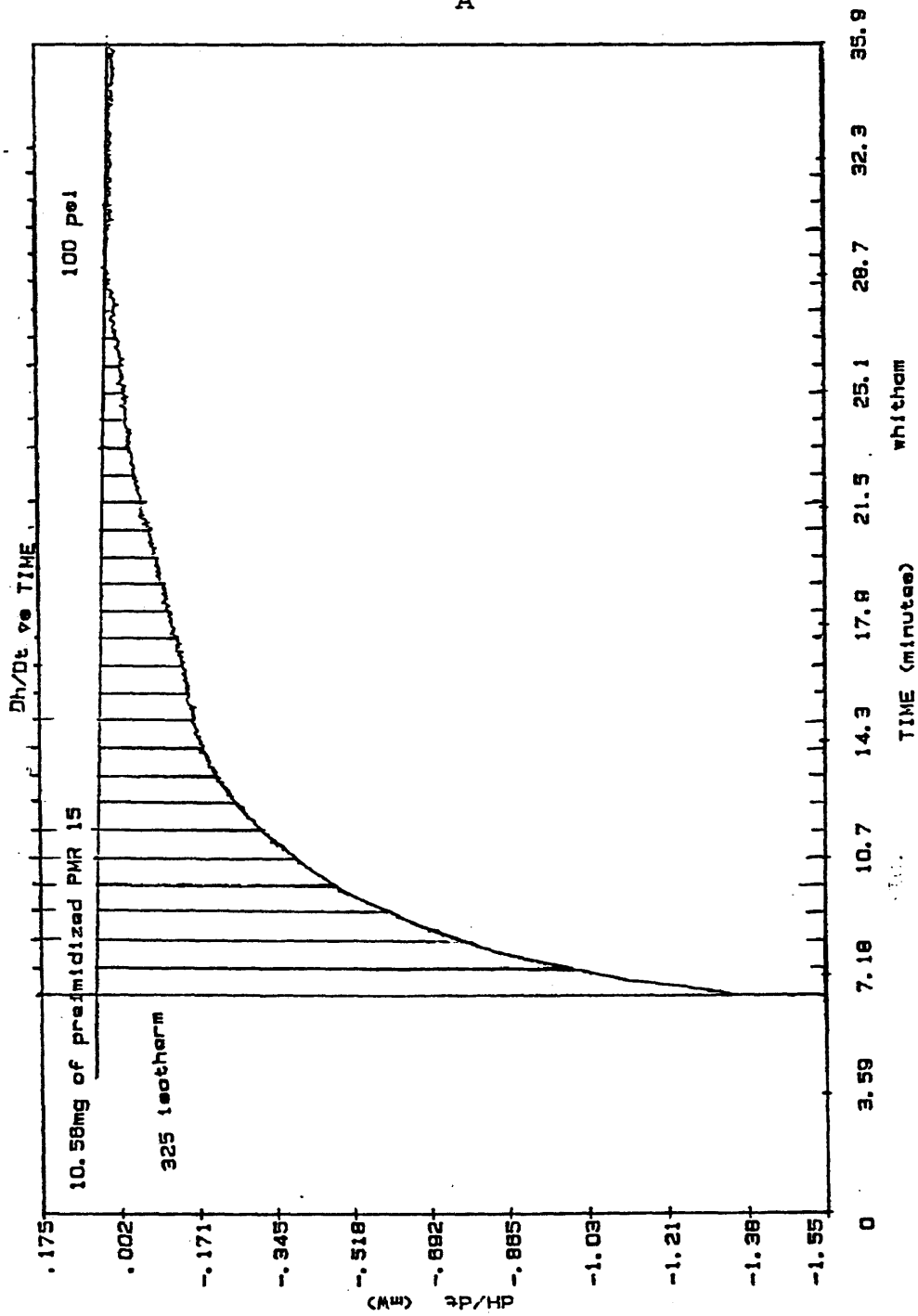


Figure E_A5

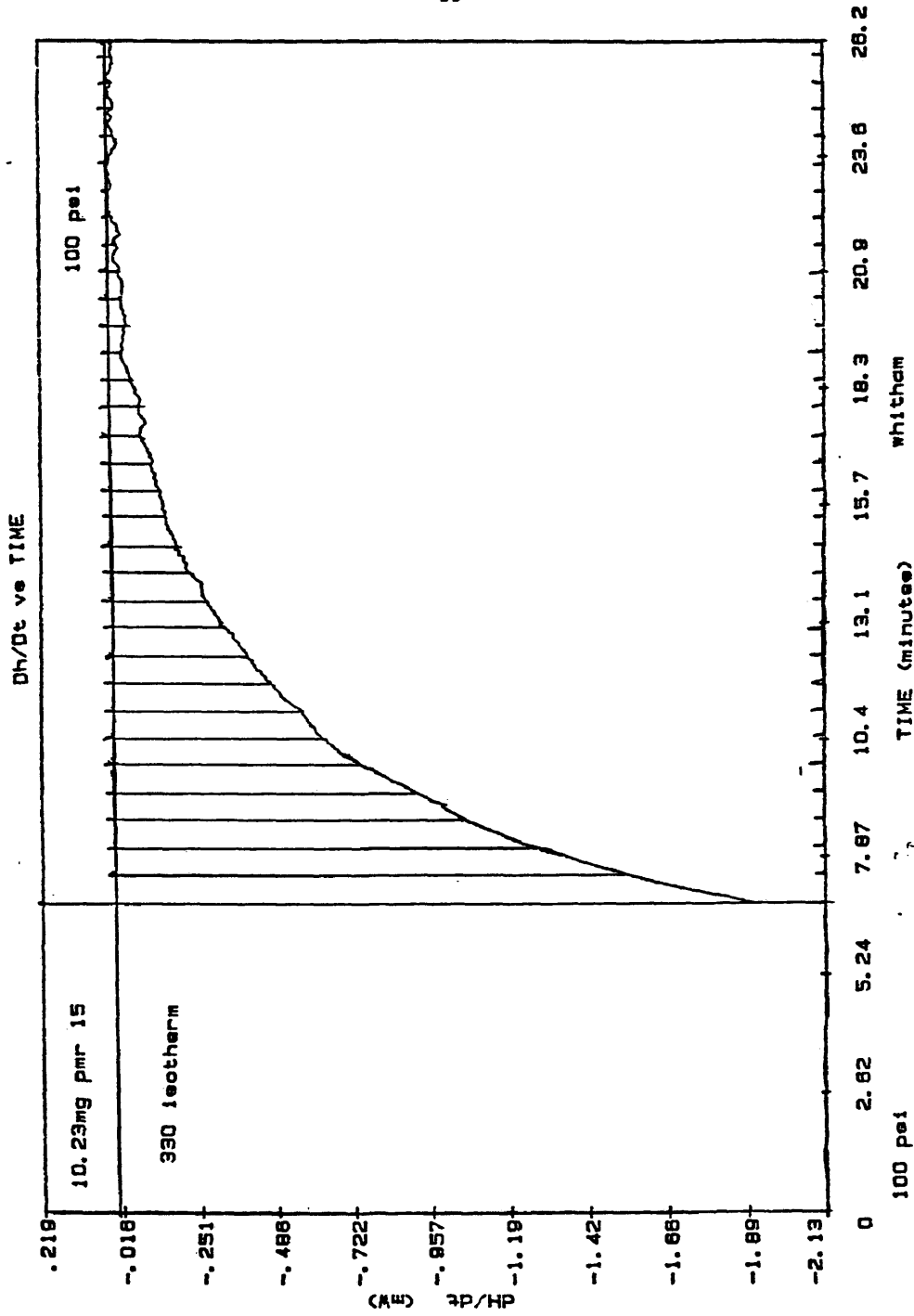


Figure E_A6

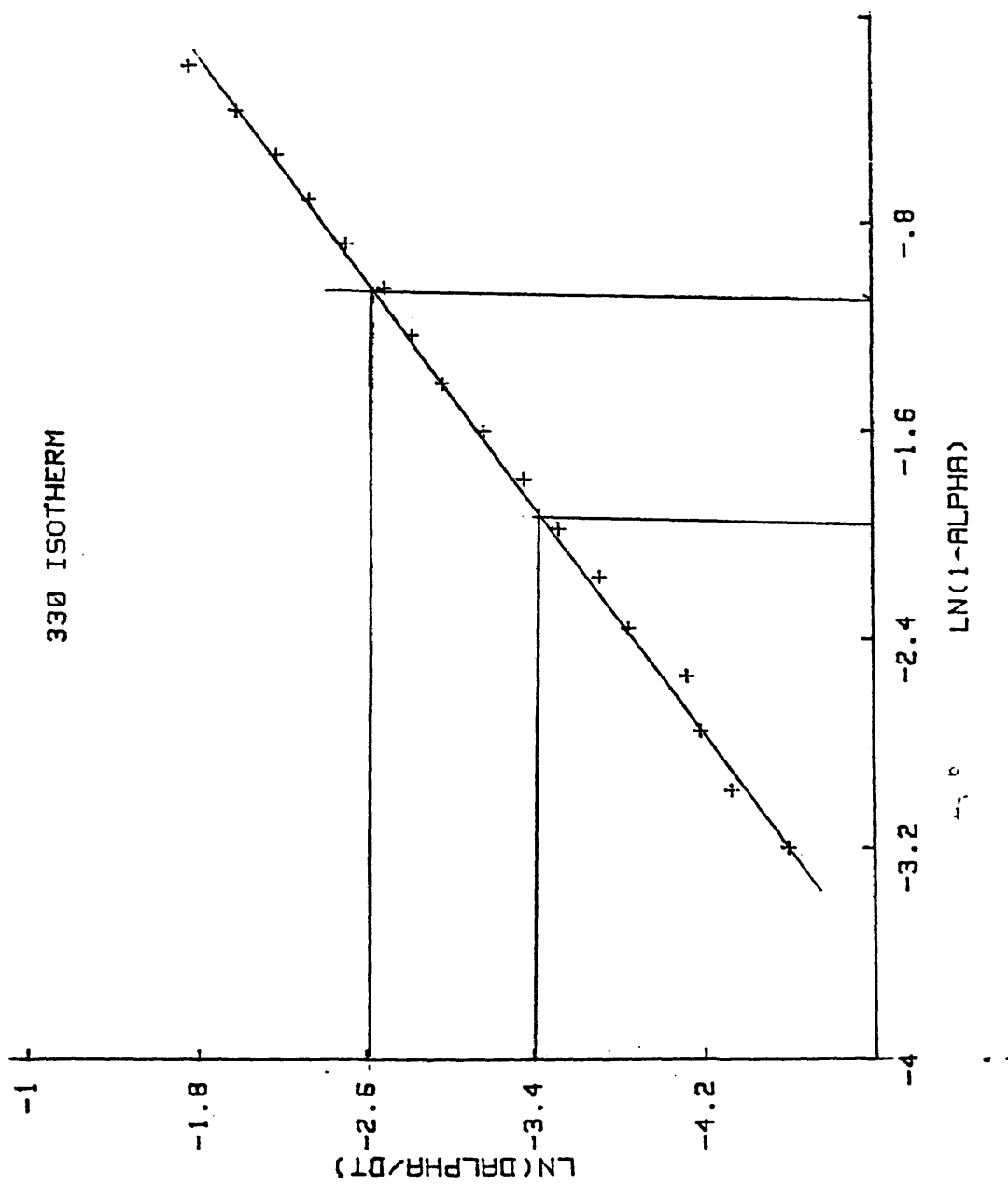


Figure E_A7

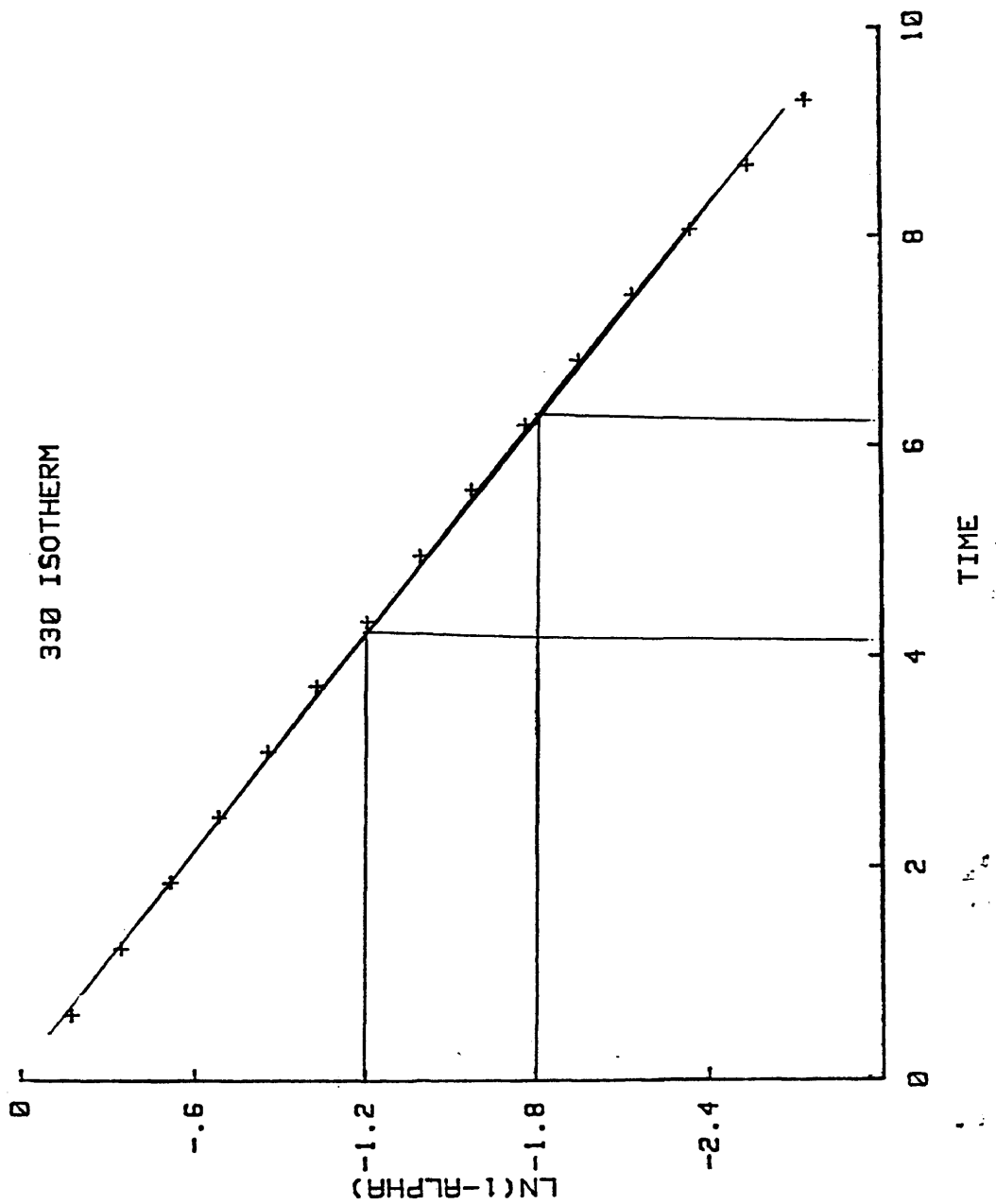
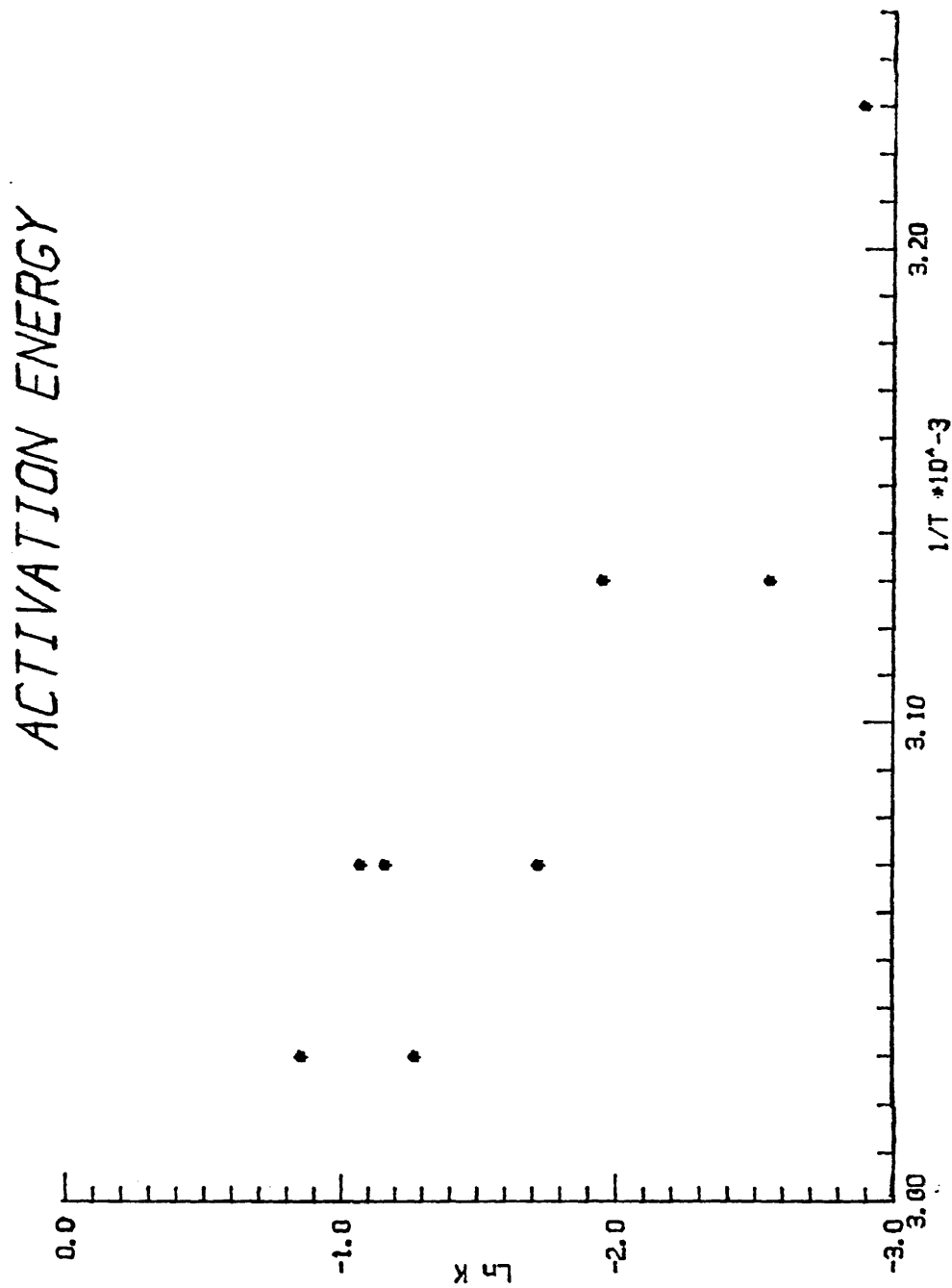


Figure E_A 8

NOTES FOR CHAPTER VIII

1. Perkin Elmer DSC 7 Manual

CHAPTER IX

Pressure Runs on the DSC

The thermal behavior of polymers can be pressure dependent as well as temperature dependent. The crosslinking reaction of the aromatic thermosetting polyimide is usually performed under pressure by industrial manufacturers and may give different products depending on the pressure. Therefore, it was imperative for our laboratory to develop a method for doing DSC runs under pressure.

The DSC 7 did not come equipped to do pressure runs. S. M. Hsu et al have published a method describing how they modified a Perkin-Elmer instrument for operation under pressures of several hundred psi.¹ We determined that the swing-away enclosure cover can contain a pressure of 100 psi without major modifications.

A flow through cover allows gases to be released from the reacting mixture directly above the sample and reference holders. We placed a valve on top of the flow through cover allowing pressure to be built up in the instrument chamber.

The instrument chamber is purged by nitrogen gas

during all runs. The gas serves the purpose of providing an inert environment for thermal reactions thereby eliminating oxidation reactions which may occur in air. The purge gas also carries heat away from the sample holder if an exothermic reaction occurs in the sample holder. If the heat energy had no way of leaving the chamber the DSC would indicate the exotherm persisted much longer than it does in reality. Restriction orifices in line with the nitrogen tank allow the nitrogen to purge at a slow rate. The optimum tank pressure is twenty psi going into the orifices.

Our method of maintaining a constant pressure is dependent on keeping the nitrogen purging from the chamber at the same rate as if the valve above the flow through cover was completely open. To accomplish this goal the line from the valve is bubbled through glycerine. By simply counting the bubbles formed when the tank pressure is 20 psi and the valve is open, the purge rate can be determined for a nonpressure run. If the tank pressure is turned up to 105 psi and the valve is completely closed, 105 psi will be slowly built up in the instrument chamber. If the valve is opened just enough to allow the purge gas to exit at the same rate as a nonpressure run, a pressure of 100 psi can be maintained during a scan. The pressure in the instrument chamber is sensed by a gauge which is put in-line before the valve.

Two effects that immediately come to mind for experiments that deal with high temperatures and pressures are the elevation of boiling points of liquids and the separation of a pressure dependent reaction from a competing nonpressure dependent reaction. We found that curing the polymer under pressure also cut down noise caused by bubbling during a reaction and made peaks sharper.

To determine the accuracy of my pressure measurement I performed an experiment I found in the literature.² The CRC reports tables of temperature-pressure data for H₂O to which I could compare to the results I obtained from my instrument. Fifty milliliters of deionized water were distilled for the experiment to insure purity. Temperature and the equilibrium vapor pressure can be related by the Claperyon equation,

$$\ln P = \frac{\Delta H_v}{RT} + C$$

The slope of a line from a graph of $\ln P$ versus $1/T$ is equal to,

$$\frac{H_v}{RT} = \frac{\lambda vM}{2.303RT}$$

where, λ =latent heat of vaporization

M =molecular weight

R =gas constant (1.9872 cal/(K*mol))

T =temperature

I used semilog paper to plot the pressure in psi versus $1/T \cdot 10^{-3}$. From the slope of this curve I could

determine the latent heat of vaporization to be 524 cal/g. The accepted value for water is 539 cal/g. Table 9 summarizes the data obtained from the experiment. Figure P1 shows the plot of table 9 data.

Table 9

Relationship of Pressure to Temperature

Gauge psi	Atm. P.	CRC Table	Temp. Obs.	1/Temp. Obs.(K)
0	15	100	102	$2.66 \cdot 10^{-3}$
19	34	125	124	$2.52 \cdot 10^{-3}$
31	46	136	134	$2.46 \cdot 10^{-3}$
50	65	148	149	$2.37 \cdot 10^{-3}$
83	98	164	162	$2.30 \cdot 10^{-3}$
123	138	178	180	$2.20 \cdot 10^{-3}$

I have an accuracy of 6 psi when I run samples under pressure. An error of 2 psi comes from my ability to read the gauge and an error of 4 psi comes from a 2 degree temperature error. Figure P2 is an example of a water under pressure run.

Figure P1

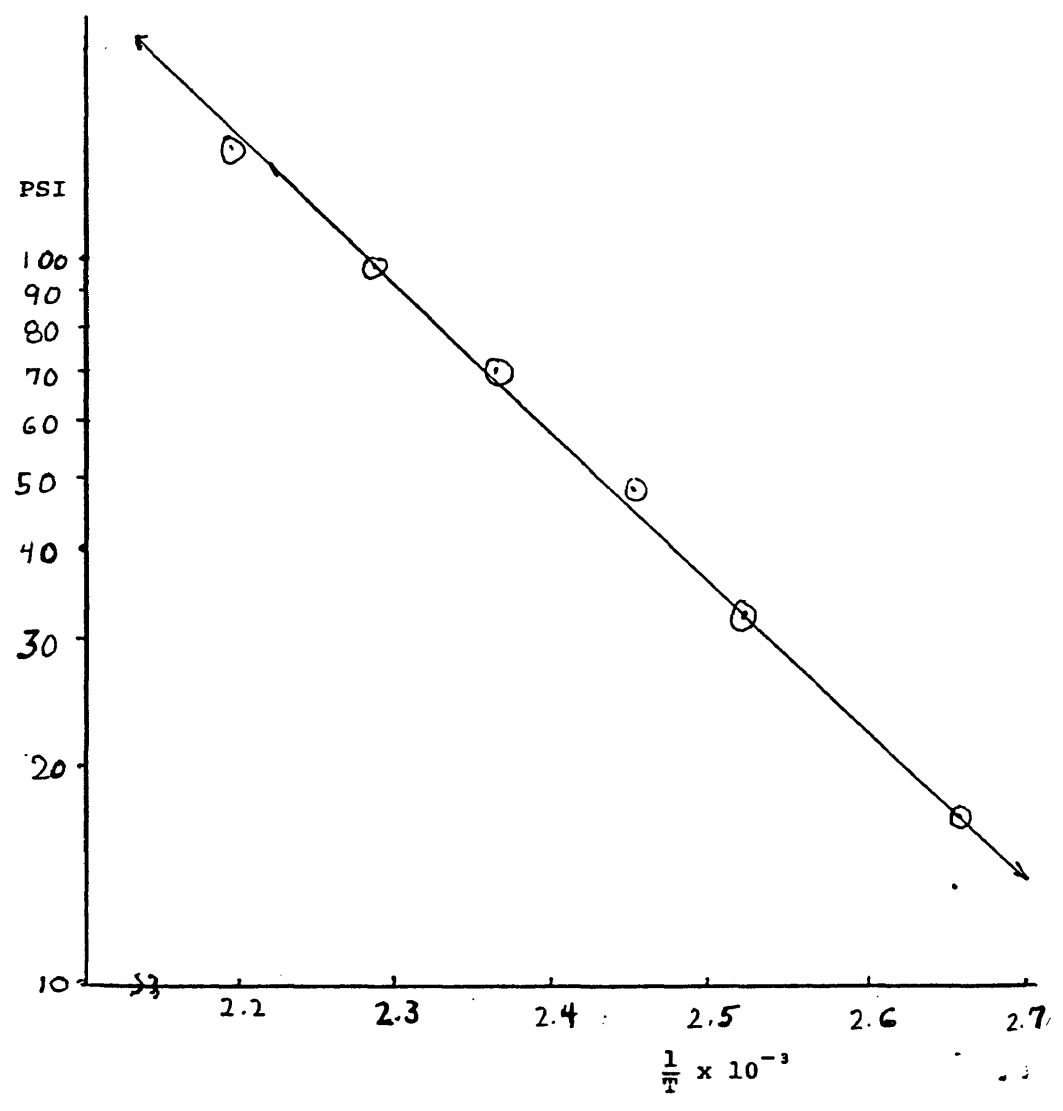
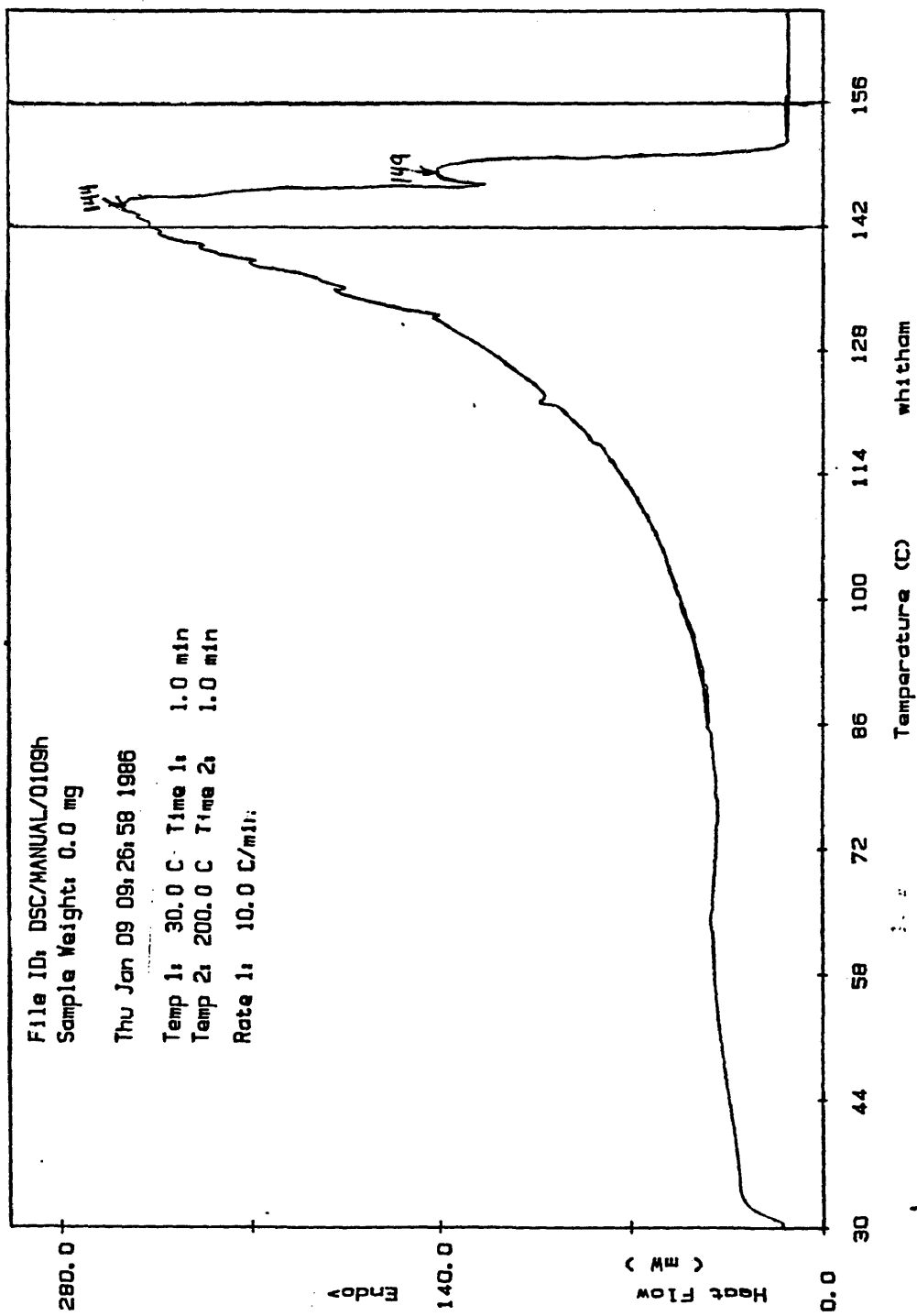


Figure P2



NOTES FOR CHAPTER IX

1. S. M. Hsu, A. L. Cummings, and D. B. Clark, SAE Reprint (821252), SAE, Inc., Warrendale, Pa., 1983.
2. Paul F. Levy, Gerrit Nieuweboer, and Ludwig C. Semanski, Thermochimica Acta, 1, 429(1970).

CHAPTER X

The Crosslinking Reaction

The presumed rate limiting step for the thermally induced crosslinking reaction is a retro Diels-Alder reaction.¹ However, the detailed nature of the crosslink has not been defined. Kinetic and energetic observations made by our laboratory and Dr. Lauvers' laboratory support a retro Diels-Alder mechanism. Figure Chem5 in chapter I shows this reaction.

Table 1 shows the data obtained by our laboratory for the aromatic thermosetting polyimide for the crosslinking reaction under 0 psi nitrogen and 100 psi nitrogen. Dr. Lauver did his experiments in a DSC under 300 psi nitrogen, and his results are also printed.

Table 1

Kinetic and Energetic Data.

<u>Pressure</u>	<u>Reaction Order</u>	<u>Preexponential A</u>	<u>E_A Kcal/mole</u>
0 psi	First	$3.3 \cdot 10^5$	13.7
100 psi	First	$5.85 \cdot 10^{13}$	21.4
300 psi	First	$4.24 \cdot 10^{13}$	44

In a study on cotton cellulose expansion, Franklin et al discussed why a retro Diels-Alder reaction can be assumed to be the rate limiting step for thermal

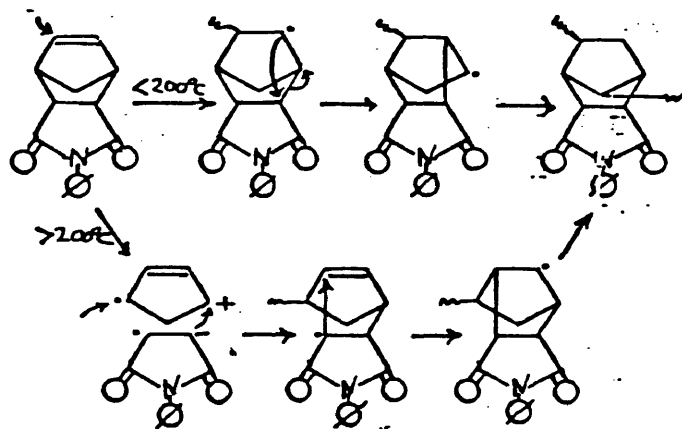
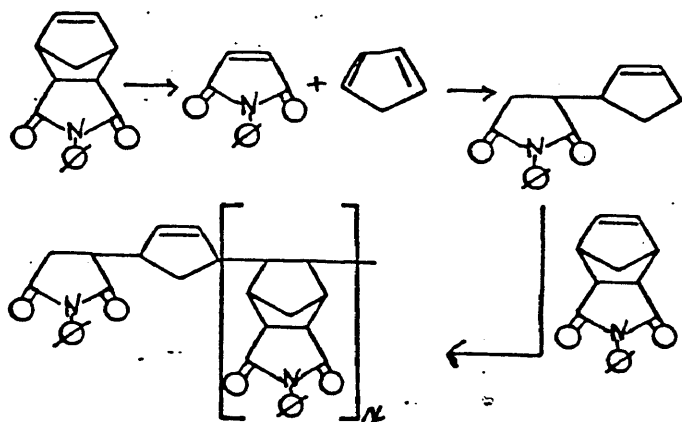
crosslinking reactions in compounds of the norbenyl moiety.² Characteristics of retro Diels-Alder reactions can be examined to support the assumption that the crosslinking reaction occurs by this mechanism.

The crosslinking reaction is first order which is characteristic of a retro Diels-Alder. The preexponential value of $A=10^{13} \text{ sec}^{-1}$ is a classic vibrational value for a first order thermal fission reaction.¹ The observed activation energies are in agreement with data for unimolecular thermal fission reactions.³ Plus, a most interesting result comes from examination of the E_A data. Notice that the E_A increases as the pressure increases. This result is expected because pressure would force the retro Diels-Alder in the opposite direction thus making the activation energy higher. In fact many Diels-Alder reactions are done at high temperatures under pressure because cyclopentadiene is a volatile reactive gas under these conditions. Crosslinking of the endcappers could proceed by a free radical addition reaction. I am not certain as to how the crosslinking can be initiated and propagated.

Model compounds containing endcapped nadimides have been studied.^{4,5,6} Kumar et al clearly demonstrated by GC/mass spec techniques that cyclopentadiene is released during the crosslinking reaction of a bisnadimide endcapped model compound.⁴ Gaylord and Martan proposed a mechanism

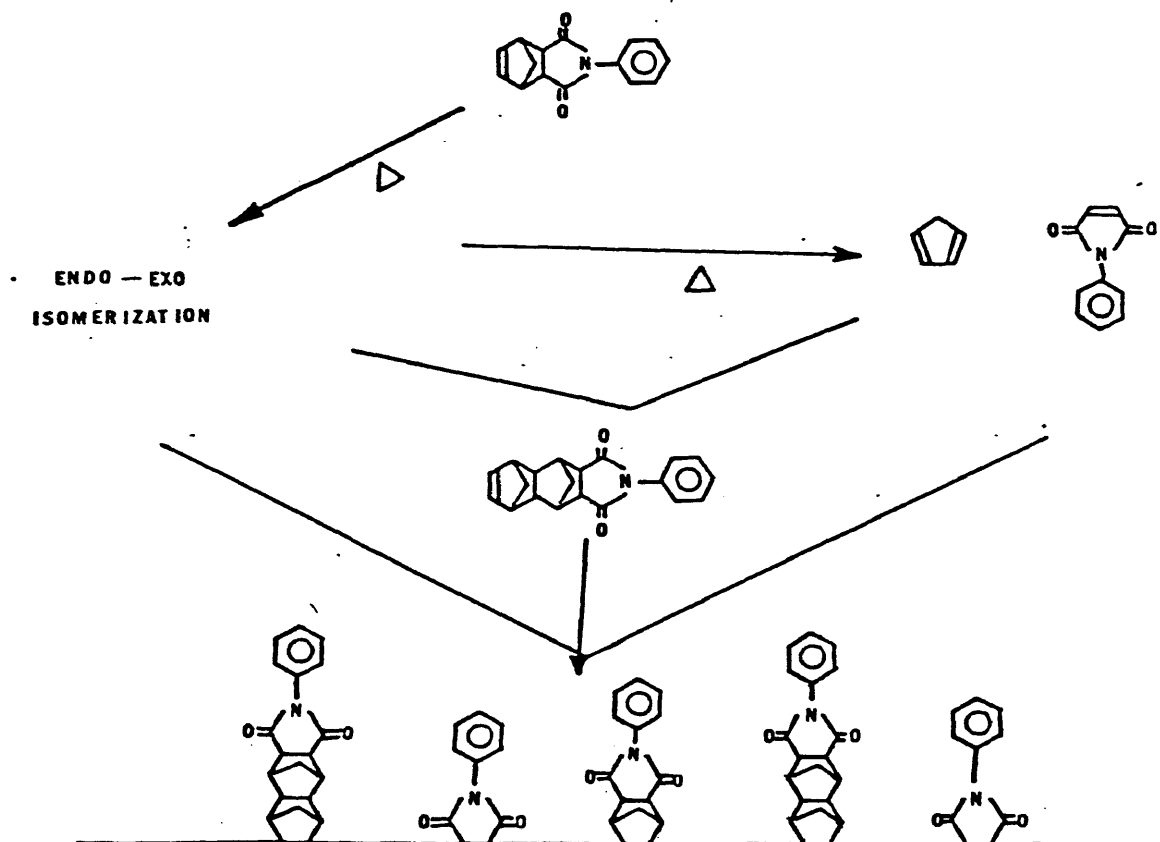
for the crosslinking of norbornene endcappers.⁵ In the Gaylord experiment a free radical was introduced in the form of a peroxyester of hydroperoxide. Figure CR-1 illustrates the mechanism. Wong and Ritchey also proposed a reaction sequence for the norbornene endcapper.⁶ Using ^{13}C -NMR, they determined that a reaction does not occur when the carbon-carbon double bond is hydrogenated. Figure CR-2 illustrates the sequence.

Figure CR-1



Reproduced from Gaylord and Martan.

Figure CR-2



Reproduced from Wong and Ritchey.

NOTES FOR CHAPTER X

1. Richard W. Lauver, J. Pol. Sci.: Pol. Chem. Ed., 17, 2529(1979).
2. W. E. Franklin, C. H. Mack, and S. P. Rowland, J. Pol. Sci. A-1, 7, 1169(1969).
3. S. W. Benson, "The Foundations of Chemical Kinetics," McGraw-Hill, New York, 1960.
4. Devendra Kumar, George M. Fohlen, and J. A. Parker, J. Pol. Sci.: Pol. Chem. Ed., 21, 565(1983).
5. N. G. Gaylord and M. Martan, ACS Pol. Preprints, 22, (1), 11(1981).
6. A. C. Wong and W. M. Ritchey, Macromolecules, 14, 825 (1981).

BIBLIOGRAPHY

Ronald S. Bauer, et.al., "Epoxy Resin Chemistry," American Chemical Society, Washington D.C. (1979).

S. W. Benson, "The Foundations of Chemical Kinetics," McGraw-Hill, New York, (1960).

Fred W. Billmeyer, "Synthetic Polymers," Anchor Books, Doubleday and Co., Inc., New York, (1972).

Fred W. Billmeyer, et.al., "Experiments in Polymer Science," John Wiley and Sons, Inc., New York, (1973).

Vera V. Daniel, "Dielectric Relaxation," Academic Press, London, (1967).

Mansel Davies, et.al., "Dielectric and Related Molecular Processes: Volume 3," The Chemical Society, London, (1977).

Peter Debye, "Polar Molecules," The Chemical Catalogue Company, Inc., New York, N.Y., (1929).

S. E. Delos, R. K. Schellenberg, J. E. Smedley, and D. E. Kranbuehl, J. Ap. Poly. Sci., 27, 4295 (1982).

John B. Enns and John K. Gillham, J. Ap. Poly. Sci., 28, 2567 (1983).

W. E. Franklin, C. H. Mack, and S. P. Rowland, J. Poly. Sci. A-1, 7, 1169 (1969).

Herbert Frohlich, "Theory of Dielectrics," Oxford University Press, London, (1949).

Henry T. Gaud, Comprehensive Analytical Chemistry, 12, 8 (1982).

N. G. Gaylord and M. Martan, ACS Poly. Preprints, 22, (1), 11 (1981).

Nora E. Hill, et.al., "Dielectric Properties and Molecular Behavior," Van Nostrand Reinhold Co., New York, N.Y., (1969).

S. M. Hsu, A. L. Cummings, and D. B. Clark, SAE Reprint, (821252), SAE, Inc., Warrendale, Pa., (1983).

J. F. Johnson and R. H. Cole, J. Am. Chem. Soc., 73, 4563 (1951).

Patricia K. Jue, "Dynamic Dielectric Analysis of the Cure Process of Some Polymer Systems," Honors Thesis, The College of William and Mary, (1983).

Theodore B. Kingsbury, "Dielectric Relaxation in the UHF and RF Regions," Masters Thesis, The College of William and Mary, (1977).

D. Kranbuehl, S. Delos, E. Yi, J. Mayer, and T. Jarvie, Proc. of the Soc. of Plastics Eng., (ANTEC), 311 (1985).

D. Kranbuehl, S. Delos, M. Hoff, and L. Weller, ACS: PMSE, 54, 535 (1986).

D. E. Kranbuehl, S. E. Delos, and P. K. Jue, SAMPE J., July/August, 18 (1983).

D. E. Kranbuehl, S. E. Delos, E. C. Yi, and J. T. Mayer, Proc. of the 2nd Intl. Conf. on Polyimides, 469 (1985).

D. Kranbuehl, S. Delos, E. Yi, M. Hoff, and M. Whitham, ACS: PMSE, 53, 191 (1985).

Devendra Kumar, George M. Fohlen, and J. A. Parker, J. Poly. Sci.: Poly. Chem. Ed., 21, 565 (1983).

Richard W. Lauver, J. Poly. Sci.: Poly. Chem. Ed., 17, 2529 (1979).

R. W. Lauver, W. B. Alson, and R. D. Vanucci, NASA-TM-79063, (n79-1621) (1979).

Paul F. Levy, Gerrit Nieweboer, and Ludwig C. Semanski, Thermochimica Acta, 1, 429 (1970).

- T. J. Lewis, "The Dielectric Behavior of Non-Crystalline Solids," in Dielectric and Related Molecular Processes, Ch. 7, The Chemical Society, London, U.K., (1977).
- J. L. McNaughton and C. T. Mortimer, "Differential Scanning Calorimetry," Perkin Elmer Corp., Norwalk, Conn., (1975).
- John O'Malley, "Basic Circuit Analysis," McGraw-Hill Book Co., New York, (1982).
- M. J. O'Neill, Analytical Chemistry, 38, no. 10, 1331 (1966).
- Perkin Elmer Thermal Analysis Newsletter, 1, (1970).
- Perkin Elmer Thermal Analysis Newsletter, 3, (1970).
- Perkin Elmer Thermal Analysis Newsletter, 9, (1970).
- Perkin Elmer, "DSC 7 Differential Scanning Calorimeter Manual," Perkin Elmer Corp., Norwalk, Conn., (1985).
- M. I. Pope and M. D. Judd, "Differential Thermal Analysis," Heydon and Sons, Ltd., New York, N.Y., (1977).
- R. Bruce Prime, Polymer Engineering and Science, 13, no. 5, 365 (1973).
- Tito T. Serafini, Chapter II: Status Review of PMR Polyimides, in "Resins for Aerospace," The American Chemical Society, Washington D.C. (1980).
- Charles Phelps Smyth, "Dielectric Behavior and Structure," McGraw-Hill Book Co., Inc., New York (1955).
- S. Sourour and M. R. Kamal, Thermochimica Acta, 14, 41 (1976).
- Murray R. Spiegel, "Complex Variables," Schaum Publishing Co., New York, (1964).

Anne K. St. Clair and Terry L. St. Clair, SAMPE Quarterly, 13, (1), 20 (1981).

Edith A. Turi, "Thermal Characterization of Polymeric Materials," Academic Press, New York, (1981).

S. Uemara, J. Poly. Sci.: Poly. Phys. Ed., 12, 1177 (1974).

E. S. Watson, M. J. O'Neill, J. Justin, and N. Brenner, Analytical Chemistry, 36, June, 1235 (1964).

Wesley Wm. Wendlandt, "Thermal Methods of Analysis," John Wiley and Sons, New York, (1974).

A. C. Wong and W. M. Ritchey, Macromolecules, 14, 825 (1981).

Eun C. Yi, "Dielectric Analysis of 3501-6," Honors Thesis, The College of William and Mary, (1985).

Philip R. Young, NASA-TM-83192, (1981).

Liu Zhenhai, Ding Mengxian, and Chen Zhongqing, Thermochemica Acta, 10, 71 (1983).

VITA

Michael Edward Whitham

Born in Washington D.C. on September 27, 1962. Graduated from Oakton High School in Vienna, Virginia in June, 1980. Received a B.S. in Biochemistry from Virginia Polytechnic Institute and State University in June, 1984. Employed as a research assistant at the military university in the NIH complex in Bethesda, Maryland from July, 1984 to December, 1984.

The author entered the graduate program in the Department of Chemistry of the College of William and Mary in January, 1985.